Fundamentals of flexoelectricity in solids

2013 Nanotechnology 24 432001

Nanotechnology **24** (2013) 432001 (36pp) doi:10.1088/0957-4484/24/43/432001

TOPICAL REVIEW

Fundamentals of flexoelectricity in solids

P V Yudin and A K Tagantsev

Ceramics Laboratory, Swiss Federal Institute of Technology (EPFL), CH-1015 Lausanne, Switzerland

E-mail: petr.yudin@epfl.ch and alexander.tagantsev@epfl.ch

Received 21 March 2013, in final form 31 May 2013
Published 2 October 2013
Online at stacks.iop.org/Nano/24/432001

Abstract
The flexoelectric effect is the response of electric polarization to a mechanical strain gradient. It can be viewed as a higher-order effect with respect to piezoelectricity, which is the response of polarization to strain itself. However, at the nanoscale, where large strain gradients are expected, the flexoelectric effect becomes appreciable. Besides, in contrast to the piezoelectric effect, flexoelectricity is allowed by symmetry in any material. Due to these qualities flexoelectricity has attracted growing interest during the past decade. Presently, its role in the physics of dielectrics and semiconductors is widely recognized and the effect is viewed as promising for practical applications. On the other hand, the available theoretical and experimental results are rather contradictory, attesting to a limited understanding in the field. This review paper presents a critical analysis of the current knowledge on the flexoelectricity in common solids, excluding organic materials and liquid crystals.

(Some figures may appear in colour only in the online journal)

Contents

Nomenclature

A	Extrapolation length
$A^{ik}_{p,j}$	Microscopic tensor linking internal strain with strain
a	Lattice constant
a_s	Substrate lattice constant
$B^{ikl}_{p,j}$	Microscopic tensor linking internal strain with strain gradient
C	Curie–Weiss constant
c_{ijkl}	Stiffness tensor
D_i	Electric displacement vector
E_i	Macroscopic electric field
e_{ijk}	Piezoelectric tensor
F	Force
f_{ijkl}	Flexocoupling tensor

G	Curvature
$G^{j}_{p,i}$	Microscopic tensor linking internal strain with the amplitude and frequency of the acoustic wave
g_{ijkl}	Correlation energy tensor
$H^{ik}_{p,j}$	Microscopic tensor linking internal strain with strain
h	Thickness
I	Trace of matrix of average quadruple density
i	Imaginary unit
M	Bending moment per unit length
M_{ij}	Tensor linking energy with time derivatives of polarization and displacement
$M^{(n)}_{p,j\ldots k}$	Multiple moments of variation of the charge density
m	Mass
N_i	Lattice translation vector
$N^{ikl}_{p,j}$	Microscopic tensor linking internal strain with strain gradient
P_i	Polarization vector (ferroelectric part)
$P_{s,i}$	Spontaneous polarization vector
P^0_j	Average dipole-moment density
Q_n	Charge of nth point charge
Q_p	Transverse effective Born charge
Q^0_{ij}	Average quadruple moment density
Q_{ij}	Average quadruple moment density, calculated without subtracting the trace
q_i	Wavevector
q_{ijkl}	Electrostriction tensor
R	Radius
R_i	Radius vector
S	Surface area
T	Temperature
T_{k}	Density of kinetic energy
T_0	Curie–Weiss temperature
t	Time
t_h	Domain wall thickness
U_i	Displacement vector
u_{jk}	Strain tensor
u_{m}	Misfit strain
V	Volume of sample
v	Volume of crystalline unit cell
$w_{p,j}$	Amplitude of atomic displacements
w^{ext}_j	External strain (atomic displacements)
w^{int}_j	Internal strain (atomic displacements)
x_i	Cartesian coordinates
α	Inverse dielectric susceptibility
β_{ijkl}	Fourth-order dielectric stiffness
γ_{ij}	Tensor linking energy with square of polarization time derivative
ε_{ij}	Dielectric permittivity tensor
ε_0	Dielectric permittivity of vacuum
ε_{b}	Background dielectric permittivity
ε_{f}	Ferroelectric part of dielectric permittivity
ϑ_{ijk}	Tensor linking energy with polarization and strain
Λ_{ij}	Tensor linking polarization and acceleration
λ	Thickness of piezoelectric layer
μ_{ijkl}	Flexoelectric tensor
ν	Poisson ratio
ρ	Charge density
ϱ	Density
σ_{ij}	Mechanical stress
Υ_{ij}	Mean strain
Φ	Thermodynamic potential defined as $\mathrm{d}\Phi_G = -P_i\mathrm{d}E_i - u_{ij}\mathrm{d}\sigma_{ij}$
ϕ	Electrostatic potential
χ_{ij}	Dielectric susceptibility tensor
Ψ_{b}	Free energy density per unit area
ω	Angular frequency

1. Introduction

The flexoelectric effect is an electromechanical effect in which the dielectric polarization exhibits a linear response to a gradient of mechanical strain. The name originates from the Latin word *flexus* meaning 'bend' and is related to the fact that a strain gradient naturally arises in bent plates. This effect can be viewed as a high-order electromechanical phenomenon with respect to the piezoelectric effect, which is a linear response of the dielectric polarization to a mechanical strain. Currently, the terms 'flexoelectric effect' and 'flexoelectricity' are used in two areas of condensed matter physics: in soft matter (liquid crystals and biological materials) [1–4] and in common solids. In this paper we are interested in the case of common solids, excluding polymers. Though the existence of the flexoelectric effect in solids was predicted in the 1950s, only very limited attention was paid to it up to the end of that century, primarily because the effect was expected to be weak. However, recently, the situation changed. First, systematic experimental studies on flexoelectricity in ferroelectric ceramics suggested that the response can be several orders of magnitude stronger than was expected based on theoretical estimates. Second, in line with the 'ever green' trend to miniaturization, as length scales decrease larger strain gradients and, correspondingly, larger flexoelectric effects are expected. Judging from the number of publications on flexoelectricity in solids (figure 1), the total volume of activity in the field is still modest but the field is evolving rapidly. Several reviews have already been published on flexoelectricity in solids [5–12], some of them quite recently. Based on these publications, one finds the big picture of the field, which leaves a mixed impression. On the one hand, the flexoelectric effect looks promising for practical applications and helps to explain a number of phenomena, especially at the nanoscale. On the other hand, the available theoretical and experimental results are rather contradictory, attesting to a limited understanding of flexoelectricity. Another feature of the development in the field is the variety of terminology and methods used in different papers, which sometimes obscures the links between different results. Under such circumstances, a unified discussion of the fundamentals of flexoelectricity is needed. Such a discussion, with an accent on the recent developments, is the main objective of the present review article.

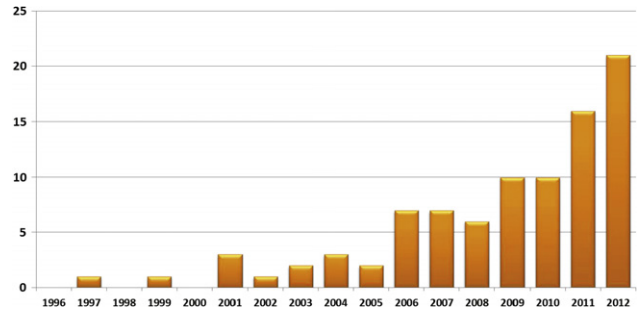

Figure 1. The number of publications on flexoelectricity in solids per year. Data from database 'webofknowledge.com', search for the keywords 'Flexoelectric/flexoelectricity', publications related only to solids are selected.

2. Historical overview and outlook of the field

The flexoelectric effect in solids was first identified theoretically by Mashkevich and Tolpygo [13, 14] based on their studies of lattice dynamics in crystals. The first phenomenological framework for the description of this effect was offered by Kogan [15] in 1964, who did it in the context of electron–phonon coupling in centrosymmetric crystals, where the flexoelectric coupling may play an important role. In 1965 the microscopics of the flexoelectric effect was addressed by Harris [16]. In 1968 a phenomenological framework for the description of the effect was proposed by Mindlin [17]. The first microscopic calculations of the coefficients controlling flexoelectricity were performed by Askar *et al* [18] in 1970 for a number of simple crystals. By that time, only very limited experimental information on the flexoelectric effects in solids had been collected [6]. All the aforementioned theoretical and experimental activity did not deal with ferroelectrics.

Flexoelectricity in ferroelectrics, the materials in which this effect looks to be interesting for practical applications, was first addressed by Bursian and coworkers [19–21]. They characterized flexoelectricity in the classical ferroelectric $BaTiO_3$ and demonstrated switching of spontaneous polarization driven by a strain gradient. These authors also developed a phenomenological theory of the flexoelectric effect in a finite plate of a ferroelectric. One of the results of this theory—that the flexoelectric effect should be strongly enhanced in materials with high dielectric permittivity (ferroelectrics)—played a decisive role in the development of the whole field. Meanwhile, on the experimental side, an important manifestation of the flexoelectric effect was identified by Axe *et al* [22] based on the analysis of phonon spectra in ferroelectrics. These authors uncovered a strong impact of this effect on the low-energy phonon spectra in perovskite ferroelectrics. It was also pointed out that the flexoelectric coupling may readily lead to the formation of modulated incommensurate structures in dielectrics. In 1981, a Landau-type theory for the flexoelectricity in ferroelectrics was offered by Indenbom *et al* [23]. Before this paper, in studies of the flexoelectric effect in solids, the term 'flexoelectric effect' was not used. It was sometimes called 'non-local piezoelectricity' [21]. The term 'flexoelectric effect' in application to solids was introduced by Indenbom *et al* [23], who borrowed it from the physics of liquid crystals, where this term was used for the description of a similar phenomenon. At that time, as also clear from the terminology used, the effect was commonly treated as a tight analogue of piezoelectricity. The situation changed as a result of the theoretical works by Tagantsev [24, 25] in the late 1980s, who demonstrated, using both phenomenological and microscopic approaches, that the situation is more complicated and that there are non-trivial dynamic and surface contributions to the flexoelectric response, having no analogs in piezoelectricity. He also formulated a simple framework enabling the calculations of the flexoelectric coefficients from the dynamical matrix of the crystal.

There was a very limited interest in flexoelectricity in solids before the systematic experimental studies of the effect in ferroelectric ceramics by Cross and coworkers in early 2000s [7, 26–29]. In some systems, e.g. $(Ba, Sr)TiO_3$ ceramics, the flexoelectric effect was found to be much stronger than was expected based on order-of-magnitude estimates for crystals. Later, the flexoelectric response was characterized in a number of ferroelectric ceramics [30–34] and single crystals [22, 35–40], using direct (polarization response of a strain gradient in finite samples) or indirect (from phonon spectra or data on thermodynamically linked effects) methods. The most detailed information was obtained on $SrTiO_3$ crystals by Zubko *et al* [41, 42].

Experimental studies of the flexoelectric effect stimulated the interest of theorists.

First, the flexoelectricity was addressed in terms of microscopic theories. The ionic contribution to flexoelectricity was evaluated for several perovskite ferroelectrics and bi-atomic crystals by Sharma and coworkers [43] using the framework offered by Tagantsev [25]. *Ab initio* calculations of this contribution were performed by Hong *et al* [44] and Ponomareva *et al* [45] for $SrTiO_3$, $BaTiO_3$, and their solid solution. The first-principles calculations of the purely electronic contribution to flexoelectricity have been done by Hong and Vanderbilt for a number of crystals, including classical perovskites [46]. The concept behind these calculations, stemming from the classical work by Martin [47], was formulated by Resta [48]. The electronic contribution to flexoelectricity in carbon nanosystems was evaluated by Dumitrica *et al* [49] and Kalinin and Meunier [50] using *ab initio* calculations.

The specifics of flexoelectricity in a finite sample was another intriguing issue for theorists. The conventional phenomenological approach was bridged [51] to Bursian's theory [21] and the importance of the surface effects in the flexoelectric behavior of ferroelectrics was identified by Tagantsev and Yurkov [51]. It was shown by Indenbom *et al* [23], Eliseev *et al* [52], and Yurkov [53] that taking flexoelectricity into account will lead to a modification of the electrical and mechanical boundary conditions.

An important breakthrough in the field was due to the work by the group of Cross [54–56], who demonstrated piezoelectric meta-materials, e.g. composite materials made of non-piezoelectrics but exhibiting the macroscopic piezoelectric response (due to the local strain

gradients and flexoelectricity). The effective piezoelectric response of such meta-materials was shown to be comparable to that of commercial piezoelectrics. Important theoretical results on piezoelectric meta-materials and other systems exhibiting an effective piezoelectric response were reported by Fousek *et al* [57] (symmetry consideration) and by Sharma and coworkers [58–60] (continuum-theory calculations).

It was recently realized that the flexoelectric coupling may interfere with various physical phenomena in solids. The scope of relevant theoretical studies is wide. Let us mention some of them. The Landau-theory modeling of ferroic domain walls by Morozovska and coworkers [61, 62] and Yudin *et al* [63] demonstrated an essential impact of flexoelectricity on the properties of the domain walls (structure, energy, and electrical conductivity). Majdoub *et al* [64] and Zhuo *et al* [65] modeled the 'dead layer' effect on ferroelectric thin films conditioned by flexoelectricity. Modeling of flexoelectricity-driven internal bias in thin films was offered by Catalan *et al* [66, 67], while a scenario for the flexoelectricity-driven imprint was offered by Abe *et al* [68, 69] and modeled by Tagantsev *et al* [70]. The continuum-theory analysis incorporating flexoelectricity identified some unexpected manifestations of this phenomenon. For example, the Texas group of Sharma [71–73] identified an important role of flexoelectricity in the hardening of ferroelectrics at nano-indentation; Morozovska *et al* showed that the flexoelectric effect can play an important role in the electromechanical properties of moderate conductors [74].

Recent experimental studies on flexoelectricity-driven phenomena are also numerous. The results of these studies attest to the key feature of the flexoelectric effect, namely, that a strain gradient (via the flexoelectric coupling) may work as an electric field: it can induce poling, switching, and rotation of polarization; it can create a voltage offset of hysteresis loops and smear the dielectric anomaly at ferroelectric phase transitions. Below we name some of these studies. The poling of quasi-amorphous $BaTiO_3$ by special thermal treatment was reported to be assisted by flexoelectricity by the group of Lubomirsky [75]. Flexoelectricity-driven internal bias in thin films of $HoMnO_3$ was documented by Lee *et al* [76]. The active control of polarity by strain gradients in thin films was reported by Gruverman *et al* [77], who demonstrated that the polarization state of a ferroelectric $Pb(Zr, Ti)O_3$ capacitor can be reversed by strain gradients generated by bending of the underlying Si substrate. A similar phenomenon, but at the nanoscale, was studied by Lu *et al* [78], who used the inhomogeneous deformation caused by pushing with the tip of an atomic force microscope in order to switch the polarization of an ultrathin $BaTiO_3$ film. Finally, the ability of a stain gradient to smear a dielectric anomaly in ferroelectric thin films was proved experimentally by Catalan *et al* [66].

3. Description of bulk flexoelectric effect in crystals

In this section we present the fundamentals of the phenomenological and microscopic theory of the bulk flexoelectric effect in crystals. Classical and recent developments will be presented in a unified framework.

3.1. Static bulk flexoelectric effect—phenomenology

The phenomenological approach provides an adequate description of the bulk flexoelectric effect. However, in contrast to the piezoelectric response, the treatment of the flexoelectric effect in the static (e.g. in a bent plate) and dynamic (in a sound wave) situations generally requires separate treatments [6, 25]. Let us start with the static case.

Following Kogan [15] we introduce the flexoelectric effect via the constitutive equation for the electric polarization P_i

$$P_i = \chi_{ij}E_j + e_{ijk}u_{jk} + \mu_{klij}\frac{\partial u_{kl}}{\partial x_j} \tag{1}$$

where E_i, u_{jk}, and $\partial u_{kl}/\partial x_j$ are the macroscopic electric field, the strain tensor, and its spatial gradient, respectively. Hereafter the Einstein summation convention is adopted. The first two rhs terms of this equation describe the dielectric and piezoelectric responses with the tensor of the clamped dielectric susceptibility χ_{ij} and the piezoelectric tensor e_{ijk}, respectively. The last rhs term of equation (1) describes the linear polarization response to a strain gradient—*flexoelectric effect*. The strain tensor is defined as the symmetric part of the tensor $\partial U_l/\partial x_j$, $u_{jk} = 1/2(\partial U_j/\partial x_k + \partial U_k/\partial x_j)$, where U_i is the displacement of point x_j of the medium. The antisymmetric part of the tensor $\partial U_l/\partial x_j$, $\Omega_{jk} = 1/2(\partial U_j/\partial x_k - \partial U_k/\partial x_j)$, corresponding to rotations of the sample as a whole, evidently does not contribute to the polarization response. As for the gradients of Ω_{jk}, it can contribute to the polarization response. However, $\partial\Omega_{kl}/\partial x_j$ are not included in this constitutive equation since, as was shown by Indenbom *et al* [23], these can always be presented as a sum of the components of tensor $\partial u_{kl}/\partial x_j$. The fourth rank tensor μ_{klij} controlling the flexoelectric effect in equation (1), the *flexoelectric tensor*, is symmetric with respect to the permutation of the first two suffixes. In general, it is not always possible to use for μ_{klij} the 2-suffix Voigt tensor notations. However, when possible, e.g. for the crystals of the cubic symmetry, we will use these notations for μ_{klij} as for other fourth rank tensors hereafter. The coefficients in the Voigt tensor notations are used in accordance with the reference text [79], for μ_{klij} same convention as for the stiffness tensor c_{klij} is applied. The flexoelectric tensor is allowed in materials of any symmetry (including those amorphous), in a sharp contrast to the piezoelectric tensor, e_{ijk}, which is a third rank tensor and allowed only in non-centrosymmetric media. This makes the principal difference between piezoelectricity and flexoelectricity, as the latter is a general phenomenon having no symmetry limitations. Since the piezoelectric and flexoelectric tensors describe the properties of a material in the absence of a macroscopical electric field, these can also be defined as

$$e_{ijk} = \left(\frac{\partial P_i}{\partial u_{jk}}\right)_{E=0} \tag{2}$$

$$\mu_{klij} = \left(\frac{\partial P_i}{\partial(\partial u_{kl}/\partial x_j)}\right)_{E=0}. \tag{3}$$

A more advanced description of both electromechanical (piezoelectric and flexoelectric) effects is the thermodynamic one, which enables the identification of the thermodynamically related converse effects and provides a proper basis for the studies of stability of the system (see section 6.2). Such a description is given by the following expansion of the thermodynamic potential density in terms of polarization, strain, and their derivatives

$$\Phi_G = \frac{\chi_{ij}^{-1}}{2}P_iP_j + \frac{c_{ijkl}}{2}u_{ij}u_{kl} + \frac{g_{ijkl}}{2}\frac{\partial P_i}{\partial x_j}\frac{\partial P_k}{\partial x_l} - \vartheta_{ijk}P_iu_{jk} - f^{(1)}_{ijkl}P_k\frac{\partial u_{ij}}{\partial x_l} - f^{(2)}_{ijkl}u_{ij}\frac{\partial P_k}{\partial x_l} - P_iE_i - u_{ij}\sigma_{ij}. \quad (4)$$

Its differential is defined as $\mathrm{d}\Phi_G = -P_i\,\mathrm{d}E_i - u_{ij}\,\mathrm{d}\sigma_{ij}$. This expansion does not contain anharmonic terms (i.e. the electrostriction term is omitted). When nonlinear effects are of interest, these can readily be incorporated into the framework, as done in section 4.2.

If we set to zero the coefficients for the gradient-containing terms, the bulk equations of state of the material can be found by a simple minimization of the potential density (4) with respect to the polarization and strain. Such a minimization leads to linear electromechanical equations for a piezoelectric:

$$E_i = \chi_{ij}^{-1}P_j - \vartheta_{ijk}u_{jk} \quad (5)$$

$$\sigma_{ij} = c_{ijkl}u_{kl} - \vartheta_{ijk}P_i. \quad (6)$$

It is seen that equation (5) is consistent with the dielectric and piezoelectric responses introduced by (1) with

$$e_{ijk} = \chi_{il}\vartheta_{ljk}. \quad (7)$$

In turn, equation (6) describes Hooke's law and the converse piezoelectric effect. Thus the term ϑPu of expansion (4) controls the piezoelectricity in the material. For clarity of the presentation, we will drop this term in the following discussion. This discussion can be readily generalized to piezoelectrics by taking this term into account.

Thus, we address flexoelectricity using the thermodynamic potential density (4) with $\vartheta = 0$. Here it is proper to present Φ_G as the sum of two contributions:

$$\Phi_G = \Phi - \frac{f^{(1)}_{ijkl} + f^{(2)}_{ijkl}}{2}\frac{\partial(P_ku_{ij})}{\partial x_l} \quad (8)$$

$$\Phi = \frac{\chi_{ij}^{-1}}{2}P_iP_j + \frac{c_{ijkl}}{2}u_{ij}u_{kl} + \frac{g_{ijkl}}{2}\frac{\partial P_i}{\partial x_j}\frac{\partial P_k}{\partial x_l} - \frac{f_{ijkl}}{2}\left(P_k\frac{\partial u_{ij}}{\partial x_l} - u_{ij}\frac{\partial P_k}{\partial x_l}\right) - P_iE_i - u_{ij}\sigma_{ij}; \quad (9)$$

where $f_{ijkl} = f^{(1)}_{ijkl} - f^{(2)}_{ijkl}$ is called *flexocoupling tensor*. The free energy in the form given by equation (9) was introduced by Indenbom *et al* [23] for the description of the static bulk flexoelectricity.

Now that the potential density contains gradient terms, to get the equation of state, one should minimize the thermodynamic potential of the sample as a whole $\int \Phi_G\,\mathrm{d}V$ (integrating over the volume of the sample), i.e. to apply the Euler equations $\partial\Phi_G/\partial A - \frac{\mathrm{d}}{\mathrm{d}x}(\partial\Phi_G/\partial(\partial A/\partial x)) = 0$, where A stands for P and u. Such a minimization yields the bulk constitutive electromechanical equations in the form proposed by Mindlin [17]

$$E_i = \chi_{ij}^{-1}P_j - f_{klij}\frac{\partial u_{kl}}{\partial x_j} - g_{ijkl}\frac{\partial^2 P_i}{\partial x_j\partial x_l} \quad (10)$$

$$\sigma_{ij} = c_{ijkl}u_{kl} + f_{ijkl}\frac{\partial P_k}{\partial x_l}. \quad (11)$$

It is seen that, in the case where the strain gradient and the polarization are homogeneous, equation (10) reproduces the flexoelectric effect introduced by (1) with

$$\mu_{klij} = \chi_{is}f_{klsj}. \quad (12)$$

Equation (12) links the flexoelectric and flexocoupling tensors, suggesting that the flexoelectric response should be enhanced in materials with high dielectric constants (high-K materials) such as ferroelectrics [23]. It is also clear from this equation that via the flexoelectric coupling the strain gradient works as an electric field.

Equation (11) enables us to recognize the thermodynamically conjugated effect to the static bulk flexoelectric response—*converse flexoelectric effect*, which consists of the contribution to the mechanical stress, proportional to the gradient of polarization [23].

An approximate form of the constitutive equations (10) and (11), where the last rhs term in (10) is neglected and equation (11) is rewritten in terms of E, neglecting the appearing contribution $\propto\frac{\partial^2 u_{ik}}{\partial x_j\partial x_l}$, is also used [7]:

$$P_i = \chi_{ij}E_j + \mu_{klij}\frac{\partial u_{kl}}{\partial x_j} \quad (13)$$

$$\sigma_{ij} = \mu_{ijkl}\frac{\partial E_k}{\partial x_l} + c_{ijkl}u_{kl}. \quad (14)$$

In the case of relatively small 'exogenous' gradients (produced, for example, by mechanical bending of a sample) this form of the constitutive equations is suitable. However, in the case of the 'endogenous' strong gradients (at domain boundaries and interfaces or the lattice displacement waves like phonons) the application of this form is limited.

It is worth mentioning that the last term in equation (8) does not contribute to the bulk constitutive electromechanical equations. This can be concluded directly from the fact that its contribution to the thermodynamic potential of the sample can be transformed to an integral over the surface of the sample: $-\frac{1}{2}(f_1 + f_2)\int uP\,\mathrm{d}S$. Thus, the thermodynamic potential density (9) provides a full phenomenological description of the static bulk flexoelectric effect.

It is instructive to compare the converse effects for the piezoelectric and flexoelectric responses. It can be seen from equations (5), (6), (10), and (11) that in both cases the converse effect is controlled by the same tensor as the direct one[1]. Based on equations (5) and (6), one can discuss

[1] As it must be for the thermodynamically conjugated effects.

the symmetry between the converse and direct piezoelectric effects. Namely, as follows from equation (5), under the short-circuited conditions ($E = 0$), strain induces polarization while, as follows from equation (6), under the mechanically free conditions ($\sigma = 0$), *polarization induces strain*. However, equations (10) and (11) suggest a certain asymmetry between the direct and converse flexoelectric effects: as clear from equations (10) and (11), in the absence of an electric field, a strain gradient induces homogeneous polarization while, for the converse effect, in a mechanically free sample, homogeneous polarization *does not induce* a strain gradient. This asymmetry provoked a judgment that a sensor based on the flexoelectric effect will not behave as an actuator [7]. This judgment, however, is not supported by the accurate analysis of the flexoelectric behavior of a finite sample [51]. We will address this issue in section 5.1.

3.2. Microscopics of static bulk flexoelectric effect

At the microscopic level, the flexoelectric response is controlled by the redistribution of the bound charge of a crystal driven by a strain gradient, where ionic and electronic contributions can be distinguished. The theories of this phenomenon provide relationships between the flexoelectric tensor introduced phenomenologically and the microscopical parameters of the material (e.g. the dynamical matrix which describes the energy of interatomic interactions in the crystal). In this subsection we will briefly outline such theories.

The microscopic theory of the static bulk flexoelectric effect has been developed using two methods: the first is based on a calculation of the average polarization induced in a finite sample by a homogeneous strain gradient in the absence of a macroscopic electric field, in agreement with definition (1)–(3). Such a polarization corresponds to one that can be experimentally measured by integrating the short-circuiting current passing between the plates of a capacitor containing the sample subjected to the strain gradient [25]. Alternatively, one can use the so-called long-wavelength method, originally introduced into the lattice dynamics theory by Born and Huang [80]. In this method, one considers a sinusoidal wave of elastic deformation and calculates the amplitude of the induced polarization wave, based on lattice mechanics of crystals and the basic definition of polarization. Then the microscopic expressions for the flexoelectric tensor can be found by comparing the results of these calculations with the amplitude of the induced polarization wave calculated within the basic constitutive equation (1) [25, 46, 48]. Both methods can be readily used for calculating the flexoelectric response of ionic crystals, when treating the ions as point charges [25]. The general situation where the charge in the crystal is not necessarily localized can be treated using the continuum-charge-density approach offered by Martin [47] in terms of the long-wavelength method. Though this approach is equally applicable to the case of point charges, it is useful indeed for calculating the purely electronic contribution to the flexoelectric response, as was demonstrated by Resta [48] and Hong and Vanderbilt [46].

In the subsections below, we will address the microscopics of the electromechanical response in terms of point-charge and continuum-charge-density approaches, using both finite-sample and long-wavelength methods, which enables us, as we will see later, to unify the theoretical results obtained in the field. The issue is subtle in view of ambiguities associated with the microscopic definition of polarization. It will be shown that the polarization response is mainly due to parts of atomic displacements, which appear due to the discrete nature of the crystal. These parts are known as *internal strains* [80] and may be obtained from real displacements by subtraction of parts corresponding to deformation of a crystal by the laws of continuum elastic media, known as *external strains*[2].

3.2.1. Finite crystal: point-charge approximation. Consider the flexoelectric response of a finite crystal which is modeled as consisting of point charges Q_n located at points with coordinates $R_{n,i}$ where n enumerates charges and i is the Cartesian suffix. This can be done by calculating the variation of the average dipole-moment density of the sample

$$\delta P_i = V_{\text{fin}}^{-1} \sum_n Q_n (R_{n,i} + w_{n,i}) - V^{-1} \sum_n Q_n R_{n,i} \quad (15)$$

where $w_{n,i}$ is the displacement of the charge (from its original position at $R_{n,i}$) induced by the deformation, and V and V_{fin} are the sample volume before and after the deformation; the summation over all the charges of the sample is implied. To evaluate the flexoelectric tensor, μ_{klij}, the calculation should be carried out under the condition of vanishing macroscopic electric field in the sample, in accordance with definition (3). This equation actually describes the total electromechanical response of the system, including piezoelectricity. We will include the latter in the following treatment as well, which provides a good benchmark for discussing flexoelectricity.

In general, the displacements $w_{n,i}$ can be presented in the form

$$w_{n,i} = \int_{x_j^0}^{R_{n,j}} \frac{\partial U_i}{\partial y_j} \, \mathrm{d}y_j + w_{n,i}^{\text{int}} \quad (16)$$

where x_j^0 are the coordinates of an immobile reference point. The first rhs term in this equation, also known as external strain [80], represents the contribution of the unsymmetrized strain $\partial U_i/\partial x_j$ taken in the so-called elastic medium approximation, the other contribution is referred to as internal strain. The difference between the external and internal strains can be understood as follows. Consider a crystal and a continuous medium with elastic constants identical to those of the crystal. Then, let us mark in the medium a mesh corresponding to the positions of the atoms in the crystal (see figure 2). If we deform the medium according to the unsymmetrized strain $\partial U_i/\partial x_j$, then the deformation of this mesh indicates the external strains of the atoms, figures 2(b), (e), (h). A model, where deformation of a crystal is described by external strains only is hereafter referred

[2] The terminology where displacements are called strains may be confusing, however we keep it following the classic book by Born and Huang [80].

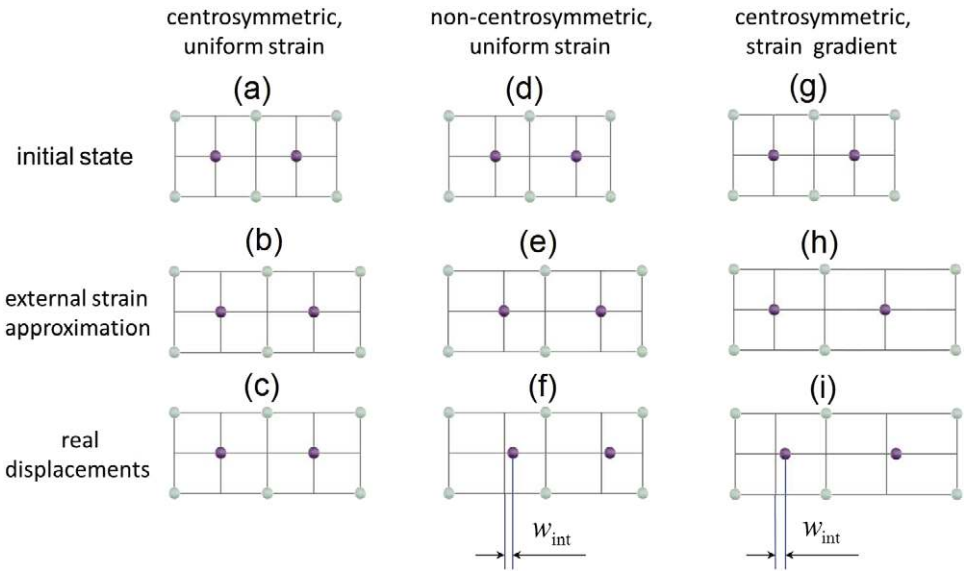

Figure 2. Schematic of atomic displacements in two neighboring unit cells of a crystal caused by application of a macroscopic strain. Cases of uniform macroscopic strain in centrosymmetric (a)–(c) and non-centrosymmetric materials (d)–(f) and of homogeneous strain gradient in centrosymmetric materials (g)–(i) are illustrated. Initial state before application of strain is shown (a), (d), (g); displacements in approximation of external strain (b), (e), (h) and real displacements, comprising external and internal strains (c), (f), (i). The mesh is attached to the light-colored atoms. It deforms according to the external strain approximation.

to as an *external strain approximation*. For a material where all atoms are centers of inversion, the external strain fully describes the atomic displacements caused by a homogeneous deformation, figures 2(b) and (c). However, in the general case, in view of the discrete nature of the crystal, it behaves differently from an elastic medium and the external strain approximation does not hold. Then there appears a difference between the real displacement of an atom and its external strain.

This difference is known as internal strain [80] and is described by the second rhs term in equation (16). Under a homogeneous deformation, internal strains appear only in material where not all atoms (or none of them) are centers of inversion [80], figures 2(e), (f). At the same time, under a deformation gradient, internal strains, in general, appear in materials of any symmetry, figures 2(h), (i). It is also worth mentioning that typically the magnitudes of external strains are much larger than those of internal strains. For instance, if a sample, the dimensions of which are about L, is under a strain u_{11}, the external strains are about Lu_{11}, while the internal strains are much smaller than the lattice constant of the material.

In the lowest, to within the amplitude of the deformation, approximation, the internal strains can be presented as linear functions of the strain tensor and its gradient [25]:

$$w^{\text{int}}_{n,j} = H^{ik}_{n,j} u_{ik} + N^{ikl}_{n,j} \frac{\partial u_{ik}}{\partial x_l}. \tag{17}$$

For the case of an ideal crystalline lattice, $H^{ik}_{n,j}$ and $N^{ikl}_{n,j}$ can be calculated in terms of lattice dynamics theory [25, 80]. Obviously $H^{ik}_{n,j} = H^{ki}_{n,j}$ and $N^{ikl}_{n,j} = N^{kil}_{n,j}$. Though we leave the lattice dynamics theory behind the calculations of the N and H factors out of the scope of this paper, we would like to make an important remark. This theory as used in these calculations deals only with small elastic deformations of the ideal lattice. Thus, only small relative variations of the interatomic distances are considered and any strong variations of the lattice (such as the dislocation formation or atom hopping in highly anharmonic crystalline lattices) are not covered. The flexoelectric effect associated only with such small relative variations of the interatomic distances will be discussed in this paper, except for section 4.3.4.

Now inserting (17) and (16) into (15) and keeping the lowest terms in the amplitude of the deformation, we find for the variation of the average polarization of the sample induced by the mechanical perturbation:

$$\delta P_j = V^{-1} \sum_n Q_n H^{ik}_{n,j} u_{ik} + V^{-1} \sum_n Q_n N^{ikl}_{n,j} \frac{\partial u_{ik}}{\partial x_l} + \delta P^{\text{ext}}_j. \tag{18}$$

The first and second rhs terms of this equation are conditioned by the internal strains. The first one controls piezoelectricity. For a piezoelectric, the sum $\sum_p Q_p H^{ik}_{p,j}$ taken over the crystalline unit cell is not, in general, zero [80] and the first rhs term of (18) is dominated by the bulk contribution. Then, neglecting the surface contribution to the sum over the sample, one can pass from the summation over the sample to that over the unit cell, and comparing the result with the basic relationship (2), one derives the microscopic expression for the piezoelectric tensor [80]

$$e_{ijk} = v^{-1} \sum_p Q_p H^{ik}_{p,j} \tag{19}$$

where the summation is taken over the ions in a unit cell of volume v. In the application of this expression to real ionic systems, the Q_p have the meaning of the transverse Born

effective charges [47] rather than just ionic charges. A similar treatment leads to the flexoelectric tensor given by

$$\mu_{ikjl} = v^{-1} \sum_p Q_p N^{ikl}_{p,j} \tag{20}$$

where the summation is again taken over the ions in a unit cell.

Next we discuss the last rhs term from (18). This term is conditioned by the external strains (the integral term in (16)) and the change of the sample volume. It explicitly depends on the termination of the ionic sample, eventual reconstruction of its surface, and the presence of the additional free charges on it. For the case of a response to a homogeneous strain in the macroscopic sample of a piezoelectric, this term can be eliminated using the condition of the absence of the macroscopic electric field in the sample [25]. This contribution, however, cannot be fully eliminated in the case of the flexoelectric response, bringing about the so-called *surface flexoelectric effect*, which will be addressed separately in section 5.3.

Equation (18) also describes an additional contribution to the integral flexoelectric response of a finite sample—the so-called *contribution of the surface piezoelectricity to flexoelectric response*. It is related to the fact that the sum $\sum_n Q_n H^{ik}_{n,j}$ taken over the distorted layer adjacent to a face of the sample should not, in general, be equal to zero, in view of the symmetry-breaking effect of the interface. We will discuss this contribution separately in section 5.2.

The approach presented above deals with a model viewing a solid as a system of point charges, which is a reasonable approach to describing electromechanical effects in ionic solids. It is suitable for a quantitative evaluation of bulk flexoelectricity in this kind of solid. The tensor $N^{ikl}_{n,j}$ above, which links the internal strains and strain gradients, can be calculated from the dynamic matrix of the material [25], which in turn can be obtained from *ab initio* lattice dynamics simulations. Using this tensor and the transverse Born ionic charges (obtained, e.g., from Berry-phase calculations) one can calculate the μ-tensor using equation (20). This approach was implemented by Pradeep Sharma and coworkers from the University of Texas to calculate the flexoelectric coefficients for a number of materials [43]. We will discuss the results of these calculations in section 6.3.1.

Summarizing this subsection we can state that the treatment of the polarization response to a strain gradient in the point-charge approximation given above identifies the bulk flexoelectric response as originating from the internal strains induced by the gradient of the elastic deformation. This is a direct analogy to the piezoelectric response, which is controlled by internal strains that depend on the elastic deformation itself.

3.2.2. Long-wavelength method: point-charge approximation. There exists an alternative approach to that discussed in the previous subsection, the so-called long-wavelength method, which provides an assessment of bulk flexoelectricity in a crystal without dealing with the surface contributions. Within this approach one considers an elastic wave in the crystal with a wavelength which is much larger than the typical interatomic distance and calculates the amplitude of the induced polarization wave. Then the flexoelectric tensor can be found by comparing the results of the calculations with the amplitude of the induced polarization wave calculated using the basic constitutive equation (1). In this subsection we will outline the implementation of this method to the calculation of the flexoelectric tensor in a model of the ionic crystal, following [6]. In such a model the ions are considered as point charges placed at the points with the coordinates

$$R_{p,j}(\vec{N}) = N_j + y_{p,j} \tag{21}$$

where $\vec{N}$ is the lattice translation vector and $y_{p,j}$ is the vector specifying the position of the pth ion in the elementary unit cell.

Consider an elastic wave characterized by a wavevector $\vec{q}$ and an angular frequency ω. In general, the ionic displacements in such a wave can be written in the form

$$w_{p,j}(\vec{N}, t) = \exp(\mathrm{i}\vec{q}\vec{R}_p - \mathrm{i}\omega t)\tilde{w}_{p,j}(\vec{q}, \omega) \tag{22}$$

where $\tilde{w}_{p,j}$ are the amplitudes of the ionic displacements and t stands for the time[3]. The amplitude, $\tilde{P}_j$, of the polarization wave

$$P_j(\vec{x}, t) = \exp(\mathrm{i}\vec{q}\vec{x} - \mathrm{i}\omega t)\tilde{P}_j(\vec{q}, \omega) \tag{23}$$

can be found using the definition of the polarization

$$\frac{\partial P_j}{\partial x_j} = -\delta\rho \tag{24}$$

where $\delta\rho$ is the elastic-wave-induced variation of the charge density, which is averaged over a macroscopic scale.

In the point-charge model now considered, the microscopic charge density reads

$$\rho^{\mathrm{mic}}(x_i) = \sum_{p,\vec{N}} Q_p \delta(x_i - R_{p,i}) \tag{25}$$

where Q_p stands for the charge of the pth ion in the unit cell and $\delta(\vec{x})$ denotes the delta-function defined in the 3D space. In this model, the linear response of the charge density to the displacement wave (22) can readily be found in the form

$$\delta\rho^{\mathrm{mic}}(x_i) = -\sum_{p,\vec{N}} Q_p \frac{\partial}{\partial x_j}\delta(x_i - R_{p,i}) w_{p,j} \tag{26}$$

corresponding to the amplitude of the wave of the average charge density [6]

$$\delta\tilde{\rho}(\omega, \vec{q}) = \frac{\mathrm{i}}{v}\sum_p q_j \tilde{w}_{p,j} Q_p. \tag{27}$$

Using (27) and the Fourier representation of (24), one finds the equation for the amplitude of the polarization wave

$$\tilde{P}_i q_i = \frac{1}{v}\sum_p q_j \tilde{w}_{p,j} Q_p. \tag{28}$$

[3] The physical quantities are the real parts of the corresponding complex functions.

The amplitude of the polarization wave satisfying this equation reads

$$\tilde{P}_j = \frac{1}{v}\sum_p \tilde{w}_{p,j} Q_p. \tag{29}$$

Strictly speaking, equation (28) taken in this form defines only the longitudinal polarization component. In solution (29) the transverse components of the polarization are introduced consistently with the case of a finite sample, equation (18). In the long-wavelength limit (i.e. at $\vec{q} \to 0$) we are interested in, the amplitude of the atomic displacements $\tilde{w}_{p,j}$ can be expanded in powers of q, ω, and the amplitude of the acoustic wave $\tilde{U}_i$ to find [25]

$$\tilde{w}_{p,j}(\vec{q},\omega) = \tilde{U}_j + \mathrm{i}A^{ik}_{p,j} q_k \tilde{U}_i - B^{ikl}_{p,j} q_k q_l \tilde{U}_i - \omega^2 G^i_{p,j}\tilde{U}_i. \tag{30}$$

Here the first rhs term is independent of the suffix p. It corresponds to the wave of external strains while the rest of the rhs terms of this equation correspond the wave of internal strains. The factors A, B, and G, controlling the internal strains, can be expressed in terms of the moments of the dynamic matrix of the crystal (with the contribution of the macroscopic electric field being excluded). The factor $A^{ik}_{p,j}$ satisfies the relationships $A^{ik}_{p,j} = A^{ki}_{p,j}$ [80] and $A^{ik}_{p,j} = H^{ik}_{p,j}$ [25]. Obviously $B^{ikl}_{p,j} = B^{ilk}_{p,j}$. In addition, the results from [25] readily suggest that $N^{ikl}_{p,j} = B^{ikl}_{p,j} + B^{kil}_{p,j} - B^{lik}_{p,j}$.

Inserting (30) into (29) one finds the amplitude of the polarization wave, which, using the aforementioned relationships for the factors A and B, can be cast in a form suitable for comparison with the phenomenological results given above:

$$\tilde{P}_i = \mathrm{i}e_{ijk}\frac{q_k\tilde{U}_j + q_j\tilde{U}_k}{2} - \mu_{kjis}q_s\frac{q_k\tilde{U}_j + q_j\tilde{U}_k}{2} - \frac{\omega^2}{v}\sum_p G^j_{p,i}Q_p\tilde{U}_j \tag{31}$$

where the tensors e_{ijk} and μ_{kjis} come from equations (19) and (20). In equation (31), $\mathrm{i}(q_k\tilde{U}_j + q_j\tilde{U}_k)/2$ and $-q_s(q_k\tilde{U}_j + q_j\tilde{U}_k)/2$ are nothing but the Fourier components of the strain tensor and its gradient. Taking this into account, one sees that the result of the long-wavelength method, (31), readily reproduces those for the piezoelectric and static bulk flexoelectric responses obtained in the finite-sample approach (equations (1), (19), and (20)). Note that the first rhs term of (30), corresponding to a wave of external strains, does not contribute to the polarization wave, again in agreement with the conclusion drawn from the above finite-sample treatment. This follows from the electroneutrality of the elementary unit cell, $\sum_p Q_p = 0$.

Equation (31) also contains an ω-dependent contribution. Since in the elastic wave $\omega^2 \propto q^2$, this term will also contribute to the polarization proportionally to the strain gradient in the wave. This is the so-called *dynamic flexoelectric response*, which will be addressed separately in section 3.3.

3.2.3. Long-wavelength method: continuum-charge-density. The results on the electromechanical response presented in the previous subsection in the point-charge approximation can be generalized to the case of an arbitrary distribution of the bound charge in the crystal, using the approach developed in the seminal paper by Martin [47]. To do this, following Martin, we use instead of (26) a more general presentation for the variation of the microscopic charge density defined as

$$\delta\rho^{\mathrm{mic}}(x_i) = \sum_{p,\vec{N}} \left.\frac{\partial\rho(x_i)}{\partial R_{p,j}(\vec{N})}\right|_{E=0} w_{p,j} \tag{32}$$

where

$$\left.\frac{\partial\rho(x_i)}{\partial R_{p,j}(\vec{N})}\right|_{E=0} \equiv f_{p,j}(x_i - R_{p,i}(\vec{N})) \tag{33}$$

is the variation of charge density at point $\vec{x}$ per unit displacement of atom at $R_{p,j}(\vec{N})$ holding all other atoms fixed and macroscopic electric field constant. In view of the translational invariance of the problem, the function $f_{p,j}(\vec{x})$ is independent of the lattice vector $\vec{N}$. The condition $E = 0$ corresponds to the definition (1)–(3) of the electromechanical response. In addition, this condition eliminates the long-range interactions so that $f_{p,j}(\vec{x})$ is short range, i.e. the characteristic range of $f_{p,j}(\vec{x})$ is much smaller than any wavelength. It was shown by Martin that the electromechanical response can be described in terms of multiple electric moments of the function $f_{p,j}(\vec{x})$, which are well defined in view of short-range character of $f_{p,j}(\vec{x})$. Specifically, using (32) instead of (26), equation (29) for the amplitude of the polarization wave can be generalized to the form [47]

$$\tilde{P}_i = \frac{1}{v}\sum_p \tilde{w}_{p,j} \times (M^{(1)}_{p,ij} - \mathrm{i}q_k M^{(2)}_{p,ikj} - q_k q_l M^{(3)}_{p,ikl} + \cdots) \tag{34}$$

where the multiple moments of the function $f_{p,j}(\vec{x})$ are defined as

$$M^{(1)}_{p,ij} = \int \mathrm{d}^3x f_{p,j}(\vec{x}) x_i, \tag{35}$$

$$M^{(2)}_{p,ikj} = \tfrac{1}{2}\int \mathrm{d}^3x f_{p,j}(\vec{x}) x_i x_k, \tag{36}$$

$$M^{(3)}_{p,ikl} = \tfrac{1}{6}\int \mathrm{d}^3x f_{p,j}(\vec{x}) x_i x_k x_l, \tag{37}$$

and so on. Here $M^{(1)}_{p,ij}$ is the effective charge tensor [81] for the pth atom in the unit cell. It is directly related to the transverse Born effective charge Q_p, satisfying the charge neutrality condition

$$\sum_p M^{(1)}_{p,ij} = 0. \tag{38}$$

In the high-symmetry cases, one may have

$$M^{(1)}_{p,ij} = Q_p\delta_{ij}. \tag{39}$$

It is instructive to compare (34) with the result of the point-charge approximation (29). In this approximation

$f_{p,j}(\vec{x}) \propto \frac{\partial}{\partial x_j}\delta(\vec{x})$ so that all moments of $f_{p,j}(\vec{x})$ except for $M^{(1)}_{p,ij}$ are zero. Thus, in view of relationship (39), the result of the continuum-charge-density approach is consistent with that of the point-charge approximation. This also enables us to identify the $M^{(1)}$-term in (34) as a *ionic contribution* to the static bulk flexoelectric effect. It is essential that, in view of (38), this contribution is zero in the external strain approximation, where the amplitudes $\tilde{w}_{p,j} = \tilde{U}_j$ are the same for all the atoms of the unit cell.

In general, the higher moments of $f_{p,j}(\vec{x})$ are not zero, contributing to (34), i.e. to the electromechanical response of the system. The fact that there is no sum rule like (38) for these moments enables us to identify a remarkable feature of the corresponding contribution: it exists even in the absence of internal strains. One can trace a parallel between the new contribution and the ionic one [6]: now redistributing the electronic density driven by external strains plays the role of internal strains. Hereafter, when discussing the polarization response which appears in the absence of internal strains, we will use the term 'electronic contribution'.

Expansion (34) was used by Martin [47] to analyze piezoelectricity: the q-linear terms of (34), with the atomic displacements coming from (30), yield an equation for the piezoelectric response incorporating the effect of a higher moment of $f_{p,j}(\vec{x})$:

$$\tilde{P}^{\text{piez}}_i = \frac{\mathrm{i}\tilde{U}_s q_k}{v}\sum_p (A^{sk}_{p,j}M^{(1)}_{p,ij} - M^{(2)}_{p,iks}) \tag{40}$$

where $A^{sk}_{p,j}$ is introduced in (30). Here, in addition to the ionic contribution, there appears an electronic one conditioned upon the quadruple moment, $M^{(2)}_{p,iks}$, of the function $f_{p,j}(\vec{x})$. Using (40) one can derive a microscopic expression for the piezoelectric tensor, incorporating the new contribution. According to Martin [47] the ionic and electronic contributions to piezoelectricity can be comparable.

Martin's approach also provides a generalized description for the static bulk flexoelectric response. Using (30) for the atomic displacements, the q^4-terms of (34) yield:

$$\tilde{P}^{\text{flex}}_i = -\frac{\tilde{U}_s q_k q_l}{v} \times \sum_p (B^{skl}_{p,j}M^{(1)}_{p,ij} + M^{(3)}_{p,ikls} - A^{sk}_{p,j}M^{(2)}_{p,ilj}). \tag{41}$$

Here, the term dependent on $M^{(1)}$ controls the ionic contribution, which corresponds to (20) in the point-charge approximation. The term dependent on the octuple moment $M^{(3)}$ controls an electronic contribution [46, 48], i.e. according to the terminology that we have accepted, a contribution which is present in the absence of internal strains. The polarization response corresponding to the last rhs term of (41) is of a mixed nature. On one hand, we cannot classify it as ionic, since it is not controlled by the effective charge tensor. On the other hand, we cannot classify it as electronic, since it requires the appearance of internal strains. In contrast to the other contributions, it is explicitly symmetry sensitive—it is zero in materials where every atom is a center of inversion, since in such materials $A^{sk}_{p,j} = 0$ [80].

Comparing (41) with the definition of the flexoelectric tensor (3) and taking into account the permutational symmetry of the relevant tensors, in view of the identity [23]

$$\frac{\partial^2 U_i}{\partial x_k \partial x_j} = \frac{\partial u_{ij}}{\partial x_k} + \frac{\partial u_{ik}}{\partial x_j} - \frac{\partial u_{kj}}{\partial x_i}, \tag{42}$$

(which implies $2\tilde{U}_i q_k q_j = q_k(\tilde{U}_i q_j + \tilde{U}_j q_i) + q_j(\tilde{U}_i q_k + \tilde{U}_k q_i) - q_i(\tilde{U}_j q_k + \tilde{U}_k q_j)$), one finds the electronic contribution to the flexoelectric tensor in the form

$$\mu^{\text{el}}_{iljk} = \frac{1}{v}\sum_p (M^{(3)}_{p,jkil} + M^{(3)}_{p,jkli} - M^{(3)}_{p,jilk}). \tag{43}$$

Until recently, this contribution to the flexoelectric response had not been discussed in the literature. Its existence was pointed out by Resta [48]. His analytical treatment of the problem and that from a recent publication by Hong and Vanderbilt [46] are based on Martin's approach and are close to that presented above.

Resta's framework employs the response function of the local microscopic electric field to an atomic displacement, calculated at fixed macroscopic field, instead of the response function of microscopic charge density (32). Since the field and the charge density are linked via the Poisson equation, Resta's framework is equivalent to that developed above [48]. Naturally, the final result of his calculation for a cubic mono-atomic crystal, $\mu^{\text{el}}_{11} = M^{(3)}_{1,1111}/v$, is consistent with (43).

The analytical treatment by Hong and Vanderbilt [46] differs from the extended Martin's treatment given above by the definition of the response function of the local microscopic charge density to an atomic displacement. In contrast to Martin, these authors have defined this response function at a fixed electrical displacement $\vec{D}$ (not at macroscopic electric field $\vec{E}$):

$$\delta\rho^{\text{mic}}(x_i) = \sum_{p,\vec{N}} \left.\frac{\partial\rho(x_i)}{\partial R_{p,j}(\vec{N})}\right|_{\vec{D}=\text{const}} w_{p,j} \tag{44}$$

where

$$\left.\frac{\partial\rho(x_i)}{\partial R_{p,j}(\vec{N})}\right|_{\vec{D}=\text{const}} \equiv f^{(D)}_{p,j}(x_i - R_{p,i}(\vec{N})). \tag{45}$$

The analytical results by Hong and Vanderbilt can be presented in a form analogous to (43)

$$\mu^{\text{eld}}_{iljk} = \frac{1}{v}\sum_p (M^{(3,D)}_{p,jkil} + M^{(3,D)}_{p,jkli} - M^{(3,D)}_{p,jilk}) \tag{46}$$

where the octuple moments, $M^{(3,D)}_{p,jkil}$, of the charge density variation are calculated using $f^{(D)}_{p,j}(\vec{x})$ instead of $f_{p,j}(\vec{x})$. However, μ^{eld}_{iljk} does not directly give the electronic contribution to the flexoelectric tensor μ^{el}_{iljk}. In general, the relationship between these tensors should depend on the shape of the sample used in the calculations and on the electronic contribution to the dielectric permittivity $\varepsilon^{\text{el}}_{il}$. Such a relationship can be obtained from the flexoelectric equation

of state for the electronic contribution to the polarization

$$P_i = (\varepsilon_{il}^{\mathrm{el}} - \delta_{il}\varepsilon_0)E_l + \mu_{klij}^{\mathrm{el}}\frac{\partial u_{kl}}{\partial x_j} \tag{47}$$

where ε_0 is the dielectric constant of vacuum. For a simple open-circuit parallel-plate capacitor geometry where $\vec{E} = -\vec{P}/\varepsilon_0$, using (47) one finds

$$\mu_{iljk}^{\mathrm{el}} = \varepsilon_{js}^{\mathrm{el}}\mu_{ilsk}^{\mathrm{eld}}/\varepsilon_0. \tag{48}$$

Concerning the calculation of the flexoelectric response involving $f_{p,j}^{(D)}(\vec{x})$ one should mention that Martin's arguments ensuring that the moments of the function $f_{p,j}(\vec{x})$ are well defined are no longer applicable. Thus, the existence of well defined moments $M_{p,jkil}^{(n,D)}$ is not self-evident. Hong and Vanderbilt [46] applied their approach to calculations of the component μ_{11}^{eld} for a number of insulating crystals. We will address the results of these calculations in section 6.3.2.

While discussing the electronic contribution one should comment on its magnitude. Based on order-of-magnitude estimates one can expect, in analogy with Martin's conclusion concerning piezoelectricity, that, in 'normal' dielectrics, the electronic and ionic contributions are comparable. However, in materials with high dielectric constants (high-K materials), such as ferroelectrics, the situation is different. In such materials, the anomalously strong polarization response results from an anomalous sensitivity of some components of internal strains, specifically of those related to the ferroelectric soft mode. In terms of our treatments, this translates into anomalously high values of some components of $B_{p,j}^{skl}$ [21]. At the same time, the electronic contribution is not expected to be sensitive to the ferroelectric softness of the lattice. Thus, in high-K materials, which are of primary interest for applications, the flexoelectric response is expected to be dominated by the ionic contribution.

To summarize this subsection, we can state that the treatment of the polarization response to a strain gradient in terms of Martin's charge-density-response approach enables the identification of a contribution complementary to that associated purely with internal strains (ionic contribution). The additional (electronic) contribution is associated with the direct response of the electron density to the elastic deformation. This result is analogous to Martin's development for the piezoelectric response. Here, it is worth mentioning that the multiple expansion (with up to the octuple moments involved) can also be used for the description of the ionic contribution[4].

3.3. Dynamic flexoelectric effect

Now we will discuss the so-called *dynamic flexoelectric effect*. While the static bulk flexoelectric effect can be viewed as an analogue of the piezoelectric effect, the phenomenon treated below has no analogue in piezoelectricity. As was mentioned in section 3.2.2, the polarization wave following an elastic wave in solids (31) contains a contribution which is explicitly dependent on the wave frequency ω, being proportional to ω^2. Since in an acoustic wave $\omega^2 \propto q^2$ (q is the wavevector of the wave), the amplitude of this contribution is proportional to the strain gradient amplitude in the wave, thus providing an additional contribution to the flexoelectric response. This contribution is called the dynamic flexoelectric effect. In the time domain, it corresponds to the polarization response to accelerated motion of the medium. In the point-charge approximation, using equation (31), the relationship describing this response is:

$$P_i = \Lambda_{ij}\ddot{U}_j \tag{49}$$

with

$$\Lambda_{ij} = \frac{1}{v}\sum_p Q_p G_{p,i}^j. \tag{50}$$

One of the first discussions of the flexoelectric response by Harris [16] actually dealt with the dynamic flexoelectric effect. Microscopic and phenomenological theories of this effect were offered by Tagantsev [24].

On the microscopic side, the tensor $G_{p,i}^j$ can be calculated in terms of the lattice dynamic theory. It has been shown that the effect is controlled by the mass difference of the ions making up the crystal, so that in a hypothetical case where the masses of all the ions are the same then Λ_{ij} vanishes. For the case of a crystal with two ions per unit cell, Λ_{ij} can be cast in the form [24]

$$\Lambda_{ij} = \chi_{ij}\frac{m_2 - m_1}{2Q} \tag{51}$$

where m_1, m_2 are the masses of ions having charges Q and $-Q$, respectively; χ_{ij} is the ionic contribution to the dielectric susceptibility of the crystal.

On the phenomenological side, the dynamic flexoelectric effect can be taken into account by adding a mixed term to the density of kinetic energy [6]

$$T_{\mathrm{k}} = \frac{\varrho}{2}\dot{U}_i^2 + \frac{\gamma_{ij}}{2}\dot{P}_i\dot{P}_j + M_{ij}\dot{U}_i\dot{P}_j \tag{52}$$

where ϱ is the density and γ_{ij} is a phenomenological tensor controlling the dynamics of polarization. The dynamic constitutive equations fully incorporating the bulk flexoelectric response can be described by minimizing the action $\int\int(T - \Phi + u_i\sigma_i)\mathrm{d}V\mathrm{d}t$ (the integral being taken over the volume of the sample and time) with respect to $\vec{P}$ and $\vec{U}$. With Φ coming from equation (9) and T_{k} from (52), such a minimization yields:

$$E_i = \chi_{ij}^{-1}P_j - f_{klij}\frac{\partial u_{kl}}{\partial x_j} + M_{ij}\ddot{U}_j - g_{ijkl}\frac{\partial^2 P_i}{\partial x_j \partial x_l} + \gamma_{ij}\ddot{P}_j \tag{53}$$

$$\varrho\ddot{U}_i = c_{ijkl}\frac{\partial u_{kl}}{\partial x_j} + f_{ijkl}\frac{\partial^2 P_k}{\partial x_l \partial x_j} - M_{ji}\ddot{P}_j. \tag{54}$$

The last two rhs terms of equation (53) control the spatial and frequency dispersion of the polarization response.

[4] One can treat the displacements of all ions of the unit cell but one as conditioned upon the displacements of the latter. This way the charge response function to the displacement of this ion (like (32)) can be introduced. The further consideration is identical to equations (34)–(41), formally treating the displacements of the rest of the ions as the driving force for the variation of the charge density of the crystal.

However, when we consider macroscopic manifestations of the flexoelectric response (e.g. in a dynamically bent sample or in ultrasonic acoustic wave), where $1/q$ is much larger than the typical microscopic scales and ω is much smaller than the typical optical phonon frequencies, these terms can be neglected. Thus, setting $\vec{E} = 0$ in (53) we see that the $M_{ij}\ddot{U}_j$ term indeed provides a contribution to polarization corresponding to the dynamic flexoelectric effect given by equation (49) with

$$\Lambda_{ij} = \chi_{is} M_{sj}. \tag{55}$$

It is instructive to eliminate $\ddot{U}_i$ between equations (53) and (54) to find a relationship controlling the total flexoelectric response in the dynamic case

$$\begin{aligned} E_i = \chi_{ij}^{-1} P_j - \left(f_{klij} - \frac{1}{\varrho} M_{is} c_{sjkl} \right) \frac{\partial u_{kl}}{\partial x_j} \\ - \left(g_{ijkl} - \frac{1}{\varrho} M_{is} f_{sjkl} \right) \frac{\partial^2 P_k}{\partial x_l \partial x_j} \\ + \left(\gamma_{ij} - \frac{1}{\varrho} M_{is} M_{js} \right) \ddot{P}_j. \end{aligned} \tag{56}$$

From this equation we can see that in view of the dynamic flexoelectric effect, the role of the flexocoupling tensor f_{klij} is now played by the *total flexocoupling tensor*

$$f^{\text{tot}}_{klij} = f_{klij} - \frac{1}{\varrho} M_{is} c_{sjkl}. \tag{57}$$

Thus, in the dynamic case, the flexoelectric response is controlled by the 'total' flexoelectric tensor $\mu^{\text{tot}}_{klis} = \mu_{klis} + \mu^{\text{d}}_{klis}$, where the dynamic contribution is defined as

$$\mu^{\text{d}}_{klij} = -\frac{1}{\varrho} \chi_{in} M_{ns} c_{sjkl}. \tag{58}$$

Both the phenomenological and microscopic relationships, (58) and (51), suggest that, like the static contribution, the dynamic contribution should be enhanced in high-K materials. Order-of-magnitude estimates show (see section 6.1.1) that the components of tensors μ^{d}_{klij} and μ_{klij} are expected to be comparable.

A remarkable feature of the bulk flexoelectric effect is that, in an acoustic wave, the relation between the static and dynamic contributions is frequency independent. The dynamic contribution to the flexoelectric effect makes it qualitatively different from the piezoelectric effect. For the latter, the polarization and strain in a moving medium are linked by the same relations as in the static case, i.e. $P_i = \chi_{ij} E_j + e_{ijk} u_{jk}$.

One should mention that, despite the fact that the components of the tensors μ^{d}_{klij} and μ_{klij} are expected to be comparable, the dynamic flexoelectric effect does not always provide a contribution comparable to that of the static effect. In an acoustic wave, the dynamic effect works at full strength, however, in quasi-static experiments, i.e. where the smallest dimension of the sample is less than the acoustic wavelength corresponding to the frequency of the external perturbation, the dynamic effect is negligible. This feature of dynamic flexoelectricity can be readily shown with a treatment similar to that of the piezoelectric resonance in a finite sample. We do not present such a treatment here, but we elucidate the origin of this phenomenon. First, note that relationship (56) applied to the static case yields $\mu^{\text{tot}}_{klis} = \mu_{klis}$, as is clear from the fact that $\mu^{\text{d}}_{klij} \frac{\partial u_{kl}}{\partial x_j}$ depends linearly on[5] $c_{sjkl} \frac{\partial u_{kl}}{\partial x_j} = \frac{\partial \sigma_{sj}}{\partial x_j}$, which vanishes in view of the equation of static mechanical equilibrium $\frac{\partial \sigma_{sj}}{\partial x_j} = 0$. In the quasi-static case, the equation of static mechanical equilibrium is satisfied to a high accuracy, implying that $\mu^{\text{d}}_{klij} \frac{\partial u_{kl}}{\partial x_j}$ is negligible. In an acoustic wave, the system is far from the static mechanical equilibrium and the dynamic effect works at full strength.

4. Manifestations of bulk flexoelectric effect in crystal

4.1. Phonon dispersion

One of the direct manifestations of flexoelectric coupling is related to phonon spectra in solids. In terms of phonons, the flexoelectric interaction can be interpreted as a repulsion between transverse acoustic (TA) and soft-mode transverse optic (TO) branches. This effect was documented in perovskite ferroelectrics by Axe *et al*, who studied the dispersion of the phonons in $KTaO_3$ [22] and $PbTiO_3$ [82] by means of neutron scattering. The temperature dependence of the dispersion curves obtained for $KTaO_3$ is shown in figure 3. As is seen from the figure, with decreasing temperature the soft optical branch moves downward closer to the acoustic one and causes a bending of the latter. The temperature-driven acoustic phonon branch bending has also been observed in $SrTiO_3$ by Hehlen *et al* [38] by means of Brillouin scattering (which allows one to trace acoustic branches in the vicinity of the Γ-point). Axe and coworkers have discussed the branch bending effect in terms of lattice mechanics analysis [22]. In this subsection we rewrite such an analysis in terms of the continuum Landau theory, this way linking this effect with the flexoelectric coupling in the material.

Within the validity of the continuum model we consider the long-wavelength part of the spectrum. We start from equations (53) and (54), where we rewrite the strain in terms of acoustic displacement, $u_{kl} = \frac{1}{2}\left(\frac{\partial U_k}{\partial x_l} + \frac{\partial U_l}{\partial x_k} \right)$. To describe the phonons, we search for solutions for polarization and displacement in the form $P = \tilde{P} e^{i\omega t - i\vec{q}\vec{x}}$, $U = \tilde{U} e^{i\omega t - i\vec{q}\vec{x}}$. Since we are interested in the transverse modes, in which electric field does not arise, we omit the term related to electric field and obtain the following set of linear homogeneous equations:

$$\begin{aligned} \omega^2 \gamma_{ij} \tilde{P}_j = \chi_{ij}^{-1} \tilde{P}_j + q_j q_l g_{ijkl} \tilde{P}_k \\ + q_j q_l f_{ijkl} \tilde{U}_k - \omega^2 M_{ij} \tilde{U}_j \end{aligned} \tag{59}$$

$$\varrho \omega^2 \tilde{U}_i = q_j q_l c_{ijkl} \tilde{U}_k + q_j q_l f_{ijkl} \tilde{P}_k - M_{ji} \omega^2 \tilde{P}_j. \tag{60}$$

Eigenfrequencies of the system (corresponding to acoustic and optic branches) may be found from the condition of

[5] Here, to be rigorous, in view of the modified definition (11) of stress, we must put the sign $\approx$ instead of $=$. However, for the macroscopic strain gradients in question, the flexoelectric correction to the equation of static mechanical equilibrium is really small.

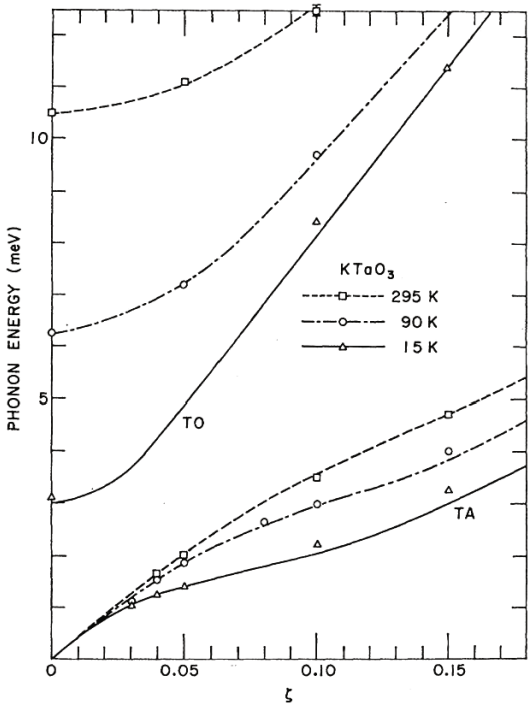

Figure 3. Temperature dependence of dispersion curves for transverse acoustic (TA) and soft-mode optic (TO) phonons with wavevector $q = a^*(\zeta, 0, 0)$ in $KTaO_3$, where a^* is the reciprocal lattice constant. Reprinted with permission from [22]. Copyright 1970 by the American Physical Society.

zero determinant of this set of equations. Let us illustrate the acoustic branch bending for the case of the cubic crystalline lattice symmetry and the q-vector directed along a four-fold axis, which corresponds to the conditions of the experiment by Axe *et al* (figure 3). In this case, the transverse modes are two-fold degenerate and not coupled with the longitudinal mode. The dispersion of the transverse modes may be readily derived from equations (59) and (60) by applying the zero determinant condition to get:

$$(\omega^2 - \omega_A^2)(\omega^2 - \omega_O^2) = \frac{(\omega^2 M - q^2 f_{44})^2}{\varrho\gamma}, \tag{61}$$

$$\omega_A^2 = \frac{c_{44} q^2}{\varrho}, \tag{62}$$

$$\omega_O^2 = \frac{\alpha + g_{44} q^2}{\gamma}, \tag{63}$$

where ω_A and ω_O are the TA and TO phonon frequencies in the absence of flexoelectric coupling. In view of the cubic symmetry of the tensors under consideration we used the expressions $M_{ij} = M\delta_{ij}$, $\gamma_{ij} = \gamma\delta_{ij}$ and $\chi_{ij}^{-1} = \alpha\delta_{ij}$ for their components.

The trend of the phonon branch repulsion can be identified by treating the case of weak interaction between the branches. In this case the relative shift of the acoustic branch may be calculated from equation (61) by setting $\omega = \omega_A$ everywhere except for the first parenthesis in the lhs to get:

$$\frac{\Delta\omega_A}{\omega_A} = -\frac{q^4 (f_{44}^{\text{tot}})^2}{2\varrho\gamma\omega_A^2(\omega_O^2 - \omega_A^2)}, \tag{64}$$

$$f_{44}^{\text{tot}} = f_{44} - \frac{1}{\varrho} M c_{44}. \tag{65}$$

The repulsive character of the interaction between the branches is seen from the sign in expression (64). As for its magnitude, it is controlled by the total flexoelectric coupling coefficient, (65), which has both dynamic and static contributions. This fact must be taken into account when extracting information about the flexocoupling tensor from scattering experiments. Formulas (64) and (65) work best in the vicinity of the Γ-point, where the mode coupling, being conditioned by high powers of the wavevector, is weak. Thus these formulas may be directly applied to evaluate the shift of the acoustic branch in Brillouin scattering experiments (e.g. those by Hehlen *et al* [38]). The difference of frequency squares in the denominator in the rhs of equation (64) indicates the amplification of the effect when the optical branch approaches the acoustic one (e.g. with decreasing temperature). The trend of the branch repulsion described above holds when interaction between them is strong. In the case of strong coupling, the contributions of static and dynamic flexoelectric effects to the acoustic branch bending become frequency-weighted, as controlled by expression (61). As noticed by Axe *et al* [22], if the strength of flexoelectric effect exceeds some threshold (once the acoustic branch touches the x-axis in figure 3), there will be a phase transition into an incommensurate phase; we discuss this situation in section 6.2.

4.2. Manifestations of flexoelectricity in domain walls

The flexoelectric effect plays an important role in ferroelectric domain walls (DWs), where large strain gradients arise because of a sharp change of the order parameter in the direction normal to the wall. To correctly describe the polarization and strain distributions in a domain wall, one has to take the flexoelectric coupling into account. In this section we consider such a description of the DW internal structure in the framework of Landau theory.

4.2.1. Polarization profile in domain walls. The problem of polarization and strain profiles in the DWs requires appending the thermodynamic potential Φ, coming from (9), with nonlinear contributions related to the fourth-order dielectric stiffness β_{ijkl} and electrostriction tensor q_{ijkl}.

$$\Phi_{\text{w}} = \Phi + \tfrac{1}{4}\beta_{ijkl} P_i P_j P_k P_l - q_{ijkl} u_{ij} P_k P_l. \tag{66}$$

The polarization and strain profiles in a DW may be found through minimization of the thermodynamic potential of the sample as a whole, $\int \Phi_{\text{w}}\, \mathrm{d}V$ (integrating over the volume of the sample) with boundary conditions corresponding to the two domain states, separated by the DW under consideration.

We illustrate the manifestation of the flexoelectric effect in ferroelectric domain walls for the case of a planar 180° DW in a perovskite crystal in the tetragonal phase. Following Yudin *et al* [63], consider an electrically neutral DW (parallel to the vector of spontaneous polarization in the domains),

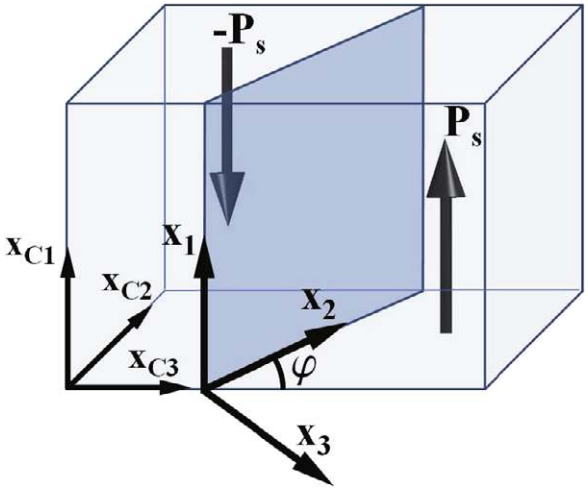

Figure 4. Neutral wall orientations in the tetragonal phase and the corresponding reference frame; φ is the dihedral angle between the wall plane and the (001) plane.

tilted at an angle φ with respect to the crystallographic axes figure 4. In the reference frame related to the domain wall, the problem can be treated as one-dimensional with polarization and strain depending only on the coordinate x_3 normal to the wall, and the boundary conditions:

$$\vec{P} = \pm\vec{P}_{\rm s}|_{x_3=\pm\infty}; \qquad u_{ij} = u^{\rm s}_{ij}|_{x_3=\pm\infty}, \quad i,j = 1,2,3 \tag{67}$$

where $\vec{P}_{\rm s}$ and $u^{\rm s}_{ij}$ are the spontaneous polarization and strain in the bulk. In such a treatment, the elastic variables may be eliminated using the conditions of mechanical compatibility and mechanical equilibrium [63, 70], which leads to equations controlling the polarization profile in the form [63]:

$$\alpha' P_1 + \beta'_1 P_1^3 + \beta'_2 P_1 P_2^2 - g_1 \frac{\partial^2 P_1}{\partial x_3^2} = f_{\rm a} \sin(4\varphi) A_1 P_1 \frac{\partial P_1}{\partial x_3} \tag{68}$$

$$\alpha'' P_2 + \beta''_1 P_2^3 + \beta'_2 P_2 P_1^2 - g_2 \frac{\partial^2 P_2}{\partial x_3^2} = f_{\rm a} \sin(4\varphi) \left(A_2 P_2 \frac{\partial P_2}{\partial x_3} + A_3 P_1 \frac{\partial P_1}{\partial x_3} \right). \tag{69}$$

Here all the terms conditioned by the flexoelectric coupling are in the rhs of equations (68) and (69); $f_{\rm a}$ is the anisotropic part of the flexocoupling tensor defined as

$$f_{\rm a} \equiv (2f_{44} - f_{11} + f_{12}). \tag{70}$$

The coefficients $\alpha', \beta'_1, \alpha'', \beta''_1, \beta'_2$ as well as A_1, A_2, A_3 may be represented in terms of β_{ijkl}, q_{ijkl} and c_{ijkl} tensor components and the wall tilt angle φ.

In the absence of the flexoelectric coupling (with $f_{\rm a}$ set to zero) equations (68) and (69) allow a solution with only one non-zero polarization component P_1. Such a solution is referred to as the Ising wall, its profile is shown in figure 5(a). When taken into account, the flexoelectric effect provokes the appearance of the additional polarization component P_2 in the wall. This is conditioned by the coupling term $f_{\rm a} \sin(4\varphi) A_3 P_1 \frac{\partial P_1}{\partial x_3}$ in equation (69), which does not vanish when $P_2 \to 0$, making the Ising solution impossible. This coupling leads to a structure of the domain wall with a polarization vector rotating in the opposite directions on the two sides of the wall, the so-call bichiral structure of the wall (figure 5(b)) [63]. Thus taking into account the flexoelectric coupling is of qualitative importance for the description of the internal structure of ferroelectric domain walls.

The mechanism by which the flexoelectric coupling leads to the appearance of the second polarization component may be elucidated as follows. The change of the 'main' P_1-component in the DW region creates a deformation gradient

$$\frac{{\rm d}u}{{\rm d}x_3} \propto \frac{\rm d}{{\rm d}x_3}(P_1^2 - P_{\rm s}^2) \tag{71}$$

via the electrostriction coupling. In turn, the deformation gradient creates the other polarization component $P_2 \propto \frac{{\rm d}u}{{\rm d}x_3}$ via the flexoelectric effect. In equation (69), this

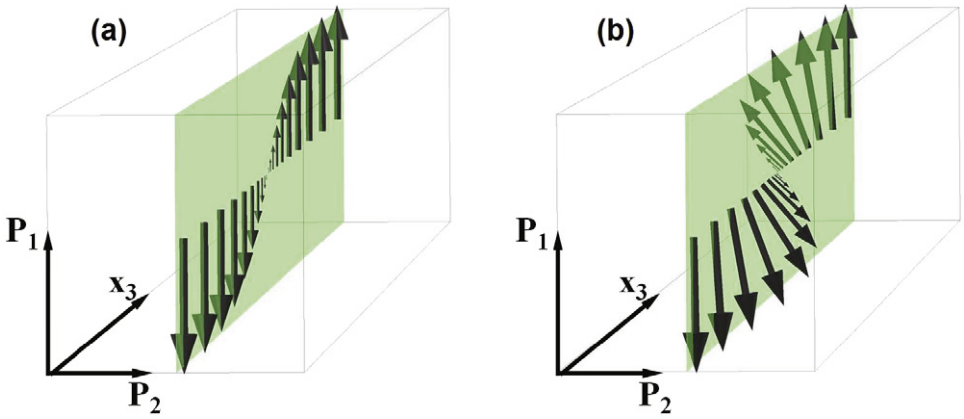

Figure 5. Schematic of the structures of the neutral 180° domain walls addressed. (a) The Ising-type structure occurring when the wall is normal to the cubic crystallographic directions or/and when the flexoelectric coupling is isotropic or neglected; (b) the bichiral structure occurring for the oblique orientation of the wall provided that the flexoelectric coupling is anisotropic. Reprinted with permission from [63]. Copyright 2012 by the American Physical Society.

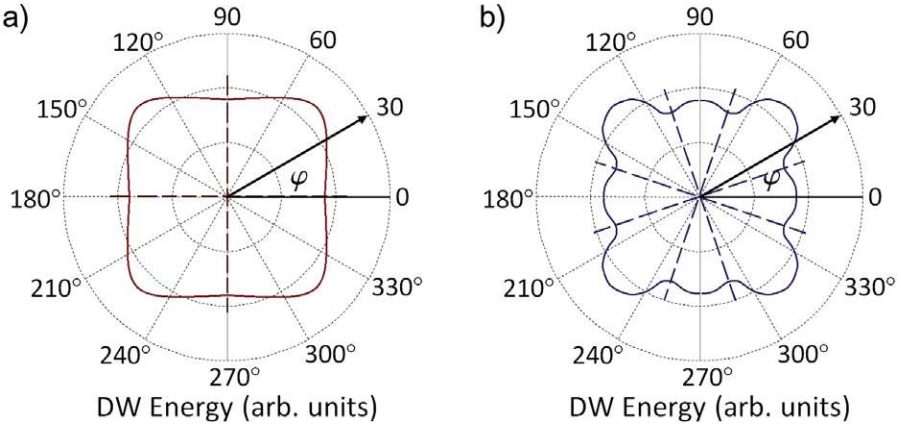

Figure 6. Schematic polar plots for the angular dependence of the domain wall energy. (a) Flexoelectric effect is neglected; (b) flexoelectric effect is taken into account. The schematic plot corresponds to the case where the flexoelectric coupling is strong enough, leading to splitting the energy minima; energetically preferred wall orientations are shown with dashed lines.

two-step interaction appears as a direct coupling between the polarization components, because the mechanical variables are eliminated. The magnitude of the P_2 component driven by the flexoelectric effect can be roughly estimated as [63]:

$$P_2 \approx \frac{\sqrt{g_1} f_a \sin(4\varphi) A_3 P_s^2}{g_2 \sqrt{-\alpha'}}. \tag{72}$$

Its value is expected to be comparable to the spontaneous polarization P_s. However, for typical perovskites the factor A_3 is small, which is linked with the smallness of q_{12} component of the electrostriction tensor, and as a result P_2 is one to two orders of magnitude smaller than P_s.

Another important aspect is the influence of the flexoelectric coupling on the intrinsic energy of ferroelectric domain walls. DW energy is defined as the energy excess of the state with the wall over the single domain state:

$$E_W = \int_{-\infty}^{\infty} \{\Phi_w(x_3) - \Phi_w(\infty)\}\, dx_3. \tag{73}$$

Of interest is the angular dependence of the DW energy, since its minima indicate preferable DW orientations. As known from the work by Dvorak *et al* [83], the DW energy $E_W^{(q)}$ in the absence of flexoelectric coupling (with f_a set to zero) is a periodic function of φ with a period of $\pi/2$, reaching minima at $\varphi = \frac{\pi n}{2}$ or $\varphi = \frac{\pi n}{2} + \frac{\pi}{4}$, $n = 0, 1, 2, 3$, depending on the sign of the anisotropic part of the stiffness tensor $c_{11} - c_{12} + 2c_{44}$. The angular dependence of $E_W^{(q)}$ is schematically shown in figure 6(a) for the case in which $\varphi = \frac{\pi n}{2}$ are the points of minima (such as in $BaTiO_3$).

Taking into account the flexoelectric coupling leads to a qualitatively different DW energy angular dependence. The flexoelectric effect does not affect the energy of the DWs with highly symmetric orientations $\varphi = \frac{\pi n}{4}$, $n = 0, 1, 2, 3$. For oblique wall orientations, the flexoelectric effect decreases the energy[6]. If the flexoelectric coupling is strong enough this flexoelectricity-related DW energy decrease will result in splitting of the energy minima, as shown in figure 6(b). The critical f_a-value needed for such splitting to occur is of the same order as existing estimates for the flexocoupling coefficient [15, 84]. Thus the flexoelectric coupling may control the orientation of energetically preferable domain boundaries in ferroelectrics.

Above we have discussed the appearance of the polarization component in-plane of the wall. In a similar way, as was first noticed by Eliseev *et al* [85], the flexoelectric interaction may lead to the appearance of a polarization component normal to the wall. Let us treat this effect, following Eliseev *et al* [85], for the case of the (100) wall orientation ($\varphi = 0$ in figure 4). The equations for the polarization component normal to the wall P_3 may be written in the form:

$$\tilde{\alpha} P_3 + \tilde{\beta}_1 P_3^3 + \tilde{\beta}_2 P_3 P_1^2 + \frac{\partial \phi}{\partial x_3} - g_3 \frac{\partial^2 P_3}{\partial x_3^2} = F_{12} A_n P_1 \frac{\partial P_1}{\partial x_3} \tag{74}$$

$$\frac{\partial \phi}{\partial x_3} \approx \frac{P_3}{\varepsilon_b} \tag{75}$$

where ϕ is electrostatic potential, ε_b is the background dielectric permittivity[7]; the coefficients $\tilde{\alpha}$, $\tilde{\beta}_1$, $\tilde{\beta}_2$ and A_n may be represented in terms of β_{ijkl}, q_{ijkl} and c_{ijkl} tensors [85]. In contrast to the in-plane polarization, which was shown to be controlled by the anisotropic part of the flexocoupling tensor, the normal polarization component is controlled by the factor $F_{12} \equiv \frac{c_{12} f_{11} - c_{11} f_{12}}{2c_{12}^2 - c_{11}^2 - c_{12} c_{11}}$. Because the P_3 component is x_3-dependent, charged layers arise in the wall with the bound charge density $\rho_b = -\mathrm{div} P$. Screening of these bound charges by free carriers may lead to an enhancement/decrease of the conductivity in the DW region; we will address this issue in the next subsection. When the screening is weak, an approximate relation for the electrostatic potential (75) may

[6] As it must be according to thermodynamics, because the flexoelectric effect introduces a new degree of freedom.

[7] Strictly speaking, here P represents not the full polarization, but only its ferroelectric part, see e.g. [86]

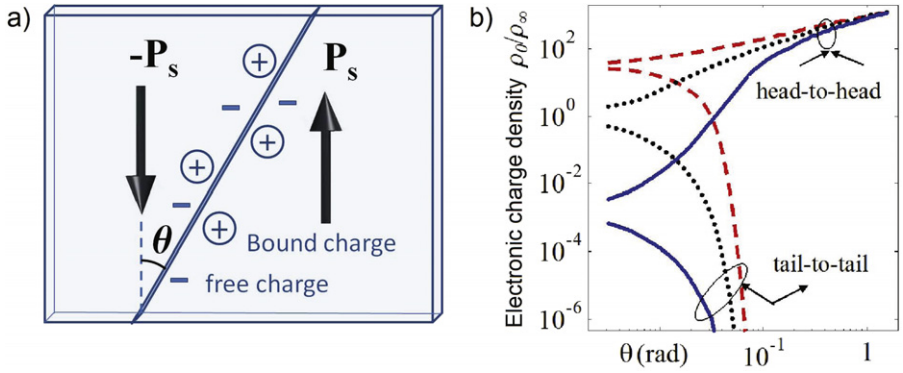

Figure 7. (a) Schematic of a charged domain wall. Bound charge due to the jump of polarization and free charge due to screening are shown. (b) Electronic concentration normalized to its bulk value plotted as a function of the wall tilt angle θ, calculated for negative, zero, and positive flexoelectric coupling coefficients $F_{12} = (-0.5, 0, 0.5) \times 10^{-10}$ m^3 C^{-1} (solid, dotted and dashed curves respectively). Material parameters of $PbZr_{0.2}Ti_{0.8}O_3$ at room temperature are used in calculations. Reprinted with permission from [85]. Copyright 2012 by the American Physical Society.

be used. In this case the magnitude of the P_3-component induced by the flexoelectric effect may be estimated as follows. From equation (68) with $\varphi = 0, P_2 = 0$ one finds $P_1 = P_s \tanh(\frac{x_3}{t_h})$, where $t_h = \sqrt{-\frac{2g_1}{\alpha'}}$ is the domain wall thickness. Then from equation (74), keeping only the fourth term in the lhs (in view of smallness of the background permittivity) and using relationship (75), one obtains:

$$P_3 \approx \frac{\varepsilon_b F_{12} A_n P_s^2}{t_h} \cdot \frac{\sinh(x_3/t_h)}{\cosh^3(x_3/t_h)}. \tag{76}$$

The magnitudes of the in-plane and out-of-plane terms, equations (76) and (72), can be compared by taking into account approximate relations: $F_{12}A_n \approx f_a A_3$, $t_h \approx \sqrt{-2g_2/\alpha'}$ and $\varepsilon_f \approx -2\alpha'^{-1}$, where ε_f is the ferroelectric part of the dielectric permittivity. From such a comparison one can see that P_3-component is smaller by a factor $\varepsilon_f/\varepsilon_b \gg 1$ than the P_2-component. This smallness is the consequence of the suppression of the normal polarization component by the depolarizing field, described, for example, in [70].

Above we have discussed the combined effect of electrostriction and flexoelectricity leading to the coupling between two different polarization components. In the case where the polarization is not the order parameter, coupling of the same type is possible between the polarization and other order parameters. For example, in $SrTiO_3$, the order parameter Ψ is related to rotations of the oxygen octahedra. It is involved in the so-called rotostriction coupling, corresponding to the $\Psi^2 u$ term in the thermodynamic potential. In view of this coupling, the order parameter gradient in the wall implies a strain gradient ($\frac{du}{dx_3} \propto \frac{d}{dx_3}(\Psi_1^2 - \Psi_s^2)$). The deformation gradient, in turn, creates the electric polarization ($P \propto \frac{du}{dx_3}$) via the flexoelectric effect. The appearance of electrical polarization in domain walls related to rotations of the oxygen octahedra outlined above has been recently theoretically addressed by Morozovska *et al* [61]. It was shown that, in $SrTiO_3$ below the antiferrodistortive phase transition, the electric polarization normal to the plane of the wall can attain a value of 0.1 μC cm^{-2}.

4.2.2. Conduction of domain walls. The question of conductivity of ferroelectric domain walls is customarily discussed in the context of the domain walls with a jump of the normal polarization component, the so-called charged DWs [86–88]. In contrast to neutral 180° DWs, charged 180° DWs are inclined with respect to the spontaneous polarization vector in the domains (figure 7(a)). The bound charge in the wall increases with increasing θ from 0 to $\pi/2$. The screening of the bound charge by free carriers makes conductivity in the wall region different from that in the bulk, and this effect may be appreciable. However, there exists an alternative mechanism leading to variation of the free charge density (conductivity) in domain walls, which is related to the flexoelectric coupling. This mechanism is conditioned by the flexoelectricity-induced, normal to the wall, component of the polarization discussed in the previous subsection. Below we address this mechanism, following Eliseev *et al* [85].

In general, to find the distribution of free and bound charges ρ_f and ρ_b in the DW region, equation (74) should be solved self-consistently with the Poisson equation $-\varepsilon_b \frac{d^2\phi}{dx_3^2} = \rho_b + \rho_f$. In the case under consideration, the screening is weak ($\rho_f \ll \rho_b$) [85], and an approximate expression for the electrostatic potential may be derived from (75) and (76) to get:

$$\phi \approx \tfrac{1}{2} F_{12} A_n P_s^2 (\tanh^2(x_3/t_h) - 1). \tag{77}$$

Expression (77) represents a potential well or hump, depending on the DW orientation (head-to-head or tail-to-tail) and the sign of the flexoelectric coefficient F_{12}. This potential well/hump causes local band bending and leads to a redistribution of free carriers. In the case of an n-type non-degenerate semiconductor, a simple expression may be obtained for the spatial distribution of the free charge density $\rho_f(x_3)$ in the DW region [89]:

$$\rho_f(x_3) = \rho_\infty \exp\left(\frac{e\phi(x_3)}{k_B T}\right) \tag{78}$$

where $k_B = 1.3807 \times 10^{-23}$ J K^{-1}, T is the absolute temperature, $e = 1.6 \times 10^{-19}$ C is the electron charge, and

ρ_∞ is the free charge concentration in the bulk. From (77) and (78) one obtains the following expression for the normalized variation of the free-carrier concentration in the DW:

$$\frac{\rho_0}{\rho_\infty} = \exp\left(\frac{eF_{12}A_nP_s^2}{2k_BT}\right) \tag{79}$$

where $\rho_0 = \rho_f(0)$ is the free charge density in the center of the DW. Numerical calculations based on equations (68), (74), (75) and (78) for the parameters of $PbZr_{0.2}Ti_{0.8}O_3$ with $F_{12} = -10^{-10}$ m^3 C^{-1} [85] yield the maximal value of P_3 about 0.02 C m^{-2}; the depth of the potential well is about 0.3 eV, giving one-order-of-magnitude variation of the free-carrier density in the wall. This implies that the flexoelectric coupling may lead to one-order-of-magnitude contrast of the conductivity in the wall.

The variation of conductivity related to flexoelectricity can also manifest itself in a charged domain wall, competing with the effect associated with the violation of its electroneutrality. This is illustrated in figure 7(b), where the normalized variation of the free-carrier concentration is plotted as a function of the tilt angle θ (after [85], for the material parameters of $PbZr_{0.2}Ti_{0.8}O_3$). Eliseev *et al* [90] have shown that the internal structure of ferroelectric DWs may be strongly correlated with current atomic force microscope (AFM) contrast, suggesting the use of current AFM for detecting phase transitions in DW structure.

4.2.3. Other manifestations. In this subsection we will discuss two more effects the flexoelectric coupling may induce in a domain wall. The first effect consists of the shear strain driven by the change of polarization; the second one consists of the narrowing of the domain wall. To illustrate these effects we use the example of a (001) 180° domain wall in the tetragonal phase of a perovskite ferroelectric (see figure 4 with $\varphi = 0$).

The first effect is a manifestation of the converse flexoelectric effect. For the geometry of the problem, the equation for the converse effect (11) may be written in the form:

$$\sigma_5 = c_{44}u_5 + f_{44}\frac{dP_1}{dx_3}. \tag{80}$$

For a mechanically free wall ($\sigma_5 = 0$), equation (80) implies a linear strain response to the polarization gradient:

$$\frac{\partial U_1}{\partial x_3} = u_5 = -\frac{f_{44}}{c_{44}}\frac{dP_1}{dx_3}, \tag{81}$$

where U_1 is the shear-induced mechanical displacement. The integration of equation (81) over x_3 leads to an offset of mechanical displacement U_1 between the two domains:

$$\delta U_1 = -2\frac{f_{44}}{c_{44}}P_s. \tag{82}$$

In other words, due to the flexoelectric effect one should expect a step on the surface of a crystal at the location of the domain wall, as schematically shown in figure 8. It is instructive to evaluate the magnitude of this effect. We will do this for a material with a high P_s. We take $P_s \cong 0.9$ C m^{-2}

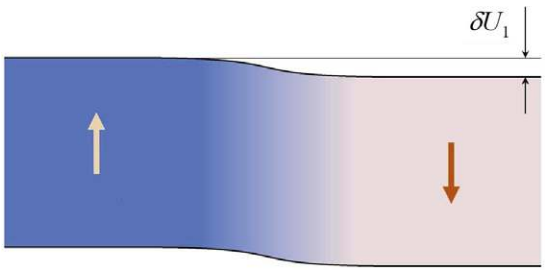

Figure 8. Deformation of the ferroelectric sample in the region of a 180° domain wall, driven by the converse flexoelectric effect. Spontaneous polarization in the two domains shown with arrows.

for $PbTiO_3$ at low temperatures and $c_{44} = 1.1 \times 10^{11}$ J m^{-3}. Following atomic estimates, the f-coefficients should be of the order of a few volts (see section 6.1). This leads us to an appreciable value of a few tenths of an ångström for the expected shift of the lattices between the two domains. This effect has been predicted by Meyer and Vanderbilt [91] using *ab initio* calculations, its value being in agreement with the above estimate.

The second effect, related to the domain wall thickness, is essentially a feedback, via the direct flexoelectric effect, from the inhomogeneous strain (81) to the polarization profile. To elucidate this effect we consider equation (10) at $E = 0$ appended with the fourth-order dielectric stiffness. To simplify the treatments we keep in this equation only the two relevant components of the polarization and strain (P_1 and u_5) to obtain:

$$\alpha P_1 + \beta_{11}P_1^3 - f_{44}\frac{\partial u_5}{\partial x_3} - g_{44}\frac{d^2P_1}{dx_3^2} = 0. \tag{83}$$

Here $\alpha = (T - T_0)/(C\varepsilon_0)$, where T is temperature, ε_0 is the dielectric permittivity of vacuum, and T_0 and C are Curie–Weiss temperature and constant respectively. Eliminating u_5 between (81) and (83) we arrive at the equation of state for the polarization P_1 in the domain wall:

$$\alpha P_1 + \beta_{11}P_1^3 - g_{44}^{\text{eff}}\frac{d^2P_1}{dx_3^2} = 0 \tag{84}$$

with a renormalized gradient term:

$$g_{44}^{\text{eff}} = g_{44} - \frac{f_{44}^2}{c_{44}}. \tag{85}$$

Equation (84) describes a domain wall with thickness $t_h = \sqrt{-2g_{44}^{\text{eff}}/\alpha}$. Thus, by renormalizing the gradient term, the flexoelectric coupling changes the thickness of the domain wall. From expression (85) one can see that the flexoelectric effect always leads to narrowing of the domain wall. The renormalized thickness of the DW as a function of the flexoelectric coupling reads:

$$\frac{t_h}{t_h^0} = \sqrt{1 - \frac{f_{44}^2}{g_{44}c_{44}}}, \tag{86}$$

where t_h^0 is the DW thickness with the flexoelectric effect neglected. According to the atomic estimates, the domain wall narrowing, given by expression (86), may be appreciable.

4.3. Internal bias and poling effect

An important feature of flexoelectricity is that it provides, in principle, a possibility of a mechanical-stimulus-driven reorientation of the spontaneous polarization between all allowed directions. In principle, the piezoelectric effect can also do this job, but only in a very limited class of ferroelectrics, exhibiting piezoelectricity in the paraelectric phase (such as Rochelle salt or KH_2PO_4). In such materials, the strain via the piezoelectric coupling makes the material polar already in the paraelectric phase. Due to this strain-induced polarity, different orientations of the spontaneous polarization in the ferroelectric phase become non-equivalent. This ensures a strain control of the spontaneous polarization in ferroelectrics with piezoelectricity in the paraelectric phase. However, most of ferroelectrics are not piezoelectric in the paraelectric phase. In this case, the electromechanics of the ferroelectric was traditionally considered to be solely governed by the electrostrictive coupling (the uP^2 term that can be taken into account in the Landau expansion (9)). This coupling, though leading to the spontaneous-polarization-induced piezoelectricity in the ferroelectric phase, cannot provide control on the sign of the spontaneous polarization. The electrostriction, in contrast to the piezoelectricity in the paraelectric phase, does not bring about a strain-induced polarity in the paraelectric phase, needed for the control of the sign of the spontaneous polarization. In such a situation, the role of the flexoelectricity becomes exclusive: it translates a mechanical stimulus (strain gradient) into the induced polarity of the paraelectric phase. As is clear from the constitutive equation (10), the strain gradient (due to the flexoelectricity) works as an electric field

$$E_i^{\text{flex}} = f_{klij}\frac{\partial u_{kl}}{\partial x_j}. \tag{87}$$

Here one can speak about *flexoelectric field* E_i^{flex}. We should stress that E_i^{flex} has nothing in common with the macroscopic electric field, since the flexoelectric effect is defined as a polarization response in the absence of an electric field. It is also worth mentioning that, in contrast to the real electric field, the introduction of a potential corresponding to the flexoelectric field cannot be consistently done since, in general, $\text{curl}\vec{E}^{\text{flex}} \neq 0$. Specifically, if one attempts to introduce such a potential by the integral relationship $\varphi(\vec{x}) = -\int_0^{\vec{x}} E_i^{\text{flex}}\, \text{d}y_i$ (as in [78]) the result will be dependent on the integration path.

In ferroelectrics, one can distinguish several situations where the flexoelectric field affects the properties of the material. First of all, if there exists a permanent average (built-in) strain gradient in the sample, the flexoelectric field leads to the *internal field* (internal bias) effect. The ferroelectric behaves as being placed in an additional dc electric field, exhibiting, for example, a switching asymmetry or a smearing of the dielectric anomaly at the ferroelectric phase transition. If the built-in flexoelectric field exceeds the coercive field of the ferroelectric, the latter can lose its bistability in the absence of an external electric field.

A specially important case of the internal field effect is the so-called *imprint* effect. In this case, the internal field appears as a result of keeping the ferroelectric for some time in a certain polarization state, while the direction of the appeared built-in field is parallel to that of the spontaneous polarization in this state. The flexoelectric field in combination with free-carrier transport can contribute to imprint.

Finally, an external strain gradient can be applied to the sample. Then, controlling the strain gradient one can, in principle, switch the polarization of the ferroelectric with a purely mechanical stimulus. Here, one can speak about *flexoelectric switching*.

The aforementioned manifestations of the flexoelectric field in ferroelectrics are addressed in sections 4.3.1–4.3.3.

The flexoelectric field may play a certain role not only in ferroelectrics. An amorphous system containing reorientable polar units can also 'feel' the flexoelectric field. This situation is addressed in section 4.3.4.

4.3.1. Internal field. The correlation between the existence of average strain gradients in ferroelectric thin films and their polarization response to an electric field was experimentally addressed by Catalan *et al* [67] and Lee *et al* [76]. The results of these experiments were interpreted in terms of an internal field effect associated with flexoelectricity.

Assuming an exponential strain decay (as a function of the distance from the substrate) in the investigated (Ba, Sr)TiO_3 thin films on a $SrRuO_3$ substrate, Catalan *et al* evaluated, based on their x-ray data, the dependence of average strain gradients in the films on the film thickness. The misfit strain between the film and the substrate was considered as the origin of the strain gradient. Using the strain gradient data obtained this way, the thickness dependence of the average flexoelectric field in the films was evaluated and the impact of this field on the dielectric anomaly at the transition was simulated. The results of the simulations were found in good qualitative agreement with the dielectric data obtained from the films.

Lee *et al* [76] investigated the strain state and ferroelectric properties of thin films of $HoMnO_3$ improper ferroelectric as conditioned by the processing conditions. The strain gradients in the films evaluated from the x-ray data were found to be in correlation with the oxygen partial pressure during the film deposition. It was suggested that the oxygen partial pressure controls the misfit strain between the films and the Al_2O_3 substrate, which in turn translates into the strain gradient in the films. Characterizing ferroelectric properties of the system, the field offset of the *PE* loops was monitored. A pronounced correlation between the field offset of the loops and the strain gradient in the film was reported. The effect was attributed to the action of the flexoelectric field caused by the strain gradient.

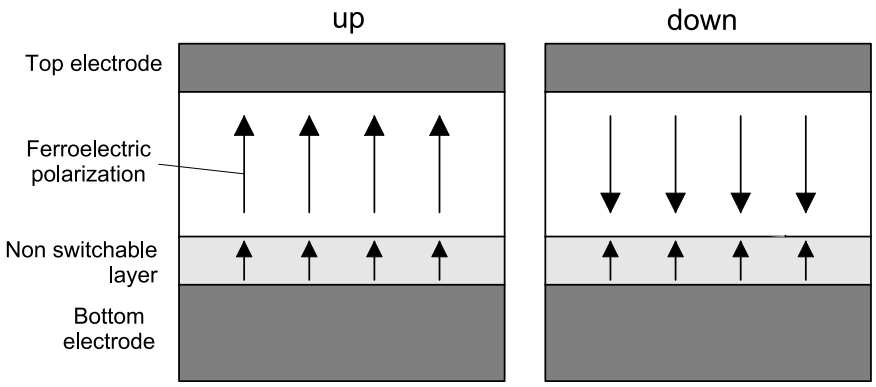

Figure 9. The model devised by Abe and coworkers [68, 69] for the voltage offset of ferroelectric loops caused by the poling effect of the strain gradient at the ferroelectric/electrode interface. In this model, the non-switchable layer cannot be switched at any applied field.

4.3.2. Imprint. The scenarios of the flexoelectricity-assisted internal field effect discussed in the previous subsection deal with a strain gradient which is basically distributed throughout the whole thickness of the film. Though one may conceive of such a situation, the simplest scenario for a dislocation-assisted stress release implies the formation of a narrow substrate-adjacent layer, where the strain gradient is mainly localized [92]. As was suggested by Abe *et al* [68, 69], such layers in ferroelectric thin films may serve as the origin of the imprint effect. A simple theory to this effect was offered by Tagantsev *et al* [70]. Let us discuss the main features of Abe's imprint model following [68, 70].

Consider a film with an in-plane bulk lattice constant a epitaxially deposited onto a substrate with an in-plane lattice constant a_s. We characterize the system with a misfit strain u_m:

$$u_m = \frac{a_s - a}{a}. \tag{88}$$

If the epitaxy is dislocation free, the film will acquire the in-plane lattice constant a_s. In this case, the film is stressed while no strain gradient occurs. The appearance of misfit dislocations relaxes the stress so that the film is less stressed; however, its main part is stressed virtually homogeneously [92]. The appearance of misfit dislocations also implies a strain gradient which is localized at the film/substrate interface. The value of strain gradient depends on the amount of the stress relaxation in the film. The largest strain gradient corresponds to full stress relaxation. Let us evaluate its value for the simplest situation where stress release is driven by edge dislocations which are formed in the ferroelectric at the film/substrate interface, having the in-plane Burgers vector equal a. To absorb the misfit strain, the distance between the dislocations laying at the interface should evidently be about

$$d_d = a/u_m. \tag{89}$$

The relaxation of the in-plane lattice constant of the film from a_s (at the substrate) to the bulk value a will take place on a distance of about d_d. Thus, the strain gradient will be mainly localized in the interface-adjacent layer of thickness d_d. The value of such a gradient can readily be evaluated as

$$\frac{\partial u_{11}}{\partial x_3} \approx \frac{u_m}{d_d} = u_m^2/a. \tag{90}$$

Here the OX_3 axis is set normal to the plane of the film.

Relationships (89) and (90) enable us to estimate possible values of the strain gradient in the substrate-adjacent layer and the thickness of this layer. Taking as typical values $u_m = 0.03$ and $a = 0.4$ nm, we find 10 nm for the thickness of this layer and 2×10^6 m^{-1} for the strain gradient in it. Such a value exceeds by many orders of magnitude typical exogenous strain gradients. If we use the classical order-of-magnitude estimate, ~10 V, for the components of the flexocoupling tensor f_{klij} (see section 6.1.1) we find an appreciable flexoelectric field ~200 kV cm^{-1}. We should recall that this is an estimate for the flexoelectric field, corresponding to full stress relaxation in the body of the film. Often the stress relaxation, which is controlled by the film thickness [93] and kinetics of the dislocation formation, is not full. Then both the strain gradient and the flexoelectric field in the surface layer become smaller.

Thus, we see that, according to the simplest scenario of dislocation-assisted stress release, a thin substrate-adjacent layer with an appreciable flexoelectric field may form in the ferroelectric films. According to Abe *et al* [68, 69], the flexoelectric field can make this layer non-switchable. A schematic of a ferroelectric capacitor containing a ferroelectric film where such a non-switchable layer is formed is shown in figure 9. It is clear from this figure that the bound charge ($\rho_b = -\mathrm{div}\vec{P}$) at the border between the non-switchable layer and the bulk of the film depends on the direction of the ferroelectric polarization in the film. For example, in the 'down' case, the bound charge is positive and larger than in the 'up' case (figure 9). The depolarizing field induced by this free charge can be appreciable. The imprint effect occurs due to the redistribution of free carriers while screening this field. When the capacitor is in a poled state for a time sufficient for an essential redistribution of the free carriers, the bound charge will be to a certain degree screened by the latter. The screening free charge is expected to be immobile during the switching characterization of the capacitor (e.g. during taking a $P - E$ hysteresis loop). Then,

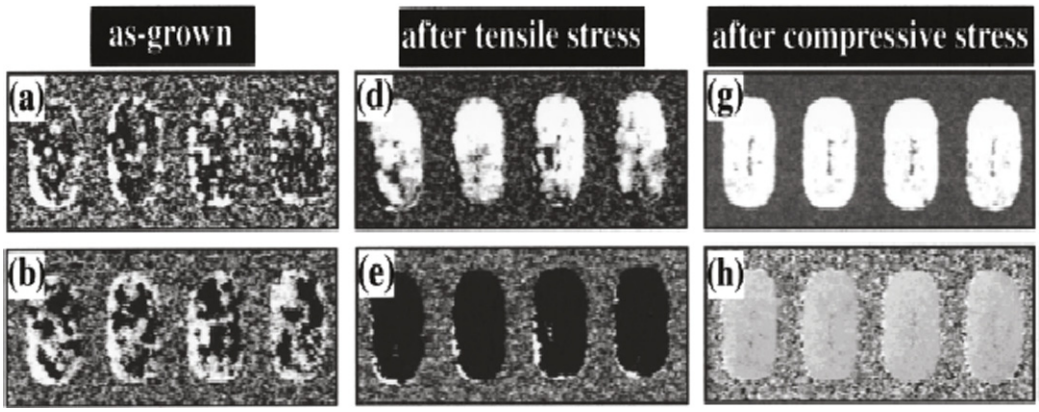

Figure 10. Piezoelectric force microscope (PFM) images illustrating the impact of substrate bending on the polarization and switching behavior of (111)-oriented PZT capacitors (ovals in the images). Before substrate bending: PFM amplitude (a) and phase (b) images of an as-grown capacitor. Up bending: PFM amplitude (d) and phase (e) images of the same capacitor. Down bending: PFM amplitude (g) and phase (h) images of the same capacitor. Reprinted with permission from [77]. Copyright 2003 AIP Publishing LLC.

the electric field of this immobile charge will make more energetically favorable the state of polarization in which the free charge redistribution took place, i.e. the imprint effect occurs. Experimentally, this effect can be seen as a field offset of the $P-E$ hysteresis loop, which is sensitive to the prehistory of the capacitor[8].

4.3.3. Flexoelectric switching and poling. The flexoelectric field makes the energies of polarization states of a ferroelectric non-equal and, thus, it can be used as a tool for the ferroelectric switching monitored by an elastic stimulus. Already in 1969, Bursian and coworkers [20] demonstrated the possibility of such switching in few-micron-thick plates of $BaTiO_3$. Specifically, it was shown that the bending of such a plate can result in the reversal of the sign of its pyroelectric coefficient. In 2003, Gruverman *et al* [77] demonstrated that the polarization state of a thin-film ferroelectric $Pb(Zr, Ti)O_3$ (PZT) capacitor on a Si substrate can be reversed by bending the structure. These authors reported a change of the sign of the piezoelectric force microscope (PFM) signal correlated with sign of the substrate curvature (figure 10). Thus, the polarization state of the films was found to correlate with the sign of both the strain and the strain gradient in the films. Because, in PZT, as a ferroelectric with a centrosymmetric paraelectric phase, the stress itself is not expected to cause any polarization reversal, the effect was attributed to a manifestation of flexoelectricity. A puzzling feature of this scenario is that the flexoelectric field evaluated by the authors based on the order-of-magnitude estimates for components of the bulk flexocoupling tensor, $\sim$10 V, (see section 6.1.1) is many orders of magnitude smaller than typical values of the coercive fields in the material. Remarkably, the same relation between the expected values of the induced flexoelectric field and the coercive field of the material holds for the experiments by Bursian and coworkers [20]. All these findings attest to a quite limited understanding of the mechanisms of flexoelectric switching.

[8] It is such behavior of the *PE*-hysteresis loops of ferroelectric (memory) capacitors, that was originally termed as imprint. In the current literature often any field offset of the $P-E$ hysteresis loops is erroneously called imprint.

Recently, flexoelectric switching on the nanoscale was experimentally addressed by Lu *et al* [78]. These authors used the inhomogeneous deformation caused by pushing with the tip of an atomic force microscope in order to switch the polarization of an ultrathin $BaTiO_3$ film. According to the author's estimates the flexoelectric field generated in this experiment is comparable to the coercive field of $BaTiO_3$.

4.3.4. Plastic flexoelectricity. In this subsection we address a kind of a strain-gradient-driven poling effect which is very different from those discussed above. Recently, Lubomirsky and coworkers [75, 94–96] presented experimental data on perovskite thin films, which strongly suggest that a strain gradient can pole an amorphous material when it is thermally treated in a special way. It was shown that during such treatment the material is passing between two different amorphous states. The initial state is centrosymmetric while the final state, which was called quasi-amorphous, is polar. Numerous examples of such a phenomenon were documented. It was shown that sputtered thin films of a number of perovskites ($BaTiO_3$, $SrTiO_3$, and $BaZrO_3$) can be prepared in the polar quasi-amorphous state, in which they exhibit appreciable pyro- and piezoelectric effects while revealing no traces of crystallinity. The originally deposited amorphous films can be turned either into the crystalline or quasi-amorphous polar states depending on the method of thermal treatment. Standard annealing leads to the crystalline material, while dragging the as-deposited film though a narrow furnace may yield the quasi-amorphous films. The authors ascribe the formation of the polar material to the effect of the strain gradients associated with the narrow furnace; it was demonstrated that an alternative poling scenario related to the electrode-film work-function difference can be excluded [96].

The following microscopic scenario for this effect was offered. It was suggested that, already in the amorphous state, perovskite films contain polar units corresponding to distorted oxygen octahedra with the B-cite atoms inside. When leaving the narrow furnace, due to a strain gradient these polar units are partially aligned, resulting in a poled quasi-amorphous state. An essential element of this scenario is the relation

between the type of the thermal treatment and type of the final state (crystalline or quasi-amorphous) of the material. A discussion of this issue goes beyond the scope of this paper and we refer the reader to the original publication [75].

The poling effect in question can be formally classified as flexoelectric. However, the mechanism offered by Lubomirsky and coworkers is qualitatively different from the microscopic mechanisms presented in section 3.2. These microscopic mechanisms deal with the displacements of bound charge on distances much smaller than the typical interatomic distances. In contrast, the mechanism of formation of the polar quasi-amorphous state, in general, is based on ionic displacements comparable with these distances [97]. Thus, one may trace an analogy between, on the one hand, elastic and plastic deformations of solids and, on the other hand, the bulk static flexoelectric effect in crystals and the poling effect in the amorphous materials in question. In each pair of the effects, one effect is associated with small atomic displacements, which are much smaller than the typical interatomic distances, whereas the other is associated with much larger displacements. In this context, we can term the poling effect in amorphous materials as *plastic flexoelectricity*. It is also clear that the estimates derived for the bulk static flexoelectric coefficient can by no means be applied to this effect. By analogy with the situation with elastic and plastic deformations, one may expect the plastic flexoelectricity to be much stronger than its 'regular' counterpart.

4.3.5. Electromechanics of moderate conductors. One of the important manifestations of flexoelectricity is in the electromechanical response of moderate conductors (where the macroscopic electric field is not necessarily screened by free carriers), e.g. in materials such as those used in solid-state electrochemical devices, including batteries, fuel cells, and electroresistive and memristive electronics. This issue was recently addressed by Morozovska *et al* [74]. These authors showed that in non-piezoelectric materials of this kind, the flexoelectricity can be important in this context.

Let us illustrate, following [74], this manifestation of flexoelectricity in the case of a thin-film parallel-plate leaky capacitor on a thick substrate containing a non-piezoelectric material. For simplicity, the material is considered to be elastically and dielectrically isotropic. In such a configuration, only one component of strain u_{33} and of electric field E_3 are involved (the OX_3 axis is normal to the plane of the films). We are interested in the displacement of the top electrode caused by the charge transport (linear response). This phenomenon is controlled by a number of factors, such as the deformation potential [98, 99], Vegard expansion [100], and the converse flexoelectric effect. The contribution of the latter can be described using the constitutive equation for the converse flexoelectric effect, taken in the form (14):

$$\sigma_{33} = \mu_{33}\frac{\partial E_3}{\partial x_3} + c_{33}u_{33} \tag{91}$$

and the Poisson equation

$$\varepsilon_{33}\frac{\partial E_3}{\partial x_3} = \rho \tag{92}$$

where ρ is the free charge density. In view of the 1D character of the problem all variables are treated as functions of only one coordinate x_3. For a film which is out-of-plane mechanically free ($\sigma_{33} = 0$), eliminating the field gradient between (91) and (92) yields a relationship between the strain and charge density:

$$u_{33} = -\rho\frac{\mu_{33}}{\varepsilon_{33}c_{33}}. \tag{93}$$

This equation enables us to link the change of the thickness of the system, $\delta h = \int_0^h u_{33}\,\mathrm{d}x_3$ (h is its original thickness), with the charge $\delta Q = \int_0^h \rho\,\mathrm{d}x_3$ entering per unit area of the system. Integrating (91) over the thickness h we find

$$\delta h = -\frac{\mu_{33}}{\varepsilon_{33}c_{33}}\delta Q. \tag{94}$$

This equation suggests that the electromechanical expansion (or contraction) of the system is controlled by the amount of free charge entering the system and the ratio of the flexocoupling coefficient to the elastic constant. In the considered geometry, the deformation potential [98, 99] and Vegard expansion [100] also lead to a contribution to δh linear in Q. However, according to the estimates by Morozovska *et al* [74] the flexoelectric contribution, in general, is expected to be appreciable, while, in particular, in perovskites such as $BaTiO_3$, $SrTiO_3$, and $Pb(Zr, Ti)TiO_3$ it is dominant.

5. Flexoelectric response in finite samples

In the previous sections we have discussed the bulk contribution to the flexoelectric response. It has been shown that the static bulk flexoelectric effect manifests itself identically in the cases of the total polarization response of a finite sample and locally in an acoustic wave. The situation is similar to the case of the piezoelectric response. At the same time, it has been demonstrated that the flexoelectric response in an acoustic wave is not fully described by the static bulk flexoelectric effect on the account of the dynamic flexoelectric effect (see section 3.3). This feature of flexoelectricity has no analogue in piezoelectricity. In this section we address in detail other features of this phenomenon that have no analogues in piezoelectricity. All these features manifest themselves once the polarization response of a finite sample as whole to a homogeneous strain gradient is considered. In the following subsections, we will be dealing with quite unusual effects. They are essentially conditioned by the surface of the sample, but nonetheless, their relative magnitudes are independent of the surface-to-volume ratio.

5.1. Flexoelectric bending

As was mentioned in section 3.1, the electromechanical constitutive equations describing the bulk flexoelectric effect[9]

$$E_i = \chi_{ij}^{-1}P_j - f_{klij}\frac{\partial u_{kl}}{\partial x_j} \tag{95}$$

$$\sigma_{ij} = c_{ijkl}u_{kl} + f_{ijkl}\frac{\partial P_k}{\partial x_l} \tag{96}$$

[9] In (95) the polarization-gradient term is dropped as being of minor importance for the problem addressed in this subsection.

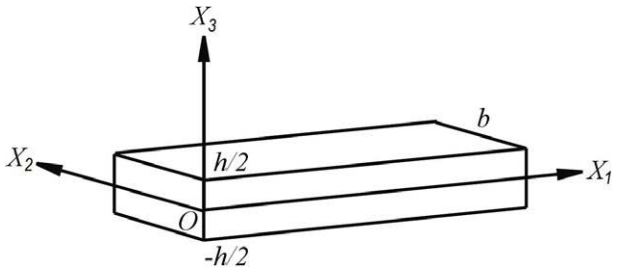

Figure 11. A thin plate of material exposed to bending and the reference frame used in calculations. The upper and lower faces of the plate are electroded.

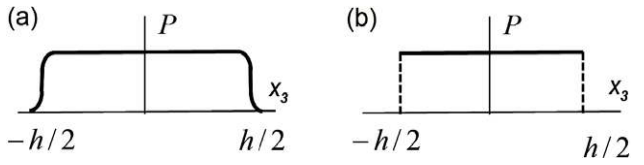

Figure 12. Polarization profiles in the plate: (a) blocking boundary conditions, (b) free boundary conditions.

suggest a certain asymmetry between the direct and converse flexoelectric responses. Namely, in the absence of an electric field, a strain gradient induces a homogeneous polarization while a homogeneous polarization has no mechanical yield. A practical situation where such asymmetry might reveal itself is bending experiments with a thin electroded plate of a centrosymmetric material (figure 11). For instance, a cylindrical bending of such a plate about the OX_2 axis will bring about non-zero strain gradients $\partial u_{11}/\partial x_3$ and $\partial u_{33}/\partial x_3$. The direct flexoelectric response to such bending can be detected by measuring the induced variation of the charge on the short-circuited electrodes. Such a response is described by equation (95), where $E = 0$ (in view of the short-circuit condition) while P_3 is directly linked with the charge. Meanwhile, one might conclude, based on equation (96), that the application of a voltage between the electrodes will not lead to any bending of the plate. Indeed, 'naturally' assuming that the voltage produces a *homogeneous polarization*, no mechanical yield is seen from equation (96).

Using similar reasoning, it was argued that a flexoelectric-based mechanical sensor, in contrast to piezoelectric-based devices, will not behave as an actuator [7, 56]. However, there are several reasons to question such a statement. First, this statement is in conflict with the results obtained by Bursian's group already in the 1960s. This group reported experimental data on electric-field-induced bending of plates of $BaTiO_3$ crystals [19]. Later, Bursian and coworkers provided a thermodynamic analysis [21], supporting their experimental findings. Second, the existence of a linear sensor-not-actuator is in a conflict with the general principles of thermodynamics, for instance, based on which one could construct a perpetual motion device [101].

Thus there appears to be a contradiction between the straightforward analysis of the constitutive equations and thermodynamics. Such an apparent contradiction was recently identified by Tagantsev and Yurkov [51] and a solution to it was outlined. The reason for this discrepancy is that the polarization-induced bending (*flexoelectric bending*) predicted by Bursian and Trunov [21] is a non-local effect that can only be obtained by considering the thermodynamics of a finite-size sample. Meanwhile, the application of the 'local' electromechanical equation (96) to the bulk of the sample does not capture this effect. The resolution of this discrepancy required a comprehensive treatment of the converse flexoelectric response of a finite sample. The full treatment of this problem is presently available only for the case of the so-called blocking boundary conditions for polarization [51], while for the general case its solution is only outlined. These two cases are discussed in following subsections.

5.1.1. Blocking boundary conditions. The application of an external voltage to an electroded plate (figure 11) does not necessarily lead to a homogeneous distribution of the polarization throughout it. A certain polarization inhomogeneity is expected in microscopically thin electrode-adjacent layers. In the simplest thermodynamic model [102], such an inhomogeneity is controlled by the boundary condition $P + A\partial P/\partial x_3 = 0$ (A is the so-called extrapolation length) at the electrode–dielectric interface. The limiting cases for the polarization distribution are illustrated in figure 12: (a) corresponds to $A \to 0$ (the so-called blocking boundary condition) and (b) to $A \to \infty$, (the so-called free boundary condition). Finite values of the parameter A provides a variety of polarization distributions.

In the present subsection we will address the electromechanical bending-mode performance of a thin plate for the case of the blocking boundary conditions, i.e. assuming that the polarization changes continuously from its bulk value to zero at the surface of the sample (figure 12(a)).

Consider a plate of a non-piezoelectric material placed in an electric field normal to it (figure 11) resulting in the polarization profile schematically shown in figure 12(a). The plate is considered to be macroscopically thick, i.e. its thickness h is much larger than the spatial scale for the polarization variation at its surface. In the main part of the sample $\frac{\partial P_k}{\partial x_l} = 0$, so that, as clear from (96), the flexoelectricity provides no mechanical input. Meanwhile, at the plate surfaces $\frac{\partial P_3}{\partial x_3} \neq 0$, implying, via equation (96), a certain mechanical yield [51, 52]. Let us show that this yield is a plate bending, accounting only for the cylindrical bending about the OX_2 axis. A straightforward way to do this is to consider the equation of balance of the bending moment for the plate. Following the basics of the elasticity theory [103], to derive such an equation, we multiply (96) by x_3 and integrate the result across an X_2X_3 cross-section of the sample (figure 11). Finally we get (for simplicity, the Poisson ratio is neglected and only one component of the strain, u_{11}, and stress, σ_{11}, are taken into account):

$$b\int_{-h/2}^{h/2}\sigma_{11}x_3\,\mathrm{d}x_3 = bf_{13}\int_{-h/2}^{h/2}\frac{\partial P_3}{\partial x_3}x_3\,\mathrm{d}x_3 + bc_{11}\int_{-h/2}^{h/2}u_{11}x_3\,\mathrm{d}x_3 \qquad (97)$$

where b is the dimension of the sample in the OX_2 direction. At mechanical equilibrium, in any X_2X_3 cross-section of the sample, the lhs term of (97) must be equal to the mechanical moment of the external forces applied to the sample. Without the first rhs term, this equation describes the bending of the sample caused by this moment. To identify the role of this term, we first evaluate it using integration by parts:

$$\int_{-h/2}^{h/2} \frac{\partial P_3}{\partial x_3} x_3 \, \mathrm{d}x_3 = -\int_{-h/2}^{h/2} P_3 \, \mathrm{d}x_3 = -h\langle P_3 \rangle \qquad (98)$$

where $\langle P_3 \rangle$ is the averaged polarization induced by the electric field in the plate. Since the spatial scale of the polarization variation at the interface is much smaller than h, with a good accuracy $\langle P_3 \rangle \approx P$, where P is the polarization in the bulk. Thus, the equation for the moment balance can be rewritten as

$$M + f_{13} h P = c_{11} \int_{-h/2}^{h/2} u_{11} x_3 \, \mathrm{d}x_3 \qquad (99)$$

where M is the bending moment per unit length (in the OX_2 direction) of the plate. It follows from equation (99) that the application of a homogeneous electric field to the plate is equivalent (via the induced polarization and the flexoelectric coupling) to the application of an external bending moment (here we can speak about *flexoelectric bending moment*). Thus, a finite mechanically free ($M = 0$) sample placed in a homogeneous electric field will bend. Note, that though the flexoelectric bending moment is conditioned by a surface effect, it is proportional to the bulk value of the polarization induced by the applied field.

Thus, the above analysis does not support the judgment, stemming from the apparent asymmetry between equations (95) and (96), that a sensor based on the flexoelectric effect will not behave as an actuator [7]. Let us show next that, moreover, a bending-mode flexoelectric sensor once working as an actuator will, in fact, be characterized by the same effective piezoelectric constant. Following [51], we will show this to be the case of a thin circular plate bending in the symmetrical flexural mode. The plate is electroded and used as a sensor or an actuator. In the first case, a force F is normally applied to its center and the charge Q induced on the electrodes is collected; the response of the system is characterized by the factor $d^{\mathrm{sen}} = Q/F$. In the second case, a voltage V is applied between the electrodes and the displacement of the center of the plate ΔL is measured; now, the response of the system is characterized by the factor $d^{\mathrm{act}} = \Delta L/V$. Virtually the same factors are customarily used for the characterization of a piezoelectric actuator/sensor[10]. For the piezoelectric device,

$$d^{\mathrm{sen}} = d^{\mathrm{act}} \qquad (100)$$

with d^{act} being equal to the d_{33} piezoelectric coefficient of the material. The goal of our treatment is to show that (100) holds for the flexoelectric actuator/sensor in question. Following Tagantsev and Yurkov, a (001) plate of a cubic material with the polarization P normal to the plate and homogeneous in its bulk is treated. In the case of symmetric bending, the curvature of the plate in all cross-sections normal to it, G, is the same. The treatment is based on the free energy density defined as $\tilde{\Phi} = \Phi + P_i E_i + u_{ij}\sigma_{ij}$, with the $\frac{g_{ijkl}}{2} \frac{\partial P_i}{\partial x_j} \frac{\partial P_k}{\partial x_l}$ term neglected, where Φ comes from (9). One also uses a result of the theory of thin plates [104] for the components of the strain tensor expressed in terms of the curvature G:

$$u_{11} = u_{22} = zG; \qquad u_{33} = -2x_3 \frac{c_{12}}{c_{11}} G; \qquad u_{12} = u_{23} = u_{13} = 0. \qquad (101)$$

(A Cartesian reference frame with the OX_3 axis normal to the plane of the plate is used.) Integrating $\tilde{\Phi}$, with the strain coming from (101), over the plate thickness, one finds the free energy density per unit area of the plate, Ψ_{b}, as a function of the polarization in the bulk of the plate, P, (see figure 12(a)) and G:

$$\Psi_{\mathrm{b}} = \frac{\chi_{33}^{-1}}{2} h P^2 + \frac{D_{\mathrm{s}}}{2} G^2 - 2hPG\tilde{f} \qquad (102)$$

$$D_{\mathrm{s}} = \frac{h^3}{6} \frac{c_{11}^2 + c_{11}c_{12} - 2c_{12}^2}{c_{11}} \qquad (103)$$

$$\tilde{f} = f_{13} - \frac{c_{12}}{c_{11}} f_{11} \qquad (104)$$

where D_{s} is a coefficient controlling the flexural rigidity of the plate for this kind of bending. A similar expression for the free energy of flexoelectric plate in the cylindrical bending mode was offered by Bursian and Trunov [21], based on purely symmetry arguments. One should note that these authors claim that they are dealing with a free energy density homogeneous over the sample. In reality, their free energy density has the meaning of the total free energy of the sample divided by its volume, which actually incorporates the surface-related effects.

For the short-circuit conditions, the minimization condition $\frac{\partial \Psi_{\mathrm{b}}}{\partial P} = 0$ leads to the equation for the direct flexoelectric effect for the plate in the symmetric flexural mode:

$$P = 2\mu_{\mathrm{pl}} G \qquad (105)$$

with

$$\mu_{\mathrm{pl}} = \chi_{33}\tilde{f}, \qquad (106)$$

which plays a role of an effective flexoelectric coefficient of the plate.

For the mechanically free plate, the minimization condition $\frac{\partial \Psi_{\mathrm{b}}}{\partial G} = 0$ leads to the equation describing the converse flexoelectric response of the plate (flexoelectric bending):

$$G = \frac{2h}{D_{\mathrm{s}}} \mu_{\mathrm{pl}} E. \qquad (107)$$

In obtaining this equation, it has been taken into account that, with a good accuracy in the plate, $P = \chi_{33}E$. The flexural

[10] Here we mean a simple device based on the longitudinal piezoelectric effect, e.g. a parallel-plate capacitor homogeneously mechanically loaded. For such a device, the relationships $d^{\mathrm{sen}} = Q/F$ and $d^{\mathrm{act}} = \Delta L/V$ can be used with ΔL standing for the voltage-induced variation of the thickness of the plate and F for the total force applied to it.

response, given by equation (107), is compatible with the result obtained by Eliseev *et al* [52] for the case of the blocking boundary conditions, when calculating the bending of a ferroelectric plate caused by the electrode-adjacent gradient of the spontaneous polarization.

Equations (105) and (107) enable a description of the sensor and actuator modes of a device based on the plate. Using the relationship between the cross-section curvature, G, and the maximal deflection, $\xi_{\max}$, for symmetric bending of a circular plate:

$$\xi_{\max} = \frac{GR^2}{2} \tag{108}$$

where R is the radius of the plate and G is given by (107), one readily finds that the both modes are controlled by the same effective piezoelectric coefficient

$$d^{\text{eff}} = d^{\text{act}} = d^{\text{sen}} = \frac{\mu_{\text{pl}} R^2}{D_{\text{s}}}. \tag{109}$$

5.1.2. General case. One can readily check that the derivation of the previous subsection is extremely sensitive to the behavior of the polarization in the microscopically thin electrode-adjacent layers. The effect is the most spectacular for the case of the free boundary conditions for polarization, corresponding to the polarization profile shown in figure 12(b). The system evidently exhibits the direct flexoelectric response. Meanwhile, for such a polarization profile, the polarization gradient is zero throughout the sample, implying (via equation (97)) no mechanical effect caused by the voltage applied to the system[11]. Thus, we arrive at a severe apparent contradiction between the conclusion just drawn above from local constitutive equations and the thermodynamics of the sample as a whole. Specifically, the former states that, for the case of the free boundary conditions, the global converse flexoelectric response of the sample vanishes while the direct response is expected. Meanwhile, the thermodynamics of the sample as a whole [21] says that such a situation is impossible.

Tagantsev and Yurkov [51] have suggested the following resolution to this contradiction. The point is that incorporating the flexoelectric coupling into the free energy density of a material leads to a modification of the boundary conditions for the bulk constitutive equations. Eliseev *et al* [52] have derived *modified boundary conditions for the polarization*, while postulating that the *classical mechanical boundary conditions* are not affected by such an incorporation. Meanwhile, generally, the mechanical boundary conditions should be modified as well [23, 53]. The modified mechanical boundary conditions were recently derived by Yurkov [53][12]. It has been shown that such a modification is not needed for the case where the polarization vanishes at the surface. This justifies the above treatment done for this case based on the classical mechanical boundary conditions. For the general case, where the polarization at the surface is not necessarily zero, the problem of the flexoelectric bending should be revisited with the modified mechanical boundary conditions which contain the surface value of the polarization. It is expected that such a treatment will yield results consistent with the thermodynamics of a finite sample: the direct flexoelectric effect implies flexoelectric bending and the effective piezoelectric coefficients characterizing the performance of a flexoelectric elements in the sensor and actuator modes are equal. However, it seems that this treatment is a mathematically challenging task which is not currently accomplished.

5.2. Surface piezoelectricity

In a finite sample, there always exist surface conditioned contributions to any effect. The size of such contributions is typically small, being controlled by the surface/volume ratio. However, there may exist a situation where the surface contribution of a strong effect can compete with the bulk contribution of another, weaker effect. This situation takes place when one is interested in the flexoelectric response of a finite sample of a non-piezoelectric material. As was mentioned in section 3.2.1, the symmetry-breaking effect of the sample surface results in the formation of surface-adjacent layers which are effectively piezoelectric. It occurs that the surface piezoelectricity can contribute appreciably to the flexoelectric response of a finite sample. This contribution has three unexpected features: (i) it is independent of the surface/volume ratio, (ii) in high-K materials, it scales as the bulk dielectric constant, (iii) its size is expected to be at least comparable to that of the bulk flexoelectric effect. We will illustrate these features in terms of a very simple model for the bending flexoelectricity in a finite sample, basically following Tagantsev and Yurkov [51]. We present a plate of nominally non-piezoelectric material as consisting of three parts: the inner part made of an 'ideally homogeneous' non-piezoelectric and two thin surface piezoelectric layers (figure 13). The thickness of each piezoelectric layer, λ, is considered to be much smaller than that of the inner part, h. Let us evaluate the polarization response to a bending of the plate, neglecting the bulk flexoelectric effect to see manifestations of the surface piezoelectricity clearer. The piezoelectric coefficients of the layers on the opposite sides of the plate should be of the opposite signs (as controlled by the orientation of the surface normal); the same is valid for the strains caused by the bending in these layers. For this reason, the induced polarizations in these layers are of the same sign. The polarization in the layer is proportional to the strain, which, in turn, is proportional to the product of the strain gradient and h. Meanwhile, when calculating the resulting change of the average polarization of the whole system one divides the bending-induced dipole moment of the sample by h. As a result, the polarization response of the system turns out to be proportional to the strain gradient

[11] Such a conclusion is compatible with a result by Eliseev *et al* [52], who argued that the electrode-adjacent variation of the spontaneous polarization causes a bending of a ferroelectric plate depending on the boundary condition for the polarization.

[12] Modified mechanical boundary conditions, very different for those obtained by Yurkov [53], were also given in [23], however without any derivation.

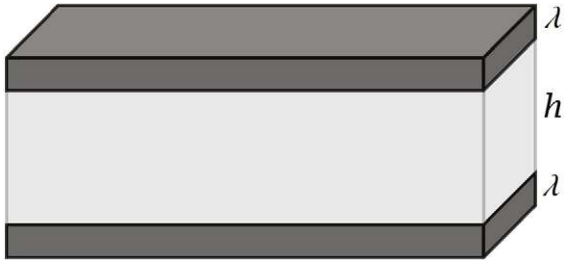

Figure 13. Model for the contribution of surface piezoelectricity to the flexoelectric response of a non-piezoelectric material. The surface layers of thickness λ model the surface-adjacent (atomically thin) layers of the material where the piezoelectricity is induced by the symmetry-breaking impact of the surface.

but independent of the plate thickness [6]. Here, we see that the surface piezoelectricity imitates the flexoelectric response, with a contribution independent of the surface/volume ratio, cf feature (i) from the list above.

The above consideration explains the surface-piezo electricity-induced flexoelectric response in the bending mode, however a similar scenario can be developed for the case where the driving force is a longitudinal strain gradient, arising, for example, once a truncated pyramid is loaded [7].

To elucidate feature (ii), let us quantify the above discussion. We characterize the top layer using the piezoelectric modulus $e_{311} \equiv e$, whereas, for the bottom layer we have $e_{311} = -e$. We also ascribe to these layers the out-of-plane component of the dielectric constant equal to ε_λ. For simplicity, we neglect the Poisson ratio so that the plate bending will result in the appearance of only one strain component, u_{11}, which can be expressed in terms of the strain gradient $\frac{\partial u_{11}}{\partial x_3}$. Thus, in the top layer $u_{11} = \frac{h}{2}\frac{\partial u_{11}}{\partial x_3}$ (to within $\lambda/h \ll 1$), while in the bottom layer $u_{11} = -\frac{h}{2}\frac{\partial u_{11}}{\partial x_3}$.

To find the bending flexoelectric response of the sample, we calculate the electrical displacement, D, induced by the strain gradient in a short-circuited capacitor containing the sandwich structure. This can be done using the electromechanical constitutive equation for the top layer appended with the standard electrostatic equations:

$$P_\lambda = \chi_\lambda E_\lambda + e\frac{h}{2}\frac{\partial u_{11}}{\partial x_3} \tag{110}$$

$$D = \varepsilon_f E_f = \varepsilon_0 E_\lambda + P_\lambda \tag{111}$$

$$2\lambda E_\lambda + hE_f = 0 \tag{112}$$

where E_λ and P_λ are the electric field and polarization in the layer; E_f, ε_f, ε_0 are the electric field in the bulk of the plate, its dielectric constant, and the dielectric constant of the free space, respectively. Note, that, in view of the short-circuit condition, the average macroscopic electric field in the plate $\langle E\rangle$ is zero, and thus D equals the average induced polarization in the plate $\langle P\rangle$. Solving this set of equations we find the relationship for the direct flexoelectric response:

$$\langle P\rangle = D = e\lambda\frac{h\varepsilon_f}{2\lambda\varepsilon_f + h\varepsilon_\lambda}\frac{\partial u_{11}}{\partial x_3} \tag{113}$$

where $\varepsilon_\lambda = \varepsilon_0 + \chi_\lambda$. For thin enough surface layers ($\lambda \ll h\varepsilon_\lambda/\varepsilon_f$), equation (113) yields the effective flexoelectric coefficient associated with the surface piezoelectricity:

$$\mu_{13}^{\text{eff}} = e\lambda\frac{\varepsilon_f}{\varepsilon_\lambda}. \tag{114}$$

Let us apply this relation to a high-K material (typically it is an incipient or a 'regular' ferroelectric in the paraelectric phase). In such a material, there is no reason for ε_λ to be high, since the special interplay of the atomic forces responsible for the high value of the bulk permittivity in ferroelectrics will be inevitably destroyed in the surface layer. Thus we see that the contribution of the surface piezoelectricity to the flexoelectric response of the plate of a high-K material should scale as its bulk dielectric permittivity, cf feature (ii) from the list above.

It is instructive to explain how the surface-driven contribution can scale as the bulk dielectric constant of the sample. Once the polarization is induced in a surface layer it results in an electric field in the bulk of the sample (due to the short-circuit electrical condition) which is parallel to the direction of the polarization. The magnitude of this field scales as ε_f. If the layer is thin enough, the polarization induced by this field in the bulk of the sample mainly controls its polarization response. That is why this response scales as ε_f.

As for the size of the effect (feature (iii) from the list above), in section 6.1.3, it will be shown that the value of μ_{13}^{eff} predicted by equation (114) can readily be comparable to the expected values of bulk flexoelectric coefficients.

The above treatment has shown how the surface piezoelectricity can contribute to the direct flexoelectric response of a finite sample in the bending mode. Meanwhile, as was shown by Tagantsev and Yurkov [51], the converse flexoelectric response of a finite sample (flexoelectric bending) driven by surface piezoelectricity also takes place, with the size controlled by the same effective flexoelectric coefficient, in direct analogy with equations (105) and (107).

5.3. Surface flexoelectricity

In this subsection we will discuss one more contribution to the polarization response of a finite sample to a homogeneous strain gradient, the so-called *surface flexoelectric effect*. Similar to the just discussed surface-piezoelectricity-driven flexoelectric response, this effect is essentially controlled by the surface of the sample, being at the same time independent of its surface-to-volume ratio. However, in contrast to the surface-piezoelectricity-driven effect, the surface flexoelectric effect is not expected to be enhanced in high-K materials. For this reason, it is of minor interest from the applied point of view. Nevertheless, we devote this subsection to the surface flexoelectric effect in view of its conceptual importance.

In section 3.2.3, it has been shown that, for the *bulk flexoelectric effect*, the external strains control the purely electronic contribution while the ionic contribution is fully conditioned by the internal strains. However, there exists a ionic contribution to the total polarization of a deformed sample associated with external strains. This contribution has been put aside in section 3.2.1 and now we address it closely to identify the surface flexoelectric effect. This effect is a delicate phenomenon. This notion was introduced by

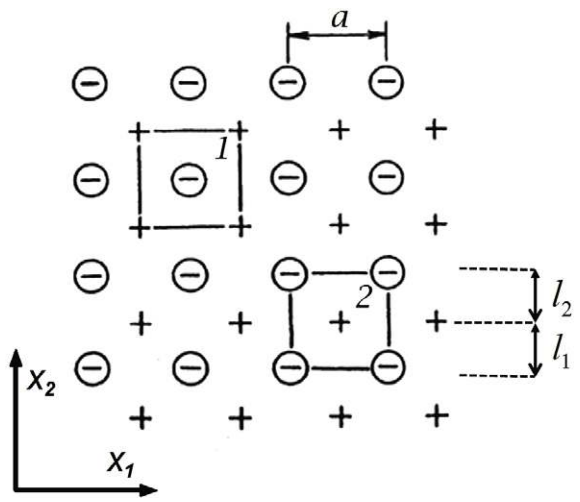

Figure 14. 2D 'ionic' structure. The signs '+' and '−' indicate the position of positive ('Q') and negative ('$-Q$') charges. '1' and '2' mark two types of unit cells.

Tagantsev [25] and currently no other theoretical treatments of it exist. Recently Resta [48] mentioned that there exist arguments which suggest the absence of this effect. In the following paragraphs we outline the treatment by Tagantsev in terms of the point-charge approximation.

Let us first illustrate, using a simple model, the existence of an appreciable surface-controlled contribution to the flexoelectric response of a finite sample. Consider a 2D 'crystal' made of point charges shown in figure 14. Let us examine its polarization response to a homogeneous strain gradient $\partial u_{22}/\partial x_2$ in the external strain approximation, i.e. only the external strains are taken into account. According to the results of section 3.2.1, the system will not exhibit any bulk flexoelectric response. Nevertheless, let us try to derive the total flexoelectric response of the system by calculating the strain-gradient-induced dipole moment per unit cell. For the cell marked with '1', the induced dipole moment is evidently controlled by the difference between the distances l_2 and l_1 (figure 14). In the external strain approximation, one readily finds

$$l_2 - l_1 = \frac{a^2}{4}\frac{\partial u_{22}}{\partial x_2} \tag{115}$$

leading to the induced dipole moment per volume of the cell:

$$P^{(1)} = \frac{Q}{v}\frac{a^2}{8}\frac{\partial u_{22}}{\partial x_2} \tag{116}$$

where Q is the charge of the positive ions and v is the volume of the unit cell with the lattice constant a. However, similar calculations for cell '2', for the induced dipole moment per unit volume yield:

$$P^{(2)} = -\frac{Q}{v}\frac{a^2}{8}\frac{\partial u_{22}}{\partial x_2}. \tag{117}$$

Results (116) and (117) are in a sharp *qualitative* conflict: equation (116) suggests the polarization is parallel to the gradient while (117) implies that it is antiparallel. To resolve this apparent paradox, we must realize that we are dealing with a surface effect. Indeed, if the sample were terminated in a way that it can be fully built of the cells '1', equation (116) would describe the response of the sample as a whole. Meanwhile, if the sample were terminated in a way that it can be fully built of the cells '2', then equation (117) is applicable. Remarkably, for normal dielectrics (not high-K materials), the effective flexoelectric coefficient corresponding to (116) and (117) is of the order of the expected values of the bulk flexoelectric coefficients (see section 6.1.1). The above model consideration suggests that there may exist an ionic contribution, coming from external strains, which is appreciable and controlled by the surface of the sample. The polarization response discussed above is tightly related to the surface flexoelectric effect, but a more involved treatment is needed to introduce this effect properly, as given below.

Consider a body deformed according to the unsymmetrized strain

$$\frac{\partial U_i}{\partial x_j} = \Upsilon_{ij} + \frac{\partial^2 U_i}{\partial x_j \partial x_l} x_l \tag{118}$$

where $\frac{\partial^2 U_i}{\partial x_j \partial x_l}$ is the homogeneous strain gradient in the body and Υ_{ij} is the mean strain; the origin is set at the center of gravity of the body. The body is presented as a set of point charges. According to (16), the external strain of the nth charge of this body reads

$$w^{\text{ext}}_{n,i} = \Upsilon_{ij} R_{n,j} + \frac{1}{2}\frac{\partial^2 U_i}{\partial x_j \partial x_l} R_{n,j} R_{n,l} \tag{119}$$

where $R_{n,j}$ is a vector linking the origin and the location of the nth charge. Using relationship (15) for the variation of the average dipole-moment density of a body under the deformation and taking into account that the relative change of its volume equals the trace of the tensor Υ_{ij}, one finds the external-strain-driven variation of the average polarization of the body as

$$\delta P^{\text{ext}}_i = \Upsilon_{ij} P^0_j - \Upsilon_{jj} P^0_i + Q^0_{jl}\frac{\partial^2 U_i}{\partial x_j \partial x_l} + I\frac{\partial^2 U_i}{\partial x_j \partial x_j} \tag{120}$$

with

$$P^0_j = \frac{1}{V}\sum_n Q_n R_{n,j}, \tag{121}$$

$$Q^0_{ij} = Q_{ij} - \frac{\delta_{ij}}{3}\text{Tr}(Q_{ij}), \tag{122}$$

$$I = \tfrac{1}{3}\text{Tr}(Q_{ij}), \tag{123}$$

$$Q_{ij} = \frac{1}{2\,\text{V}}\sum_n Q_n R_{n,i} R_{n,j} \tag{124}$$

where the sums are taken over all charges of the body of volume V (before the deformation).

The introduced entities have the following meanings: P^0_j is the average dipole-moment density of the body; Q^0_{ij} is the average quadruple moment density, calculated according to the standard definition, subtracting away the trace of the

matrix [105]; Q_{ij} is the average quadruple moment density, calculated without subtracting the trace; I is the average density of the trace of Q_{ij}. With regards to a real sample, these factors should be calculated by taking all charges of the system into account, including free charges on the surface and in the electrode (in the case of an electroded sample). One can readily check that all these factors, in general, are strongly dependent on the structure and composition of the surface of the sample and on the presence of the aforementioned free charges. In principle, one can consider these terms as interface-controlled contributions to the piezoelectric and flexoelectric response. For example, the terms $\Upsilon_{ij}P^0_j - \Upsilon_{jj}P^0_i$ were considered in the piezoelectric response by Born and Huang [80] and Martin [47], but these authors did not realize that these terms are surface-controlled.

An alternative approach to the external-strain-driven polarization response given by equation (120) has been offered by Tagantsev [25]. Following the definitions of the piezoelectric and flexoelectric tensors, (2) and (3), the condition of vanishing macroscopic electric field ($\vec{E} = 0$) during the application of any mechanical stimulus was employed for the interpretation of this response. Such an approach is adequate with regard to the conventional experimental method measuring the piezoelectric or flexoelectric response in a finite sample. In this method, an electroded sample is short-circuited (before and during the application of the mechanical stimulus) while the polarization response is evaluated by integrating the induced current. Thus, the condition $E = 0$ requires that all multiple moments of the system are zero (the system is assumed to be electroneutral on average), implying $P^0_j = 0$ and $Q^0_{ij} = 0$. The condition $P^0_j = 0$ (see equation (120)) ensures the absence of any surface-controlled contribution to the piezoelectricity. However, this condition does not require $I = 0$, since only the traceless part of the Q_{ij} tensor creates an electric field [105]. Thus, of all terms of equation (120), only the I-term can potentially contribute to the measurable flexoelectric response of a finite sample. Such a contribution is called the surface flexoelectric effect. Using (42) it can be rewritten as

$$\delta P^{\mathrm{SF}}_i = I\left(2\frac{\partial u_{ij}}{\partial x_j} - \frac{\partial u_{jj}}{\partial x_i}\right). \tag{125}$$

At this point we stop our discussion of this effect, referring the reader for more details to [6], and make the following remarks. First, similarly to the electronic contribution, this effect is controlled directly by external strains and should not be sensitive to the ferroelectric softness of the lattice. Thus it should not be enhanced in high-K materials. As a result, the surface flexoelectric effect is expected to be of minor importance for practical applications. Second, Tagantsev's treatment of this effect presented above might be too simple for its adequate description. Thus, a more involved treatment is welcome, especially in view of the recent criticism by Resta [48].

6. Size and features of the flexoelectric response

The very first discussions of the experimental data on the flexoelectric response in solids [5, 6, 23] revealed a disparity between these data and available theoretical estimates. The measured values of the flexoelectric coefficients were often found to exceed these estimates by a few orders of magnitude. More recent experimental studies (e.g. [7, 27–29, 41, 42, 77]) have confirmed this trend. Thus, a natural question arise: Do the theory and the experiment deal with the same effect? In this context, the information provided by both the theory and experiment on the size and typical features of the flexoelectric effect are of primarily interest. Below we address this issue from different sides. Order-of-magnitude estimates for the flexoelectric and flexocoupling coefficients are discussed in section 6.1. In section 6.2 we present some inequalities limiting the possible values of these coefficients. The results of microscopic calculations of the flexoelectric and flexocoupling coefficients are overviewed in section 6.3. Finally, in section 6.4, we overview experimental results on the flexoelectric effect and discuss them in the context of the available theoretical knowledge.

6.1. Order-of-magnitude estimates

6.1.1. Static bulk flexoelectricity. An order-of-magnitude estimate for the components of the flexoelectric tensor, controlling the bulk static flexoelectricity, was first offered by Kogan [15]. He gave an estimate for the flexoelectric tensor, μ_{klij}, which is valid only for materials with moderate values of the dielectric constant, underestimating the μ_{klij} of high-K materials. However, if, normalizing this tensor to the dielectric constant, one passes from μ_{klij} to the flexocoupling tensor, f_{klij}, then the estimate for f_{klij} will be valid for all materials, including high-K materials. Let us obtain such an estimate in the spirit of the work by Kogan.

Consider a simple lattice of point charges q with interatomic spacing a. Let this lattice be distorted by an 'atomic scale' strain gradient of the order of $1/a$ and with an 'atomic scale' polarization of the order of $(ea)/a^3$. Such a strong perturbation is expected to modify the energy density in the material, which is of the order of $\simeq \frac{q^2}{4\pi\epsilon_0 a}\frac{1}{a^3}$, by an amount comparable to itself. Assigning this energy change to the flexoelectric term $fP\frac{\partial u}{\partial x}$ in the free energy expansion (9) yields a rough order-of-magnitude estimate for the flexocoupling coefficient

$$f \simeq q/(4\pi\varepsilon_0 a) \sim 1\text{–}10\ \mathrm{V}, \tag{126}$$

using the electronic charge for q and a of the order of an ångström. Note that the accuracy of such a kind of 'atomic' estimate is one to two orders of magnitude.

6.1.2. Dynamic flexoelectricity. The first attempt to evaluate the size of the dynamic flexoelectric effect was made by Harris [16] for ionic crystals such as CsCl and NaCl. In a simple diatomic 1D model he obtained an estimate for the total flexoelectric coefficients

$$\mu \simeq \frac{q}{8a}\frac{m_1 - m_2}{m_1 + m_2} \tag{127}$$

where m_1 and m_2 are the masses of the ions. Some remarks are to be made concerning this estimate. First, it suggests

that Harris considers the dynamic effect as the only origin of the flexoelectric response. Second, as is clear from the text of [16], this estimate was done taking into account only the external strains, so that it has nothing in common with the bulk flexoelectric effect (see section 5.3). Third, the factor $\frac{m_1-m_2}{m_1+m_2}$ was added to this estimate without any justification. All in all, there are no grounds for this estimate, though it coincides with the true one for low-dielectric-constant materials, given below.

Let us evaluate the dynamic contribution to the total flexocoupling tensor using the phenomenological relationship

$$f^{\text{tot}}_{klij} = f_{klij} - \frac{1}{\varrho} M_{is} c_{sjkl} \tag{128}$$

for this tensor obtained in section 3.3 and a relationship for M_{is} valid for diatomic ionic crystals, which follows from (55) and (51)

$$M_{ij} = \delta_{ij} \frac{m_2 - m_1}{2Q} \tag{129}$$

where m_1, m_2 are the masses of ions having charges Q and $-Q$, respectively. Taking the components of the elastic constants of the order of the energy density in solids $\simeq \frac{q^2}{4\pi\epsilon_0 a} \frac{1}{a^3}$ and using the estimates $(m_2 - m_1)/\rho \simeq a^3$ and $Q \simeq q$, we find for the dynamic contribution to f^{tot}_{klij}

$$\frac{1}{\varrho} M_{is} c_{sjkl} \simeq q/(4\pi\varepsilon_0 a) \sim 1\text{–}10 \text{ V}. \tag{130}$$

Thus, we conclude that, in general, the magnitudes of the static and dynamic contributions to the flexoelectric response are expected to be comparable, with a reservation for the quasi-static situation (see section 3.3).

6.1.3. Surface-related contributions. There exist two surface-related contributions to the flexoelectric response of a finite sample: one due to the surface piezoelectricity (section 5.2) and the other due to the surface flexoelectricity (section 5.3).

Let us first evaluate the contribution of the surface piezoelectricity in high-K materials, using the result of the model consideration for the effective flexoelectric coefficient

$$\mu^{\text{eff}}_{13} = \lambda e \frac{\varepsilon_{\text{f}}}{\varepsilon_\lambda}, \tag{131}$$

obtained in section 5.2. It corresponds to the effective bending flexocoupling coefficient

$$f^{\text{eff}} = \frac{\mu^{\text{eff}}_{13}}{\varepsilon_{\text{f}}} = \frac{\lambda e}{\varepsilon_\lambda}. \tag{132}$$

For a conservative lower-bound estimate, we consider the surface layer to be atomically thin ($\lambda = 0.4$ nm). Then, using $e = 1$ C m^{-2} and $\varepsilon_\lambda/\varepsilon_0 = 10$, we find $f^{\text{eff}} \simeq 4$ V. This value is close to the typical value of the components of the flexocoupling tensor $f_{ijkl} \sim 1$–10 V (see section 6.1.1). Thus, we see that the surface piezoelectricity can readily compete with bulk flexoelectricity. Though the above estimate is obtained for the bending geometry, one can readily expect its validity also for the case of the longitudinal strain gradient (e.g. once a truncated pyramid is loaded).

Note that the permittivity does not enter estimate (132), suggesting that it has a 'universal' character and that it also applies to materials with moderate values of the dielectric constant.

The contribution of the surface flexoelectricity can be evaluated based on (125). Setting $I \cong q/a$ we find $f = I/\chi \cong q/(a\chi)$. For materials with moderate values of the dielectric constant, this estimate corresponds to Kogan's estimate (126), implying that in such a material the contribution of the surface flexoelectricity can be tangible. Meanwhile, this estimate suggests that in high-K materials this contribution is of minor importance.

6.2. Upper bounds for the static bulk flexocoupling coefficients

Bounds for flexoelectric coefficients in a ferroelectric can be obtained from the analysis of the parameters of its phonon spectrum. It was shown in section 4.1 that the flexoelectric effect leads to a bending of the acoustic phonon branch (see figure 3). The acoustic branch may reach the level $\omega = 0$ at some critical wavevector $q_c \neq 0$. This will happen if the flexoelectric coupling strength exceeds some threshold. The existence of the critical wavevector $q_c \neq 0$ will mean that the system becomes unstable with respect to a spatial modulation corresponding to this wavevector, and hence that the material undergoes a phase transition into an incommensurate phase. On the other hand, for materials without an incommensurate phase one can get constraints for its flexocoupling coefficients by requiring the absence of such critical wavevectors. Below, using equations (59) and (60), we derive such constraints on the flexocoupling coefficients for the case of cubic (in the paraelectric phase) ferroelectric perovskites.

To get the constraints for the flexocoupling coefficients, in general, one can require the absence of critical vectors of any direction. Being interested in the upper limits for the coefficients, let us require the absence of critical wavevectors only along highly symmetric axes of the crystal. In the materials addressed, such axes are the 4-fold, 3-fold and 2-fold axes. The requirement corresponding to each of these axes will produce a constraint.

The constraint corresponding to the 4-fold axis may be derived from equation (61). Suppose there exists a wavevector $q_c \neq 0$ with eigenfrequency $\omega = 0$. Then its magnitude must satisfy the following equation (obtained by setting $\omega = 0$ in equation (61)):

$$c_{44}\alpha + (c_{44}g_{44} - f^2_{44})q^2_c = 0. \tag{133}$$

Because the first term in equation (133) is positive, this equation will have no real solution if

$$f^2_{44} < c_{44}g_{44}, \tag{134}$$

which is the sought constraint. One readily checks that if $f^2_{44} > c_{44}g_{44}$ then a critical wavevector necessarily appears in the limit case $\alpha \to 0$.

Analogous constraints may be derived, for the wavevectors parallel to the 2-fold and 3-fold axes, by setting $q = \frac{1}{\sqrt{2}}(q_c, q_c, 0)$ and $q = \frac{1}{\sqrt{3}}(q_c, q_c, q_c)$ in equations (59) and (60). In the case of the 2-fold axis, there appear two pairs of coupled modes. The stability condition for the first one is identical to constraint (134), while the stability condition for the second one reads:

$$(f_{11} - f_{12})^2 < (c_{11} - c_{12})(g_{11} - g_{12}). \tag{135}$$

In the case of the wavevector directed along a 3-fold axis the normal modes are two-fold degenerate, and one obtains the following condition:

$$(f_{44} + f_{11} - f_{12})^2 < (c_{44} + c_{11} - c_{12})(g_{44} + g_{11} - g_{12}). \tag{136}$$

As one can check, inequality (136) follows from conditions (134) and (135) in view of the classic relationship $\frac{a+b}{2} \geq \sqrt{ab}$. Thus equations (134) and (135) form the sought set of constraints for the flexocoupling coefficients in perovskite ferroelectrics.

For the typical ferroelectrics the upper bounds for the flexocoupling coefficients given by (134) and (135) are of the order of a few volts. In particular for $BaTiO_3$[13]

$$|f_{44}| < 3.3 \text{ V}, \qquad |f_{11} - f_{12}| < 7 \text{ V} \tag{137}$$

and for $SrTiO_3$[14]

$$|f_{44}| < 2.4 \text{ V}, \qquad |f_{11} - f_{12}| < 10 \text{ V}. \tag{138}$$

Based on 'atomic' order-of-magnitude estimates for cs and gs analogous constraints can be obtained for other displacive ferroelectrics.

It is instructive to note that the above reasoning may be reformulated in terms of the ferroelectric domain wall energies. One may obtain the same upper bounds for the flexoelectric coupling coefficients by posing the requirement that a domain wall of any orientation must have positive energy. In particular, for the case of a domain wall with a normal parallel to a 4-fold axis of the perovskite crystal in the tetragonal phase, the upper bound identical to (134) may be obtained as follows.

We have shown in section 4.2.3 that, for this kind of wall, the flexoelectric coupling leads to renormalization of the gradient term

$$g_{44}^{\text{eff}} = g_{44} - \frac{f_{44}^2}{c_{44}}. \tag{139}$$

For the domain wall energy to be positive, this term must be positive as well, implying $g_{44}^{\text{eff}} > 0$, which is equivalent to (134).

Concerning the derivation of bounds (134)–(136) two remarks are to be made. First, only the lowest in q terms are used in the analysis. However, it gives a correct criterion for the instability (see the paper by Axe *et al* [22] for a more detailed analysis of the problem). Second, the constraints obtained are strict only for the case of second-order phase transitions, where in the case $\alpha \to +0$ material still stays in the paraelectric phase. However, equations (134)–(136) still give a reasonable approximation for the upper bounds of the flexoelectric coupling coefficients in a first-order phase transition (such as $BaTiO_3$) and incipient (such as $SrTiO_3$) ferroelectrics, where α approaches close to zero but does not reach it.

The upper bounds obtained are useful for the interpretation of experimental data on the flexocoupling coefficients. If the measured flexocoupling coefficients are essentially inconsistent with these constraints, this fact indicates that the explanation of the response characterized is beyond the static bulk flexoelectric effect.

6.3. Microscopic calculations of flexoelectric and flexocoupling coefficients

Among four contributions to the flexoelectric response, microscopic calculations were performed only for the static bulk flexoelectric effect. Below we will discuss the results of these calculations available in the literature for a number of materials. In section 6.3.1, we address the ionic contribution to the flexoelectricity in high-K materials (ferroelectrics), while section 6.3.2 is devoted to other relevant calculations.

6.3.1. Ionic contribution in perovskites. In ferroelectric perovskites, the ionic contribution dominates the static bulk flexoelectric response since it scales as the dielectric constant, which is enhanced in these materials. Several methods were used for the microscopic evaluation of this contribution.

Maranganti and Sharma [43] implemented an approach offered by Tagantsev [25] to calculate the flexoelectric tensor from the dynamic matrix of the crystal and the transverse Born ionic charges. These authors obtained the dynamic matrix by using a zero-kelvin density functional theory (DFT). The three independent components of the flexoelectric tensor, μ_{11}, μ_{12}, and μ_{44} were calculated (in nC m^{-1}): 0.15, −5.5, and −1.9 for $BaTiO_3$ and −0.26, −3.7, −3.6 for $SrTiO_3$, respectively. To compare the absolute values of the obtained coefficients with experimental data, one should pass from the μ_{klsj} tensor to the f_{klsj} tensor $\mu_{klij} = \chi_{is} f_{klsj}$. Then, in view of expectedly weak temperature dependence of f_{klsj}, one can use the results of a zero-kelvin theory. The values of the f_{klsj} tensor may also be compared with the order-of-magnitude estimates. However, such comparisons are hardly possible since the components of the zero-kelvin dielectric susceptibility in the DFT models used are not provided in this paper. Meanwhile, the signs of the tensor components and the relationships between them may be compared with the experimental data.

Another method to obtain the μ_{klij} tensor consists of direct calculations of the polarization response in an inhomogeneously deformed crystalline lattice. In view of the periodic boundary conditions typically required for first-principles calculations, consideration of a periodic distribution of the strain gradient (as the source of a 'static' wave of external strains) is a reasonable option. Then, once the transverse Born ionic charges are available, the amplitude of the polarization wave can be found. This approach was

[13] Calculated using parameters taken from [70].

[14] Calculated using parameters taken from [35, 79].

directly implemented by Hong *et al* [44] in their calculations for some ferroelectric perovskites. These authors introduce the static strain wave via fixing the positions of the A-site atoms (e.g. Ba in $BaTiO_3$) as a sinusoidal function of the distance, the direction of the atomic displacements and the modulation direction being parallel to a cubic crystallographic axis. Such conditions of the simulation imply conservation of the longitudinal component of the electrical displacement (the appearance of the depolarizing field) so that it should yield the μ^D_{11} component of the flexoelectric tensor defined at fixed electrical displacement

$$\mu^D_{klij} = \varepsilon_0(\delta_{is} - \varepsilon_0\varepsilon^{-1}_{is})f_{klsj} \tag{140}$$

where $\varepsilon_{is} = \varepsilon_0\delta_{is} + \chi_{is}$ is the permittivity tensor (cf the discussion concerning relationships (47) and (48)). In high-K materials, obviously, to within a good accuracy $\mu^D_{11} = \varepsilon_0 f_{11}$. The μ^D_{11} values obtained in [46] correspond to the values of f_{11} (in volts): -40 for $BaTiO_3$ and -150 for $SrTiO_3$. In view of Kogan's estimate (126) these values look too large. Since the values of f_{12} are not obtained in these calculations, we cannot check these results for compatibility with the stability conditions (137) and (138): $|f_{11} - f_{12}| < 7$ V for $BaTiO_3$ and $|f_{11} - f_{12}| < 10$ V for $SrTiO_3$. However, it is clear that, for such large values of f_{11}, these conditions can be readily violated unless in these materials the components f_{11} and f_{12} are by chance rather close in value.

A method based on a 'static' wave of external strains was also used by Ponomareva *et al* [45] for calculations of zero-kelvin values of the f_{klsj} tensor and finite-temperature values of the μ_{klij} tensor for the solid solution $Ba_{0.5}Sr_{0.5}TiO_3$. Here the effect was addressed by employing Monte Carlo simulations with an *ab initio*-calculated effective Hamiltonian; the contribution of the depolarizing energy was deliberately eliminated. These calculations confirmed the validity of the phenomenological relationship $\mu_{klij} = \chi_{is}f_{klsj}$. Three independent components of the flexocoupling tensor, f_{11}, f_{12}, and f_{44}, were obtained (in volts): 5.1, 3.3, and 0.045, respectively. These values agrees with Kogan's estimate and are consistent with the stability conditions (137) and (138) for the end members of the solid solution. A drawback of this work is that, in the *ab initio* calculations of the f_{klsj} tensor, the wavelength of the 'static' wave was only two lattice constants in size, implying that only the interaction between the local dipole and strain inside one unit cell was taken into account. Such an approximation can readily entail some 50% inaccuracy.

6.3.2. Other microscopic calculations. Using the technique employed for calculations of the flexoelectric coefficients for perovskite ferroelectrics, Maranganti and Sharma [43] addressed a number of cubic binary crystals (GaAs, GaP, ZnS, KCl, and NaCl). The dynamic matrices were calculated using the *ab initio* and shell lattice dynamics models. In all these materials, the flexoelectric coefficients found correspond to the components of the f_{klsj} (flexocoupling) tensor, having absolute values of the order of 0.1 V. Both positive and negative components were reported. The results obtained using the shell model were found in a good agreement with the shell-model results reported earlier by Askar *et al* [18]. However, it was found that the sign of the flexoelectric coefficient may depend on the lattice dynamics model used for the calculations of the dynamic matrix. The value of 0.1 V for the components of the f_{klsj} tensor is 1–2 orders of magnitude smaller than Kogan's estimate. The reason for the anomalously small flexocoupling coefficients in these materials is not clear.

The purely electronic contribution, associated with the redistribution of electronic density driven by the *external strai*ns (see section 3.2.3), was evaluated for a number of crystals by Hong *et al* [46]. The flexoelectric coefficients defined at fixed electrical displacement $\mu^{\rm eld}_{11}$ were calculated using the DFT. For the perovskites $BaTiO_3$, $SrTiO_3$, and $PbTiO_3$, it was found that $\mu^{\rm eld}_{11}/\varepsilon_0 \approx -16$ V. For NaCl, MgO, Si, and C, the reported values of $\mu^{\rm eld}_{11}/\varepsilon_0$ (in volts) are -5, -11, -12, -20, respectively. We should recall that, in these calculations, only a part of the electronic contribution is addressed. For this reason none of the obtained results are suitable for comparison with any experimental data which might in the future be collected for these materials. This reasoning holds for non-ionic Si and C as well. In these structures, where not all atoms are the centers of inversion, some redistribution of the electronic density driven by the *internal strains* should also occur. Thus, the mixed contribution from (41) should also be taken into account for a proper description of the flexoelectricity even in Si and C.

6.4. Experimental data

Flexoelectricity in solids can be directly evaluated using two different experimental methods: (i) an analysis of the phonon spectra and (ii) macroscopic characterization of the electrotechnical response of a finite sample. In general, these methods provide different information about the phenomenon.

The phonon spectra provide information on the joint action of the static and dynamic bulk flexoelectric effects. The spectra are typically obtained using neutron inelastic scattering or Brillouin scattering.

The macroscopic characterization provides information on the static bulk flexoelectric response and the contribution of the surface piezoelectricity. Such a characterization is most commonly performed using some variation of the two methods sketched in figure 15.

The first method consists of dynamically bending the material in a cantilever beam geometry in order to generate a transverse strain gradient (figure 15(a)). The flexoelectric polarization can then be measured by recording the displacement current flowing between the metallic plates. In this way the coefficient $\tilde{\mu}_{12}$ where

$$P_3 = \tilde{\mu}_{12}\frac{\partial u_{11}}{\partial x_3} \tag{141}$$

can be calculated. Since in a bent beam both the $\frac{\partial u_{11}}{\partial x_3}$ and $\frac{\partial u_{33}}{\partial x_3}$ components of strain gradient are inevitably present, $\tilde{\mu}_{12}$ is an effective flexoelectric coefficient involving a combination of flexoelectric tensor components that depends on the precise geometry of the system [41, 42], hereafter we term it as

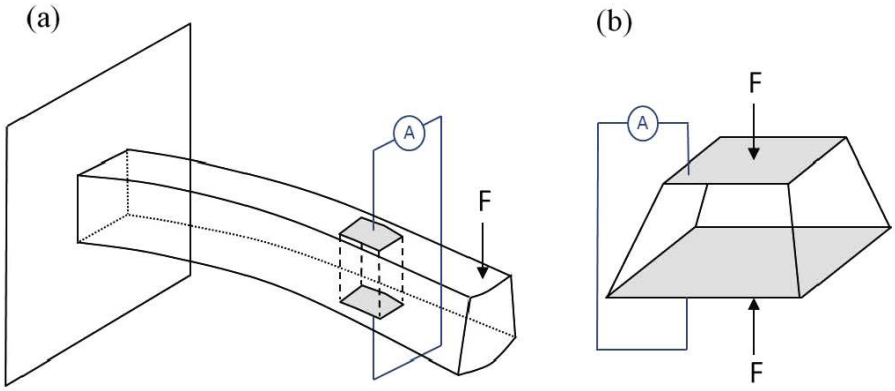

Figure 15. Methods most commonly used to quantify the flexoelectric response: (a) beam bending, (b) compression of a truncated pyramid. The action of the mechanical force is shown with arrows; the response is characterized by the current measured between the electrodes (shown in gray). Reprinted with permission from [12]. Copyright 2013 Annual Reviews.

effective transverse coefficient. In the case of an isotropic bent beam, for example, $\tilde{\mu}_{12} = -\nu\mu_{11}^{\text{mac}} + (1-\nu)\mu_{12}^{\text{mac}}$, where ν is the Poisson ratio. Here the components μ_{11}^{mac} and μ_{12}^{mac} characterize the flexoelectric response of a finite sample. In the typical case of quasi-static measurements, these components are not affected by the dynamic flexoelectric effect (see section 3.3), however, they can contain an essential contribution associated with the surface piezoelectricity (see section 5.2).

The second method for measuring direct flexoelectricity involves uniaxial compression of a truncated-pyramid-shaped sample [7], as illustrated in figure 15(b). The stress $\sigma_{33} = F/S$, generated by the pair of forces F, is different at the top and bottom surfaces of the truncated pyramid due to their different areas S, setting up a longitudinal strain gradient and thus generating a flexoelectric polarization

$$P_3 = \tilde{\mu}_{11}\frac{\partial u_{33}}{\partial x_3}. \tag{142}$$

Again, $\tilde{\mu}_{11}$ is an effective coefficient, hereafter we term it as the *effective longitudinal* coefficient. Under the assumption that the strain gradient is homogeneous over the pyramid, $\tilde{\mu}_{11}$ can be expressed in terms of the μ_{ijkl}^{mac} tensor [9]. For example, in the case of an isotropic material one finds $\tilde{\mu}_{11} = \mu_{11}^{\text{mac}} - 2\nu\mu_{12}^{\text{mac}}$.

A pyramid-shape sample can also be used for monitoring the converse flexoelectric response. Application of a voltage to such a structure gives rise to a non-uniform field distribution and hence polarization gradients that, in turn, generate strain in the sample through the converse flexoelectric effect. The induced strain can be measured using interferometric techniques [7, 31]. Such measurements always include a contribution from electrostriction, which usually dominates the signal. However, the field dependence is different for electrostriction (quadratic) and flexoelectricity (linear) and therefore the two effects can, in principle, be separated.

In classical crystalline materials, both the analysis of the phonon spectra and the macroscopic techniques are used for the characterization of flexoelectricity. In ceramics, the phonon-spectrum-based approach cannot be applied, so only the macroscopic techniques were employed. The following two subsections are devoted to the discussion of the experimental data on crystals and ceramics, respectively.

6.4.1. Crystals—phonon data. In displacive ferroelectrics (regular or incipient), the long-wavelength low-energy part of the phonon spectrum can be described using the continuum Landau-theory framework. In this framework, the interaction between the optical soft mode and the acoustic branches in the paraelectric phase is fully controlled by the flexoelectric coupling (section 4.1). Thus, the analysis of the phonon spectrum can provide information on flexoelectricity in the material. There are two limitations for this technique. First, it is always sensitive to both static and dynamic flexoelectric effects. Second, as is clear from the dispersion equation for the spectrum (61), it does not give the absolute sign of the components. At best, using this technique one may conclude that two components are of the same (or of the opposite) sign.

An accurate analysis of the Brillouin scattering data can provide information on the components of the total flexocoupling coefficient (57)

$$f_{klij}^{\text{tot}} = f_{klij} - \frac{1}{\varrho}M_{is}c_{sjkl}. \tag{143}$$

Using such an analysis Tagantsev *et al* [106] determined $|f_{44}^{\text{tot}}| = 2.2\,\text{V}$ for crystalline $SrTiO_3$ based on experimental data by Hehlen *et al* [38]. Let us explain the main points of this analysis. The transverse acoustic phonons propagating along a cubic crystallographic axis of $SrTiO_3$ are considered. Since the typically values of wavevectors of acoustic phonons probed with Brillouin scattering are small compared to the reciprocal lattice vector, relationship (64) for the description of the small nonlinearity of the dispersion of the acoustic branch in this case may be simplified to

$$\frac{\Delta\omega_A}{\omega_A} = -\frac{q^2(f_{44}^{\text{tot}})^2}{2c_{44}\alpha}, \tag{144}$$

$$f_{44}^{\text{tot}} = f_{44} - \frac{1}{\varrho}Mc_{44}. \tag{145}$$

Table 1. The effective flexoelectric coefficients of some perovskites evaluated from their phonon spectra. The sign of $f_{11}^{\text{eff}} - f_{12}^{\text{eff}}$ is actually not known.

Material	$f_{11}^{\text{eff}} - f_{12}^{\text{eff}}$	$\lvert f_{44}^{\text{eff}} \rvert$
$BaTiO_3$ [35]	<7.8	<0.15
$SrTiO_3$ [35, 106]	−1.2–1.4	1.2–2, 2.2
$KTaO_3$ [35, 39]	∼0, 1.8	2.9, 2.5

To simplify this the relations (62) and (63) were used. Once the parameters $c_{44}, \alpha = 1/\varepsilon_f$ entering relationship (144) are known, the absolute value of f_{44}^{tot} can be determined by fitting the experimental spectrum to relationship (144). Here one should note that, in [106], the dynamic flexoelectric effect was not taken into account, i.e. in (143) M_{is} was set zero. As a result, the value of 2.2 V obtained was actually attributed to the f_{44} component of the flexocoupling tensor. Clearly, relations analogous to (144) can be derived for acoustic phonon propagation in other directions, yielding information on the other components of the f_{klij}^{tot} tensor.

The information on the flexoelectric coupling can also be obtained from a treatment of the low-energy phonon spectrum of a crystal probed with the neutron scattering technique. In this case, the energy resolution is much lower than in the Brillouin scattering technique but the spectrum is available in the whole Brillouin zone. In some perovskites, the treatment of long-wavelength low-energy part of the spectrum (two branches of the soft mode + three acoustic branches) was actually done [35, 39] in terms of equations (59) and (60), however, with the contribution of the dynamic flexoelectric effect being omitted, i.e. in equations of motion (59) and (60) M_{is} was set to zero and the mode coupling is described in terms of the f_{klij} tensor only. Thus, such a treatment of a spectrum gives some effective values of the flexocoupling coefficients f_{klij}^{eff}, corresponding to a frequency-weighted sum of the static and dynamic contributions (see section 4.1). These coefficients can essentially differ from the components f_{klij}^{tot}, once the deviation of the dispersion of the acoustic branch from the linear law is appreciable (see figure 3). This issue is discussed in section 4.1. The components of f_{klij}^{eff} evaluated from the neutron scattering data are listed in table 1. The values given in table 1 contradict neither the Kogan's estimate nor the stability conditions (137) and (138). However, a quantitative comparison of these results with the experimental data or theoretical results on tensors f_{klij} and f_{klij}^{tot} is not directly possible in view of the aforementioned frequency-weighted summation.

6.4.2. Crystals—macroscopic measurements. The only crystal for which the flexoelectric response has been substantially characterized using macroscopic measurements is $SrTiO_3$. Zubko *et al* [41, 42] employed a modification of the bending method (figure 15(a)) to characterize the flexoelectric response in single crystals of this material. It was found that the measured flexoelectric response (actually it is controlled by the effective transverse coefficient $\tilde{\mu}_{12}$ from (141)) is linear in the applied strain gradient and that its temperature dependence follows that of the dielectric constant. For a beam cut according to the crystallographic cubic axes at room temperature $\tilde{\mu}_{12} = 6.1$ nC m^{-1} is reported. To get all the three independent coefficients characterizing the flexoelectric response of cubic $SrTiO_3$ the authors performed bending experiments with different orientations of the beam, finding $\tilde{\mu}_{12}$ of the same order-of-magnitude for all beam orientations. However, pure bending experiments yield only two independent equations for the three components of the flexoelectric tensor [42] and the authors combined their data with the component $f_{44} = 2.2$ V of the flexocoupling tensor taken from the Brillouin scattering data to find $f_{11} = 0.08$ V and[15] $f_{12} = 2.6$ V.

Since these components of the flexocoupling tensor were obtained using the data of static measurements in a finite sample and the phonon data, they are expected to be controlled by three effects: static bulk flexoelectricity, dynamic bulk flexoelectricity, and the surface piezoelectricity. Such an attribution is well supported. First, the experimental values of the flexocoupling coefficients are consistent with the order-of-magnitude estimates for the contributions of these effects. Second, the flexoelectric response was documented to scale as the dielectric constant of the material, which is again consistent with the theoretical predictions for these effects. However, a more quantitative comparison with the theory is hardly possible. First of all, the surface piezoelectricity may substantially affect the flexoelectric response, while no quantitative theory for this effect is currently available. Moreover, even if we assume that for some reason this effect is not active in the $SrTiO_3$ samples studied, one will still not be able to quantify the analysis of the experimental data. In view of the quasi-static regime of measurement, the bending-experiment data are fully controlled by the static bulk flexoelectric effect. Meanwhile, there is problem with use of the Brillouin data. First of all, this technique yields the components of the f_{klij}^{tot} tensor not f_{klij}. Because of the dynamic flexoelectric effect, these tensors can be essentially different. In addition, as was indicated in the preceding subsection, this technique does not yield the sign of f_{44}^{tot}.

6.4.3. Ceramics—macroscopic measurements. Using the beam-bending and pyramid-loading methods, the flexoelectric response was characterized in a number of perovskite ceramics. Particularly high coefficients $\tilde{\mu}_{11}$ and $\tilde{\mu}_{12}$ (tens of μC m^{-1} and more) have been measured close to the ferroelectric-to-paraelectric phase transitions of (Ba, Sr)TiO_3, relaxor PMN, and (Pb, Sr)TiO_3 ceramics, where the dielectric constants reach values exceeding 10 000–20 000. Measurements of the flexoelectric response as a function of temperature confirm the expected trend for scaling of μ with χ, as illustrated in figures 16(a)–(c) for several perovskite compounds in their paraelectric phases. The exact proportionality between μ and χ predicted by equation (12), however, does not always hold, as can be seen most clearly in figures 16(b), (c). For the ceramics in the paraelectric phase, the flexoelectric response was reported

[15] Actually, the components of the μ_{ijkl} flexoelectric tensor were reported in [41, 42]. To find the corresponding components of the f_{klij} tensor we take the room-temperature value of the dielectric constant in $SrTiO_3$ equal to 300.

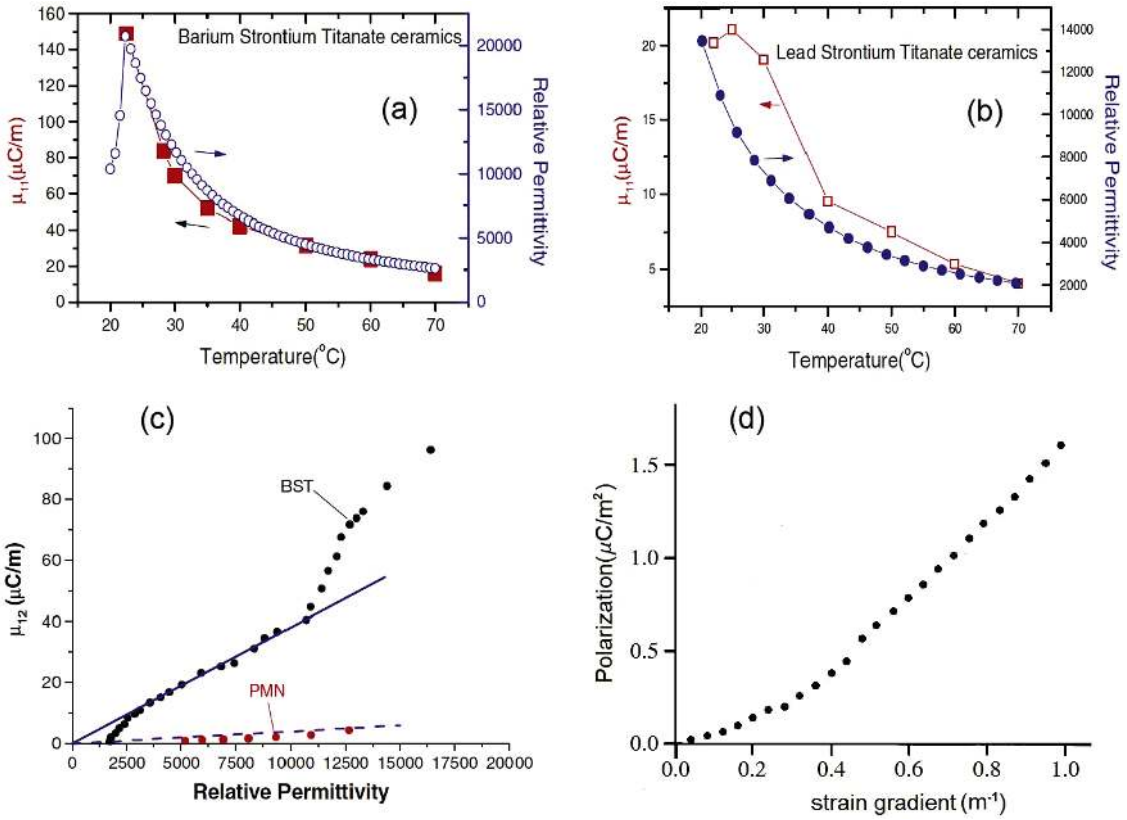

Figure 16. Temperature evolution of the effective longitudinal flexoelectric coefficient $\tilde{\mu}_{11}$ and the dielectric permittivity of (a) (Ba, Sr)TiO_3 and (b) (Pb, Sr)TiO_3 (BST) ceramics above the Curie temperature. The effective transverse flexoelectric coefficient $\tilde{\mu}_{12}$ plotted as a function of the relative dielectric permittivity for $PbMg_{1/3}$ $Nb_{2/3}O_3$ (PMN) and $Ba_{0.67}Sr_{0.33}$ TiO_3 (c). Polarization versus strain gradient in bending measurements in modified Pb(Zr, Ti)O_3 (PZT-5H) ceramics at room temperature (d). Reprinted with permission from [7]. Copyright 2006 Springer.

linear in the applied strain gradient. In contrast, the data for unpoled ceramics in the ferroelectric phase correspond to a pronounced super-linear polarization/strain gradient dependence (figure 16(d)).

The flexoelectricity in perovskite ceramics was also probed with the electrical loading of pyramidal samples, the method mentioned at the beginning of section 6.4. This method was used by Fu and coworkers to measure the converse flexoelectric effect and thus estimate the flexoelectric coefficient $\tilde{\mu}_{11}$ for BST, which was found to be in excellent agreement with measurements of the direct flexoelectric effect [31]. A similar method was also used by Hana *et al* to study converse flexoelectricity in $PbMg_{1/3}$ $Nb_{2/3}O_3$-$PbTiO_3$ [33, 107].

Originally, the results obtained for ceramics in the paraelectric phase were attributed to a manifestation of the static bulk flexoelectric effect (see e.g. [7]). However, in the context of the recent developments in the field, such an interpretation may be questioned. Firstly, it was shown that the contribution of surface piezoelectricity scales with the bulk dielectric constant. In view of this, the fact that the measured flexoelectric response scales as the bulk dielectric constant does not necessarily imply that one is dealing with static bulk flexoelectric effect. Secondly, the reported values of $\tilde{\mu}_{11}$ and $\tilde{\mu}_{12}$ often correspond to the those of the components of the flexocoupling tensor f_{klij}, lying in the range 100–900 V, which far exceeds Kogan's estimate $f_{klij} \simeq 1$–10 V for ionic solids. In addition, such high values can hardly be compatible with the constraints (135) and (134) associated with the stability of the system with respect to the formation of an incommensurate state. All in all, the mechanism behind the giant flexoelectric response in perovskite ceramics remains obscure, making it appealing for theorists. The results on the flexoelectric response in non-poled Pb(Zr, Ti)O_3 ceramics are also challenging for theorists: a pronounced super-linear polarization/strain gradient dependence (figure 16(d)) suggests a domain contribution to the flexoelectric response [29], while no relevant theory is currently available. This issue is tightly related to the problem of the flexoelectric switching discussed in section 4.3.3, where the domain-assisted flexoelectricity may be relevant.

7. Conclusions and open questions

As one may conclude from reading this review paper, flexoelectricity exhibits many facets relevant to both the fundamental properties of solids and their practical applications. It is also clear that despite the considerable effort expended on theoretical and experimental studies of flexoelectricity there exist many open issues attesting to a

limited understanding of the physics of flexoelectricity in real systems. Concluding this paper we would like to draw the attention of the reader to the most important of them.

The situation with flexoelectricity in perovskite ceramics is challenging [7]. The level of the flexoelectric response in these materials is suitable for use in practical electromechanical devices [56]. Meanwhile, the reported values of the flexoelectric constants are compatible neither with theoretical estimates nor the constraints associated with the stability of the crystalline structure of these materials (see section 6.4.3). Thus, the mechanism behind the flexoelectricity of perovskite ceramics remains obscure. This missing knowledge seems to be a serious obstacle for further practical development of flexoelectric materials.

The data on the flexoelectric response of unpoled perovskite ceramics in the ferroelectric phase suggest the presence of a domain contribution to the direct flexoelectric effect [29]. The data on the flexoelectricity-driven polarization switching [20, 77] reveals a very strong switching action of the strain gradient (much stronger than that expected for the static bulk flexoelectric effect). The presence of a strong domain contribution to flexoelectricity might resolve such a controversy. However, no theory of domain-assisted flexoelectricity is currently available.

Any comparison of the theoretical results with experimental data on flexoelectricity is still a challenging task. For the moment, one can only state that (i) the temperature dependence of flexoelectric response is often close to that of the dielectric constant, in agreement with the theoretical prediction, and (ii) the orders of magnitude of the flexocoupling coefficients in crystals are consistent with the rough estimate by Kogan. However, a more quantitative comparison with the theory is not currently possible. The phonon data cannot be compared with theoretical results since such a comparison requires theoretical values for the tensor M_{ij} (see equation (52)) controlling the dynamic contribution to the flexoelectricity, which are not currently available. The quantitative interpretation of the data obtained from macroscopic measurements is also problematic in view of a possible contribution of the surface piezoelectricity, the quantitative theory of which is not yet developed. Last, but not least, there exists a purely experimental issue: in all experiments at least two contributions to the flexoelectric response are active: either the static and the dynamic or the static and the surface-controlled.

Though a simple model for the flexoelectric response conditioned by the surface piezoelectricity was recently offered [51] no microscopic theory of the phenomenon is currently available. Such a theory might clarify the very strong flexoelectricity in perovskite ceramics. On the phenomenological side, it looks interesting to link the flexoelectric response conditioned by the surface piezoelectricity with the Landau-theory treatment of the surface piezoelectricity [108, 109].

And, finally, a most challenging issue for understanding and quantitative theoretical description is the strain-gradient-assisted preparation of perovskites in a polar (quasi)amorphous state and the notion of plastic flexoelectricity (see section 4.3.4).

Acknowledgments

The authors are indebted to Dragan Damjanovic, Gustau Catalan, Pavlo Zubko, and Anna Morozovska for useful discussions. Daniil Kitchaev is acknowledged for reading the manuscript. The authors also gratefully acknowledge funding from the Swiss National Science Foundation.

References

[1] Meyer R B 1969 Piezoelectric effects in liquid crystals *Phys. Rev. Lett.* **22** 918–21
[2] Petrov A G 2002 Flexoelectricity of model and living membranes *Biochim. Biophys. Acta (BBA)—Biomembr.* **1561** 1–25
[3] Petrov A G 2006 Electricity and mechanics of biomembrane systems: flexoelectricity in living membranes *Anal. Chim. Acta* **568** 70–83
[4] Breneman K D, Brownell W E and Rabbitt R D 2009 Hair cell bundles: flexoelectric motors of the inner ear *PLoS One* **4** e5201
[5] Tagantsev A K 1987 Pyroelectric, piezoelectric, flexoelectric, and thermal polarization effects in ionic crystals *Sov. Phys.—Usp.* **30** 588–603
[6] Tagantsev A K 1991 Electric polarization in crystals and its response to thermal and elastic perturbations *Phase Transit.* **35** 119–203
[7] Cross L 2006 Flexoelectric effects: charge separation in insulating solids subjected to elastic strain gradients *J. Mater. Sci.* **41** 53–63
[8] Maranganti R, Sharma N D and Sharma P 2006 Electromechanical coupling in nonpiezoelectric materials due to nanoscale nonlocal size effects: Green's function solutions and embedded inclusions *Phys. Rev.* B **74** 014110
[9] Ma W 2010 Flexoelectric charge separation and size dependent piezoelectricity in dielectric solids *Phys. Status Solidi* b **247** 213–8
[10] Lee D and Noh T W 2012 Giant flexoelectric effect through interfacial strain relaxation *Phil. Trans. R. Soc.* A **370** 4944–57
[11] Nguyen T D, Mao S, Yeh Y-W, Purohit P K and McAlpine M C 2013 Nanoscale flexoelectricity *Adv. Mater.* **25** 946–74
[12] Zubko P, Catalan G and Tagantsev A K 2013 Flexoelectric effect in solids *Annu. Rev. Mater. Res.* **43** 387–421
[13] Mashkevich V S and Tolpygo K B 1957 Electrical, optical and elastic properties of diamond type crystals. 1 *Sov. Phys.—JETP* **5** 435–9
[14] Tolpygo K B 1963 Long wavelength oscillations of diamond-type crystals including long range forces *Sov. Phys.—Solid State* **4** 1297–305
[15] Kogan S M 1964 Piezoelectric effect during inhomogeneous deformation and acoustic scattering of carriers in crystals *Sov. Phys. Solid State* **5** 2069–70
[16] Harris P 1965 Mechanism for the shock polarization of dielectrics *J. Appl. Phys.* **36** 739–41
[17] Mindlin R D 1968 Polarization gradient in elastic dielectrics *Int. J. Solids Struct.* **4** 637–42
[18] Askar A, Lee P C Y and Cakmak A S 1970 Lattice-dynamics approach to the theory of elastic dielectrics with polarization gradient *Phys. Rev.* B **1** 3525
[19] Bursian E V and Zaikovskii O I 1968 Changes in the curvature of a ferroelectric film due to polarization *Sov. Phys.—Solid State* **10** 1121–4
[20] Bursian E V, Zaikovskii O I and Makarov K V 1969 Ferroelectric plate polarization by bending *Izv. Akad. Nauk, SSSR Ser. Fiz.* **33** 1098–102

[21] Bursian É V and Trunov N N 1974 Nonlocal piezoelectric effect *Sov. Phys.—Solid State* **10** 760–2

[22] Axe J D, Harada J and Shirane G 1970 Anomalous acoustic dispersion in centrosymmetric crystals with soft optic phonons *Phys. Rev.* B **1** 1227–34

[23] Indenbom V L, Loginov E B and Osipov M A 1981 Flexoelectric effect and the structure of crystals *Kristalografija* **26** 1157

[24] Tagantsev A K 1985 Theory of flexoelectric effects in crystals *Zh. Eksp. Teor. Fiz.* **88** 2108–22

[25] Tagantsev A K 1986 Piezoelectricity and flexoelectricity in crystalline dielectrics *Phys. Rev.* B **34** 5883–9

[26] Ma W and Eric Cross L 2001 Observation of the flexoelectric effect in relaxor $Pb(Mg_{1/3}Nb_{2/3})O_3$ ceramics *Appl. Phys. Lett.* **78** 2920–1

[27] Ma W and Eric Cross L 2001 Large flexoelectric polarization in ceramic lead magnesium niobate *Appl. Phys. Lett.* **79** 4420–2

[28] Ma W and Eric Cross L 2002 Flexoelectric polarization of barium strontium titanate in the paraelectric state *Appl. Phys. Lett.* **81** 3440–2

[29] Ma W and Eric Cross L 2003 Strain-gradient-induced electric polarization in lead zirconate titanate ceramics *Appl. Phys. Lett.* **82** 3293–5

[30] Ma W and Eric Cross L 2006 Flexoelectricity of barium titanate *Appl. Phys. Lett.* **88** 232902

[31] Fu J Y, Zhu W, Li N and Eric Cross L 2006 Experimental studies of the converse flexoelectric effect induced by inhomogeneous electric field in a barium strontium titanate composition *J. Appl. Phys.* **100** 024112

[32] Huang W, Kim K, Zhang S, Yuan F-G and Jiang X 2011 Scaling effect of flexoelectric (Ba, Sr)TiO_3 microcantilevers *Phys. Status Solidi (RRL)* **5** 350–2

[33] Hana P 2007 Study of flexoelectric phenomenon from direct and from inverse flexoelectric behavior of pmnt ceramic *Ferroelectrics* **351** 196–203

[34] Ma W and Eric Cross L 2005 Flexoelectric effect in ceramic lead zirconate titanate *Appl. Phys. Lett.* **86** 072905

[35] Vaks V G 1973 *Introduction to the Microscopic Theory of Ferroelectrics* (Moscow: Nauka)

[36] Harada J, Axe J and Shirane G 1971 Neutron-scattering study of soft modes in cubic $BaTiO_3$ *Phys. Rev.* B **4** 155

[37] Cowley R A 1964 Lattice dynamics and phase transitions of strontium titanate *Phys. Rev.* **134** A981–97

[38] Hehlen B, Arzel L, Tagantsev A K, Courtens E, Inaba Y, Yamanaka A and Inoue K 1998 Brillouin-scattering observation of the Ta–To coupling in $SrTiO_3$ *Phys. Rev.* B **57** R13989

[39] Farhi E, Tagantsev A K, Currat R, Hehlen B, Courtens E and Boatner L A 2000 Low energy phonon spectrum and its parameterization in pure $KTaO_3$ below 80 k *Eur. Phys. J.* B **15** 615–23

[40] Shandarov S M, Shmakov S S, Burimov N I, Syuvaeva O S, Kargin Y F and Petrov V M 2012 Detection of the contribution of the inverse flexoelectric effect to the photorefractive response in a bismuth titanium oxide single crystal *JETP Lett.* **95** 618–21

[41] Zubko P, Catalan G, Buckley A, Welche P R L and Scott J F 2007 Strain-gradient-induced polarization in $SrTiO_3$ single crystals *Phys. Rev. Lett.* **99** 167601

[42] Zubko P, Catalan G, Buckley A, Welche P R L and Scott J F 2008 Strain-gradient-induced polarization in $SrTiO_3$ single crystals [phys. rev. lett. 99, 167601 (2007)] *Phys. Rev. Lett.* **100** 199906 (erratum)

[43] Maranganti R and Sharma P 2009 Atomistic determination of flexoelectric properties of crystalline dielectrics *Phys. Rev.* B **80** 054109

[44] Hong J, Catalan G, Scott J F and Artacho E 2010 The flexoelectricity of barium and strontium titanates from first principles *J. Phys.: Condens. Matter* **22** 112201

[45] Ponomareva I, Tagantsev A K and Bellaiche L 2012 Finite-temperature flexoelectricity in ferroelectric thin films from first principles *Phys. Rev.* B **85** 104101

[46] Hong J and Vanderbilt D 2011 First-principles theory of frozen-ion flexoelectricity *Phys. Rev.* B **84** 180101

[47] Martin R M 1972 Piezoelectricity *Phys. Rev.* B **5** 1607

[48] Resta R 2010 Towards a bulk theory of flexoelectricity *Phys. Rev. Lett.* **105** 127601

[49] Dumitrica T, Landis C M and Yakobson B I 2002 Curvature-induced polarization in carbon nanoshells *Chem. Phys. Lett.* **360** 182–8

[50] Kalinin S V and Meunier V 2008 Electronic flexoelectricity in low-dimensional systems *Phys. Rev.* B **77** 033403

[51] Tagantsev A K and Yurkov A S 2012 Flexoelectric effect in finite samples *J. Appl. Phys.* **112** 044103

[52] Eliseev E A, Morozovska A N, Glinchuk M D and Blinc R 2009 Spontaneous flexoelectric/flexomagnetic effect in nanoferroics *Phys. Rev.* B **79** 165433

[53] Yurkov A S 2011 Elastic boundary conditions in the presence of the flexoelectric effect *JETP Lett.* **94** 455–8

[54] Fu J Y, Zhu W, Li N, Smith N B and Eric Cross L 2007 Gradient scaling phenomenon in microsize flexoelectric piezoelectric composites *Appl. Phys. Lett.* **91** 182910

[55] Zhu W, Fu J Y, Li N and Cross L 2006 Piezoelectric composite based on the enhanced flexoelectric effects *Appl. Phys. Lett.* **89** 192904

[56] Chu B, Zhu W, Li N and Eric Cross L 2009 Flexure mode flexoelectric piezoelectric composites *J. Appl. Phys.* **106** 104109

[57] Fousek J, Cross L E and Litvin D B 1999 Possible piezoelectric composites based on the flexoelectric effect *Mater. Lett.* **39** 287–91

[58] Sharma N D, Maranganti R and Sharma P 2007 On the possibility of piezoelectric nanocomposites without using piezoelectric materials *J. Mech. Phys. Solids* **55** 2328–50

[59] Sharma N D, Landis C M and Sharma P 2010 Piezoelectric thin-film superlattices without using piezoelectric materials *J. Appl. Phys.* **108** 024304

[60] Chandratre S and Sharma P 2012 Coaxing graphene to be piezoelectric *Appl. Phys. Lett.* **100** 023114

[61] Morozovska A N, Eliseev E A, Glinchuk M D, Chen L-Q and Gopalan V 2012 Interfacial polarization and pyroelectricity in antiferrodistortive structures induced by a flexoelectric effect and rotostriction *Phys. Rev.* B **85** 094107

[62] Borisevich A Y, Eliseev E A, Morozovska A N, Cheng C-J, Lin J-Y, Chu Y H, Kan D, Takeuchi I, Nagarajan V and Kalinin S V 2012 Atomic-scale evolution of modulated phases at the ferroelectric—antiferroelectric morphotropic phase boundary controlled by flexoelectric interaction *Nature Commun.* **3** 775

[63] Yudin P V, Tagantsev A K, Eliseev E A, Morozovska A N and Setter N 2012 Bichiral structure of ferroelectric domain walls driven by flexoelectricity *Phys. Rev.* B **86** 134102

[64] Majdoub M S, Maranganti R and Sharma P 2009 Understanding the origins of the intrinsic dead layer effect in nanocapacitors *Phys. Rev.* B **79** 115412

[65] Zhou H, Hong J, Zhang Y, Li F, Pei Y and Fang D 2012 Flexoelectricity induced increase of critical thickness in epitaxial ferroelectric thin films *Physica* B **407** 3377–81

[66] Catalan G, Sinnamon L J and Gregg J M 2004 The effect of flexoelectricity on the dielectric properties of inhomogeneously strained ferroelectric thin films *J. Phys.: Condens. Matter* **16** 2253

[67] Catalan G, Noheda B, McAneney J, Sinnamon L J and Gregg J M 2005 Strain gradients in epitaxial ferroelectrics *Phys. Rev.* B **72** 020102

[68] Abe K, Komatsu S, Yanase N, Sano K and Kawakubo T 1997 Asymmetric ferroelectricity and anomalous current conduction in heteroepitaxial $BaTiO_3$ thin films *Japan. J. Appl. Phys.* **36** 5846–53

[69] Abe K, Yanase N, Yasumoto T and Kawakubo T 2002 Voltage shift phenomena in a heteroepitaxial $BaTiO_3$ thin film capacitor *J. Appl. Phys.* **91** 323–30

[70] Tagantsev A K, Cross L E and Fousek J 2010 *Domains in Ferroic Crystals and Thin Films* (New York: Springer)

[71] Gharbi M, Sun Z H, Sharma P and White K 2009 The origins of electromechanical indentation size effect in ferroelectrics *Appl. Phys. Lett.* **95** 142901

[72] Gharbi M, Sun Z H, Sharma P, White K and El-Borgi S 2011 Flexoelectric properties of ferroelectrics and the nanoindentation size-effect *Int. J. Solids Struct.* **48** 249–56

[73] Robinson C R, White K W and Sharma P 2012 Elucidating the mechanism for indentation size-effect in dielectrics *Appl. Phys. Lett.* **101** 122901

[74] Morozovska A N, Eliseev E A, Tagantsev A K, Bravina S L, Chen L-Q and Kalinin S V 2011 Thermodynamics of electromechanically coupled mixed ionic-electronic conductors: deformation potential, Vegard strains, and flexoelectric effect *Phys. Rev.* B **83** 195313

[75] Lyahovitskaya V, Feldman Y, Zon I, Wachtel E, Gartsman K, Tagantsev A K and Lubomirsky I 2005 Formation and thermal stability of quasi-amorphous thin films *Phys. Rev.* B **71** 094205

[76] Lee D, Yoon A, Jang S Y, Yoon J-G, Chung J-S, Kim M, Scott J F and Noh T W 2011 Giant flexoelectric effect in ferroelectric epitaxial thin films *Phys. Rev. Lett.* **107** 057602

[77] Gruverman A, Rodriguez B J, Kingon A I, Nemanich R J, Tagantsev A K, Cross J S and Tsukada M 2003 Mechanical stress effect on imprint behavior of integrated ferroelectric capacitors *Appl. Phys. Lett.* **83** 728–30

[78] Lu H, Bark C-W, Esque de los Ojos D, Alcala J, Eom C B, Catalan G and Gruverman A 2012 Mechanical writing of ferroelectric polarization *Science* **336** 59–61

[79] Martienssen W 1992 *Landolt-Börnstein: Numerical Data and Functional-Relationships in Science and Technology—New Series* vol III/16 and III/29a (Berlin: Springer)

[80] Born M and Huang K 1962 *Dynamical Theory of Crystal Lattices* (Oxford: Oxford University Press)

[81] Pick R M, Cohen M H and Martin R M 1970 Microscopic theory of force constants in the adiabatic approximation *Phys. Rev.* B **1** 910–20

[82] Shirane G, Axe J D, Harada J and Remeika J P 1970 Soft ferroelectric modes in lead titanate *Phys. Rev.* B **2** 155

[83] Dvorak V and Janovec V 1965 *Japan. J. Appl. Phys.* **4** 400–2

[84] Ponomareva I, Tagantsev A K and Bellaiche L 2012 *Phys. Rev.* B **85** 104101

[85] Eliseev E A, Morozovska A N, Svechnikov G S, Maksymovych P and Kalinin S V 2012 Domain wall conduction in multiaxial ferroelectrics *Phys. Rev.* B **85** 045312

[86] Gureev M Y, Tagantsev A K and Setter N 2011 Head-to-head and tail-to-tail 180 degree domain walls in an isolated ferroelectric *Phys. Rev.* B **83** 184104

[87] Vul B M, Guro G M and Ivanchik II 1973 Encountering domains in ferroelectrics *Ferroelectrics* **6** 29–31

[88] Jia C L, Mi S B, Urban K, Vrejoiu I, Alexe M and Hesse D 2008 Atomic-scale study of electric dipoles near charged and uncharged domain walls in ferroelectric films *Nature Mater.* **7** 57–61

[89] Anselm A I 1981 *Introduction to Semiconductor Theory* (Moscow: Mir) (Englewood Cliffs, NJ: Prentice-Hall) p 346

[90] Eliseev E A, Yudin P V, Kalinin S V, Setter N, Tagantsev A K and Morozovska A N 2013 Structural phase transitions and electronic phenomena at 180° domain walls in rhombohedral $BaTiO_3$ *Phys. Rev.* B **87** 054111

[91] Meyer B and Vanderbilt D 2002 *Ab initio* study of ferroelectric domain walls in $PbTiO_3$ *Phys. Rev.* B **65** 104111

[92] Speck J S and Pompe W 1994 Domain configurations due to multiple misfit relaxation mechanisms in epitaxial ferroelectric thin films. I. Theory *J. Appl. Phys.* **76** 466–76

[93] Matthews J W and Blakeslee A E 1974 Defects in epitaxial multilayers: I. Misfit dislocations *J. Cryst. Growth* **27** 118–25

[94] Lyahovitskaya V, Zon I, Feldman Y, Cohen S R, Tagantsev A K and Lubomirsky I 2003 Pyroelectricity in highly stressed quasi-amorphous thin films *Adv. Mater.* **15** 1826–8

[95] Ehre D, Lyahovitskaya V, Tagantsev A and Lubomirsky I 2007 Amorphous piezo- and pyroelectric phases of $BaZrO_3$ and $SrTiO_3$ *Adv. Mater.* **19** 1515–7

[96] Shelukhin V, Ehre D, Lavert E, Wachtel E, Feldman Y, Tagantsev A and Lubomirsky I 2011 Structural determinants of the sign of the pyroelectric effect in quasi-amorphous $SrTiO_3$ films *Adv. Funct. Mater.* **21** 1403–10

[97] Ehre D, Cohen H, Lyahovitskaya V, Tagantsev A and Lubomirsky I 2007 Structural transformations during formation of quasi-amorphous $BaTiO_3$ *Adv. Funct. Mater.* **17** 1204–8

[98] Herring C and Vogt E 1956 Transport and deformation-potential theory for many-valley semiconductors with anisotropic scattering *Phys. Rev.* **101** 944–61

[99] Liu J, Cannon D D, Wada K, Ishikawa Y, Danielson D T, Jongthammanurak S, Michel J and Kimerling L C 2004 Deformation potential constants of biaxially tensile stressed ge epitaxial films on Si(100) *Phys. Rev.* B **70** 155309

[100] Zhang X, Shyy W and Sastry A M 2007 Numerical simulation of intercalation-induced stress in Li-ion battery electrode particles *J. Electrochem. Soc.* **154** A910

[101] Yurkov A S 2012 privite communication

[102] Kretschmer R and Binder K 1979 Surface effects on phase transition in ferroelectrics and dipolar magnets *Phys. Rev.* B **20** 1065–76

[103] Timoshenko S and Woinowsky-Kreiger S 1987 *Theory of Plates and Shells* (New York: McGraw-Hill)

[104] Landau L D and Lifshitz E M 1975 *Theory of Elasticity* (Oxford: Pergamon)

[105] Landau L D and Lifshitz E M 1975 *The Classical Theory of Field* (Oxford: Pergamon)

[106] Tagantsev A K, Courtens E and Arzel L 2001 Prediction of a low-temperature ferroelectric instability in antiphase domain boundaries of strontium titanate *Phys. Rev.* B **64** 224107

[107] Hana P, Marvan M, Burianova L, Zhang S J, Furman E and Shrout T R 2006 Study of the inverse flexoelectric phenomena in ceramic lead magnesium niobate-lead titanate *Ferroelectrics* **336** 137–44

[108] Glinchuk M D and Morozovska A N 2004 The internal electric field originating from the mismatch effect and its influence on ferroelectric thin film properties *J. Phys.: Condens. Matter* **16** 3517–31

[109] Dai S, Gharbi M, Sharma P and Park H S 2011 Surface piezoelectricity: size effects in nanostructures and the emergence of piezoelectricity in non-piezoelectric materials *J. Appl. Phys.* **110** 104305